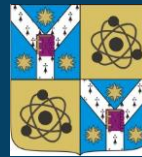


Plasma diagnostics



UNIVERSITATEA "ALEXANDRU IOAN CUZA" din IAŞI



www.uaic.ro

Iasi Plasma Advanced Research Center (IPARC)

www.plasma.uaic.ro



CONTENT

Electrical diagnosis:

- Discharge current
- Probes

Optical diagnosis:

- Emission spectra, including time and space resolved
- Absorption, including laser radiation
- Photography, including high speed imaging

Mass spectrometry and ions energy

Gas-phase FTIR spectroscopy

Electrical diagnosis: discharge current



UNIVERSITATEA "ALEXANDRU IOAN CUZA" din IAŞI

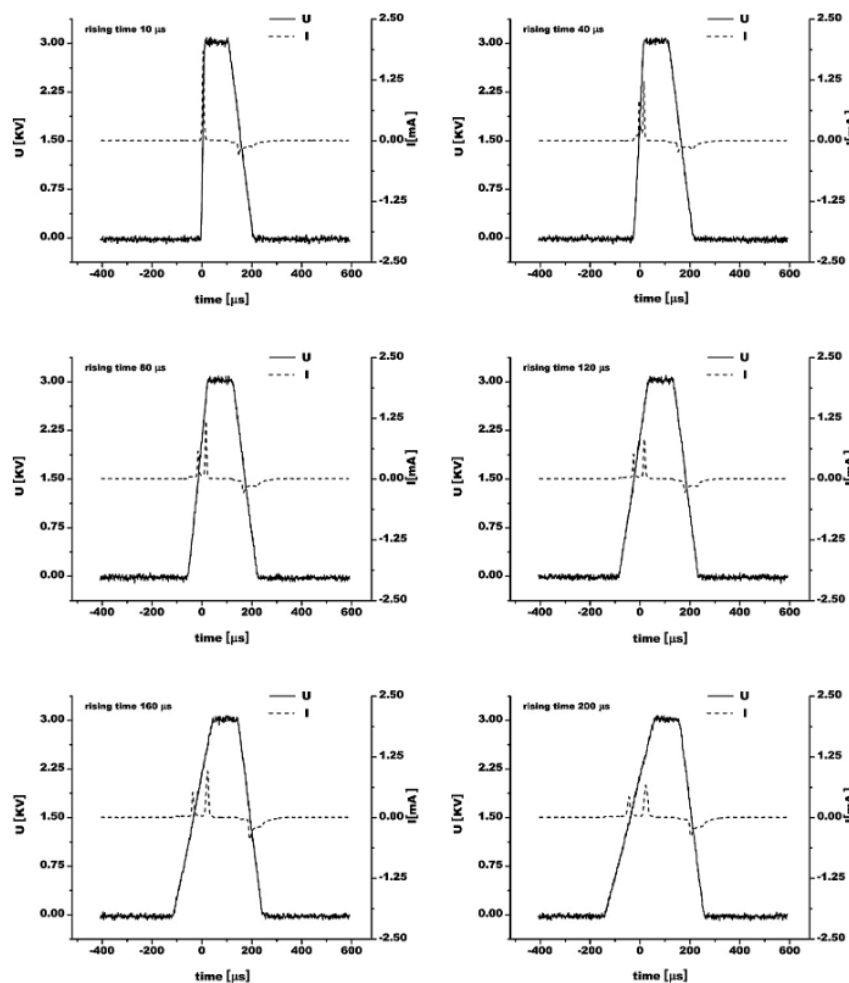
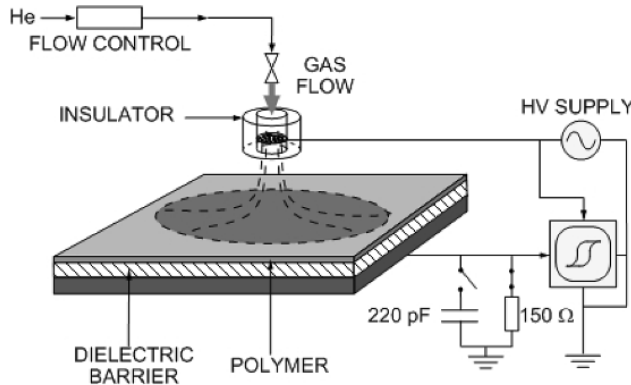
www.uaic.ro

Equipment and materials:

- Current probes
- Voltage probes
- Oscilloscopes
- Analog-to-Digital Converters (ADC)



EXAMPLE:



$$W = \frac{1}{T} \int_t^{t+T} I(t)U(t)dt$$

$$E = \int_t^{t+T} Q(t)U(t)dt$$

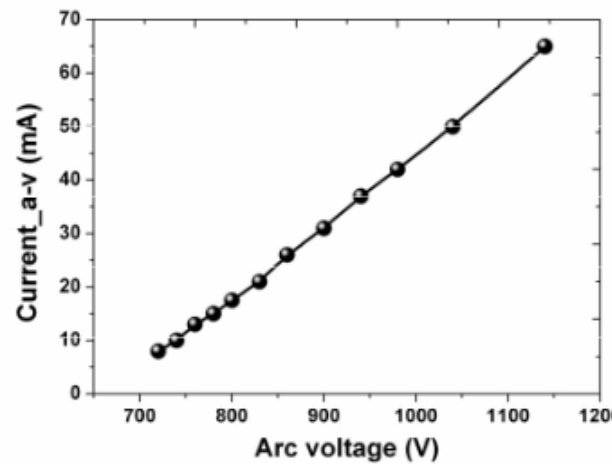
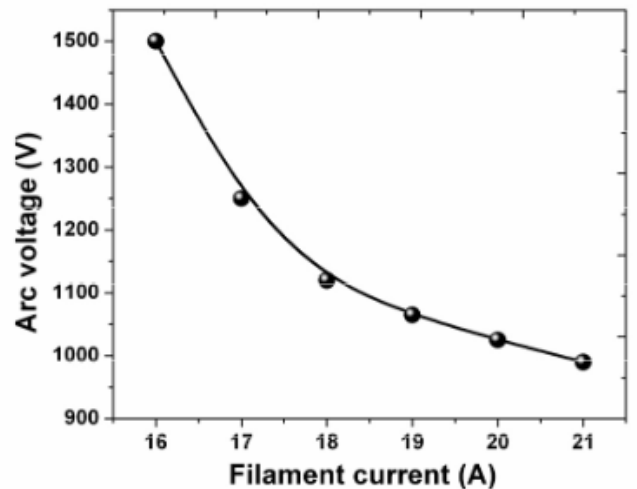
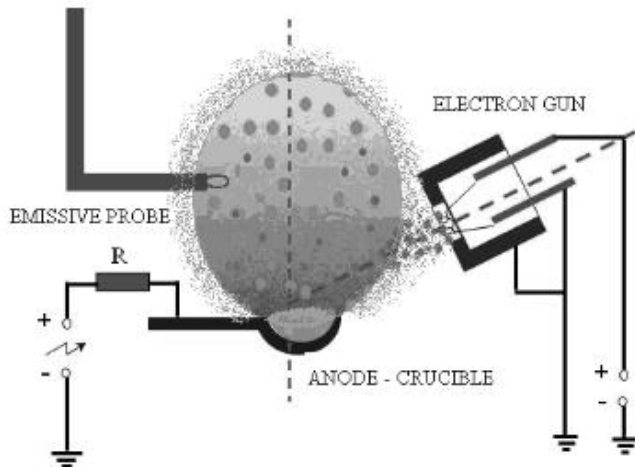
Experimental set-up and DBD voltage and current waveform for pulses with variable rising time (3 KV amplitude, 100 μs width, 100 μs falling time).



https://rjp.nipne.ro/2009_54_7-8/0689_0698.pdf



EXAMPLE:



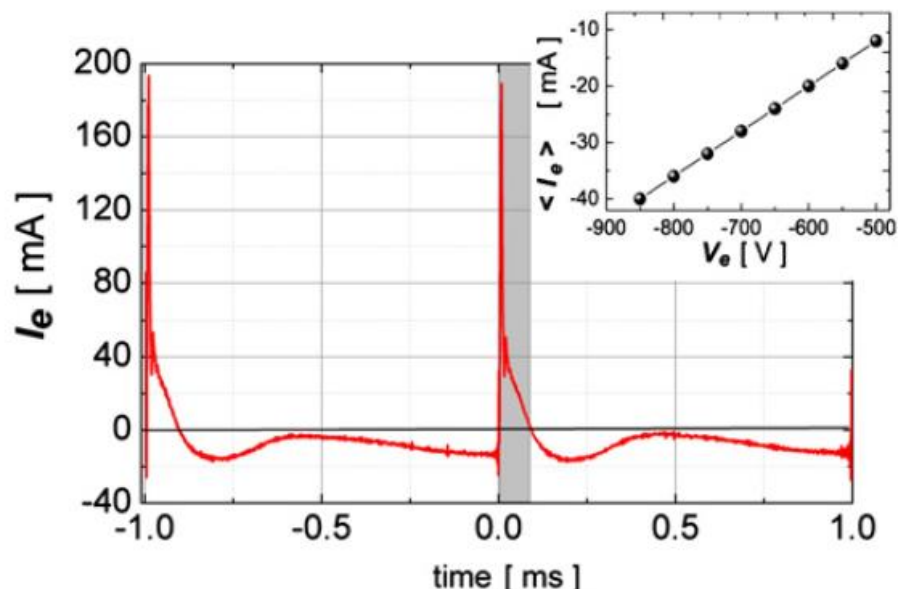
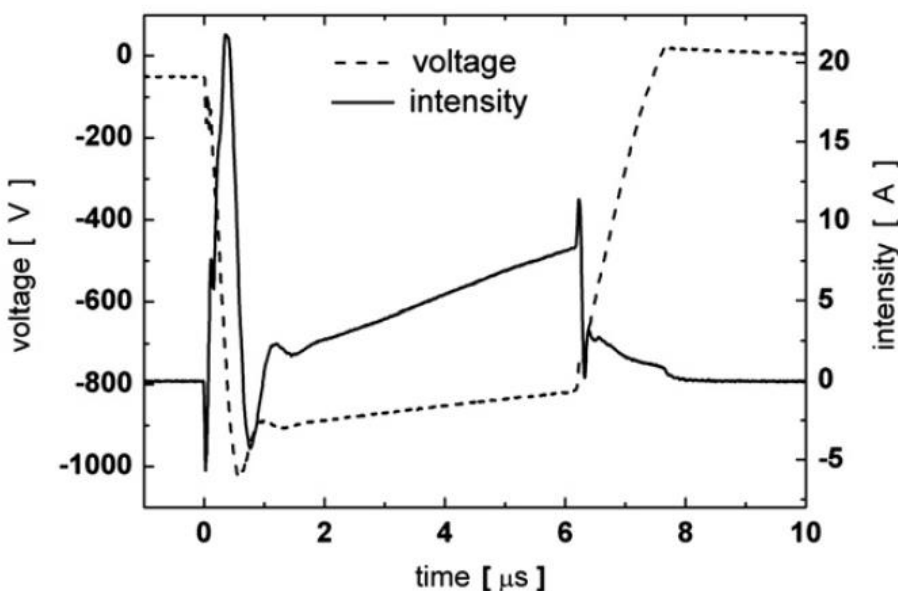
Thermionic vacuum arc (TVA): the influence of filament heating current on the arc voltage, discharge current kept constant at 200 mA; current flowing between anode and vessel walls versus arc voltage, arc current kept at 280 mA.



<https://doi.org/10.1109/DEIV.2010.5625866>



EXAMPLE:



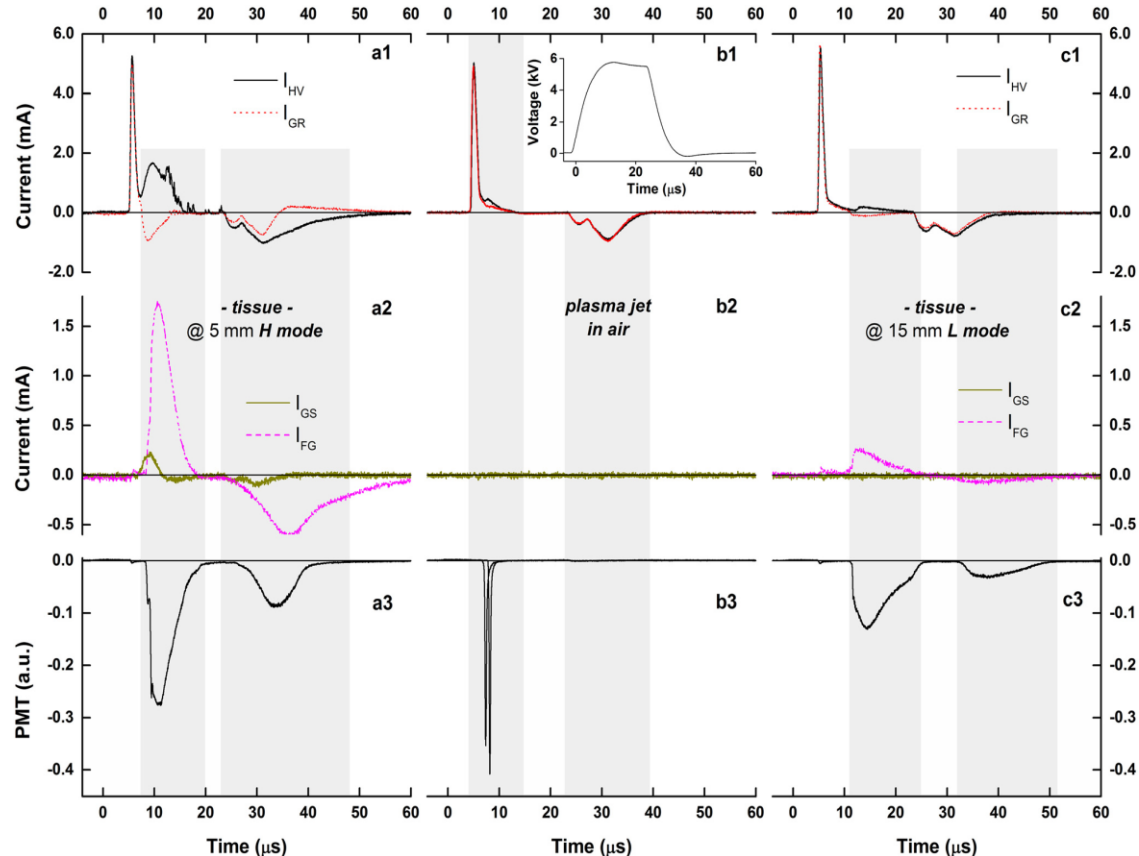
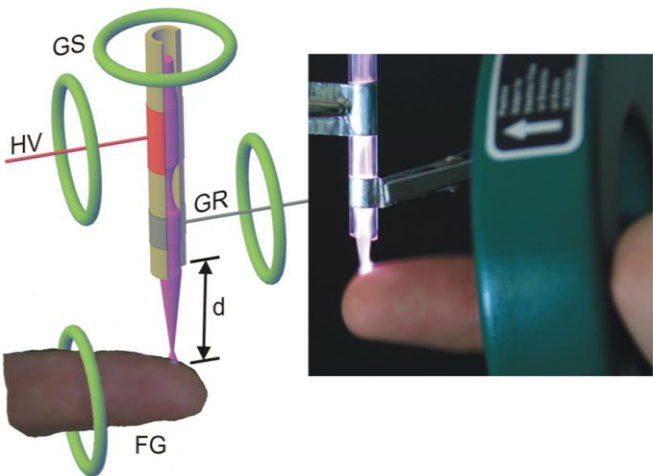
High Power Impulse Magnetron Sputtering (HIPIMS): typical variation of discharge voltage and current intensity during one discharge pulse; time variation of electrode current intensity, I_e (the inset presents the dependence of the average value of I_e on the electrode biasing potential, V_e ; the gray rectangle highlights the anode working regime of the electrode)



<http://dx.doi.org/10.1016/j.tsf.2012.02.079>



EXAMPLE:



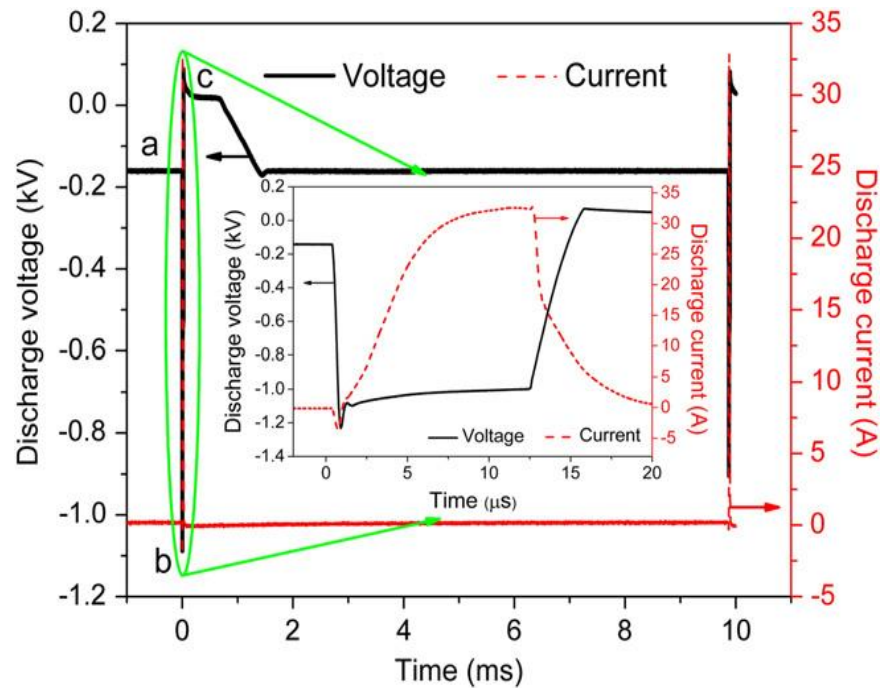
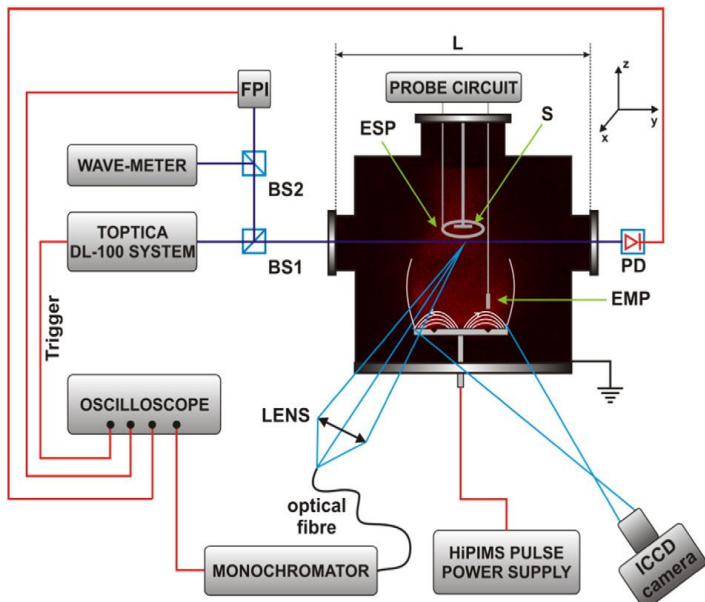
Sketch of the experimental arrangement, pointing the position of the current monitor (GS—gas, HV—high voltage, GR—ground, FG—finger). On the right side, a photography of a human finger under direct atmospheric pressure plasma jet, and the current monitor. Typical waveforms of the currents for plasma jet running in air (b column) and for the plasma jet focused on a fingertip (a and c columns); the inset shows the shape of the high voltage pulse applied on the powered electrode.



<https://dx.doi.org/10.1063/1.4804319>



EXAMPLE:



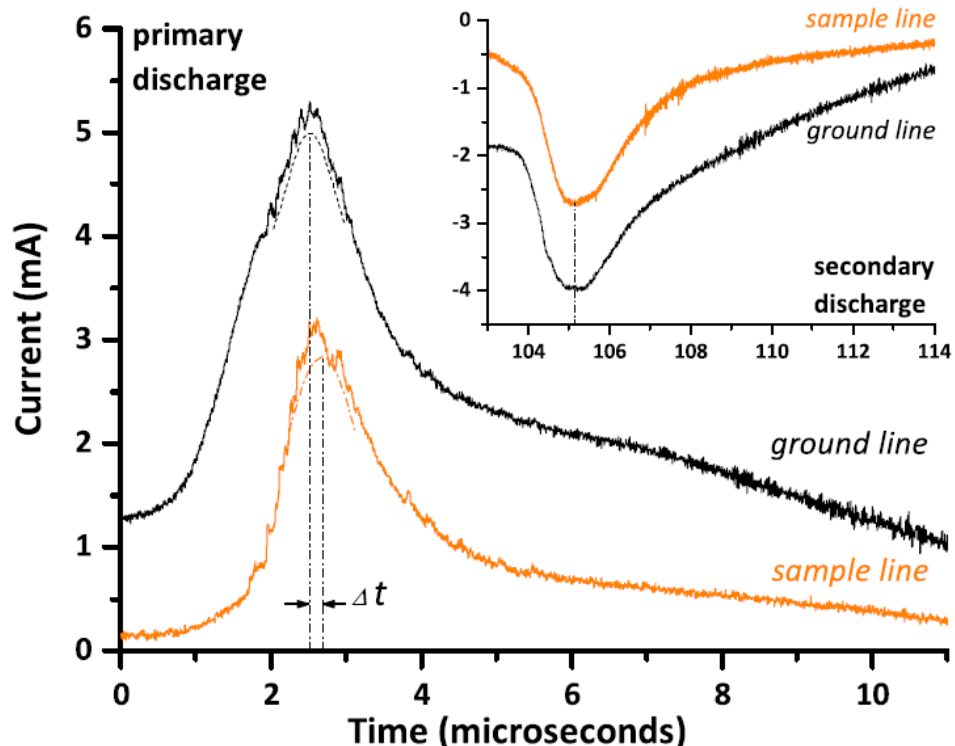
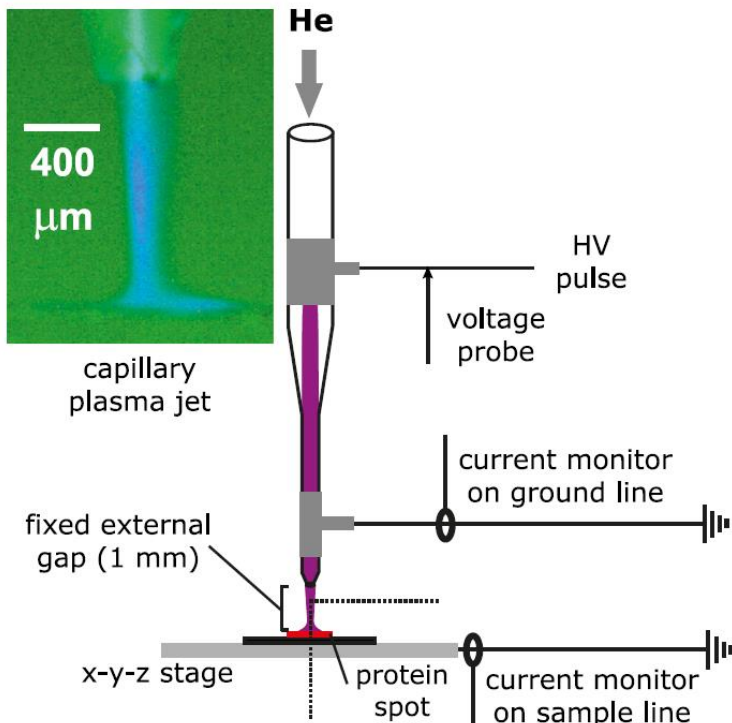
High Power Impulse Magnetron Sputtering (HIPIMS): simplified schematic of the experimental device (FPI—Fabry-Pérot interferometer, PD—photodiode, BS—beamsplitter, ESP—electrostatic probe, EMP—emissive probe, S—substrate, L—optic distance of the laser beam probing the plasma volume); typical waveforms of both the discharge current intensity and voltage during one period of the high power pulse showing all three phases: a) pre-ionization phase (constant discharge current intensity of about 8 mA); b) power pulse on-phase (12 μ s pulse duration with details in inset image); c) afterglow plasma.





EXAMPLE:

$$neVd = I / (eS) \longrightarrow 5 \times 10^{13} \text{ cm}^{-3}$$



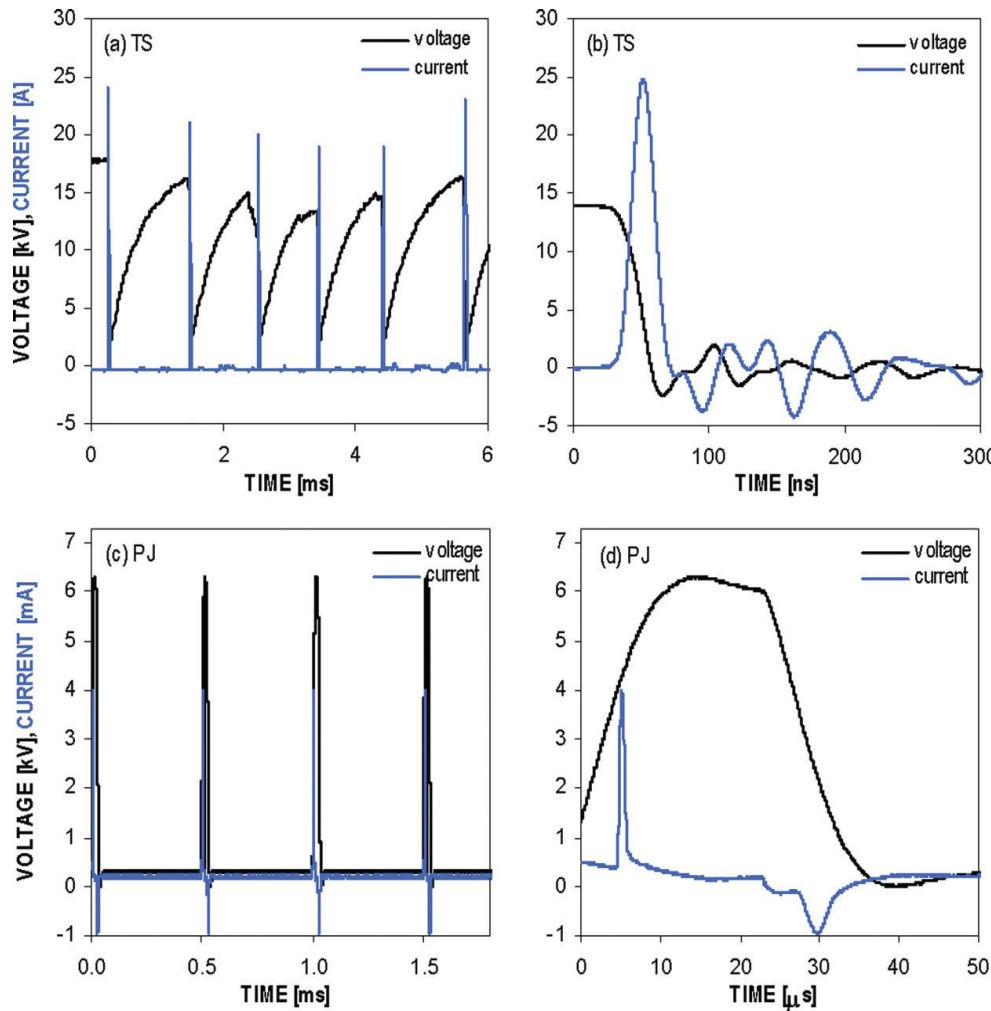
Details of the experimental arrangement used to generate and characterize the **capillary plasma jet**, in helium at atmospheric pressure. Current traces during primary and secondary (graph inset) discharges, recorded on ground line and sample line.



<https://dx.doi.org/10.1063/1.4907349>



EXAMPLE:



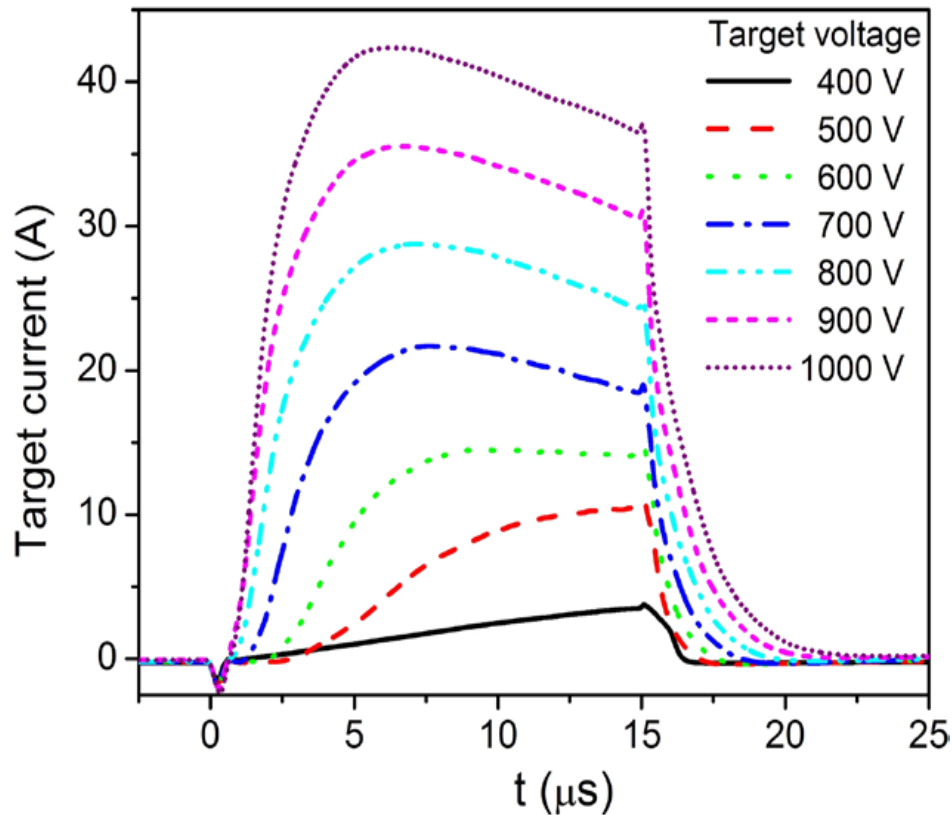
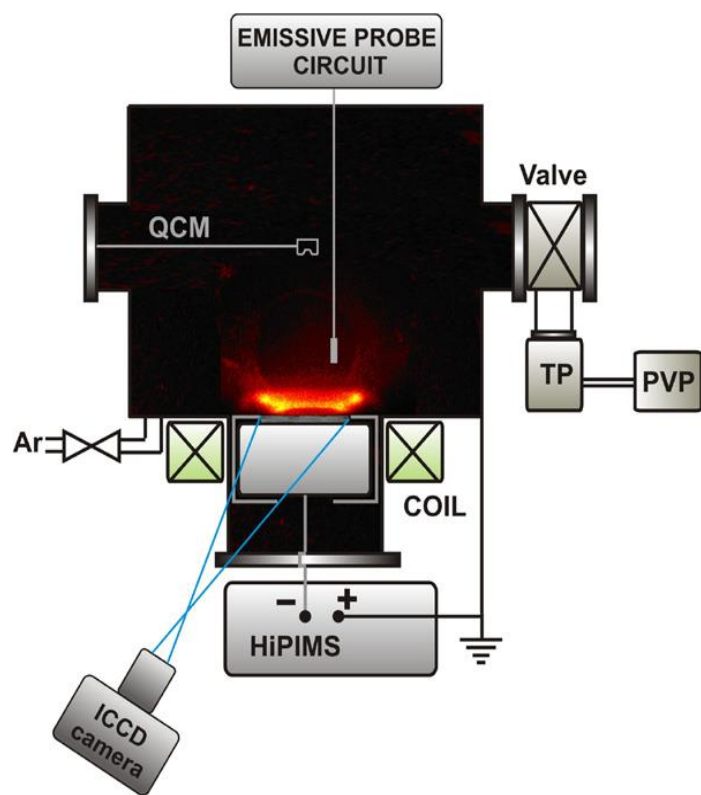
Typical current and voltage waveforms of the transient spark (TS) in air [(a) and (b)] and the pulse-driven dielectric barrier discharge plasma jet (PJ) in helium [(c) and (d)] in different time scales.



<https://dx.doi.org/10.1116/1.4919559>



EXAMPLE:



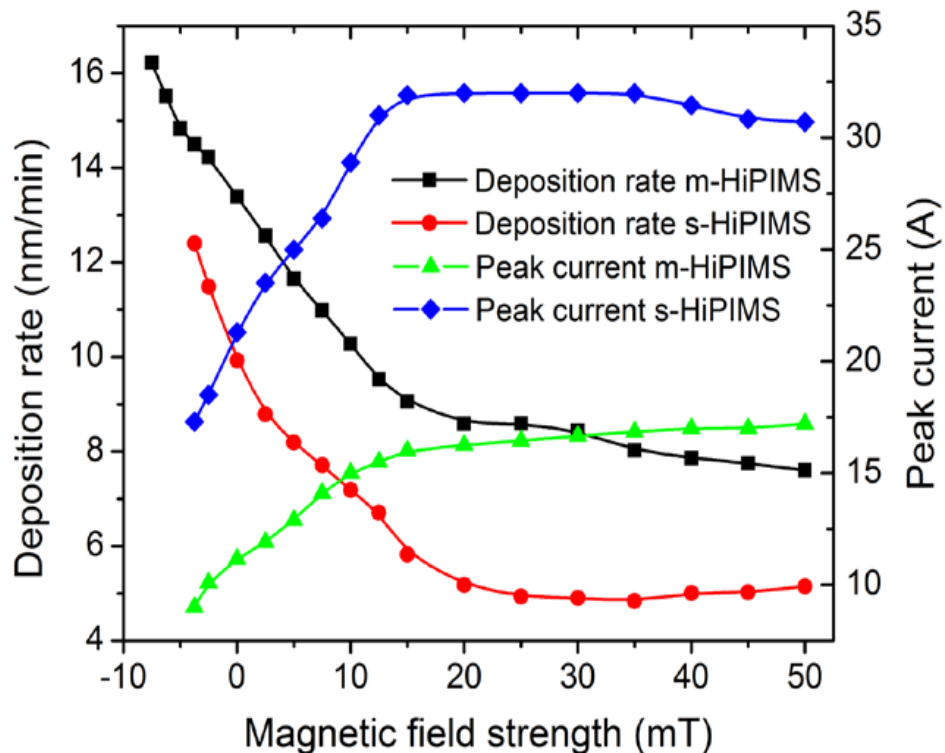
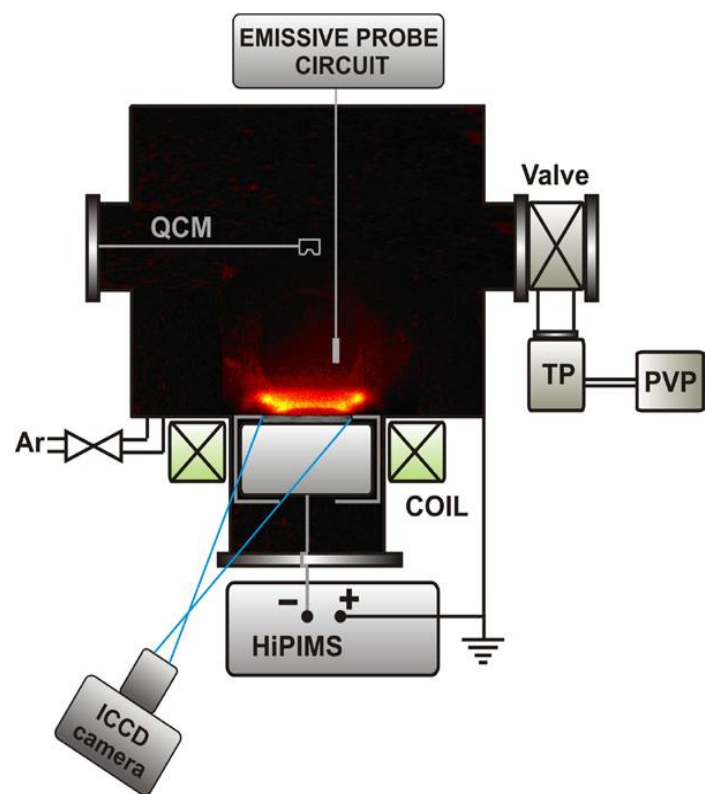
High Power Impulse Magnetron Sputtering (HiPIMS): Target current waveforms of a HiPIMS discharge operated with a pulse duration of 15 μs , working gas pressure of 1 Pa, average power of 100 W, and different cathode voltages.



<https://dx.doi.org/10.1088/0022-3727/48/49/495204>



EXAMPLE:



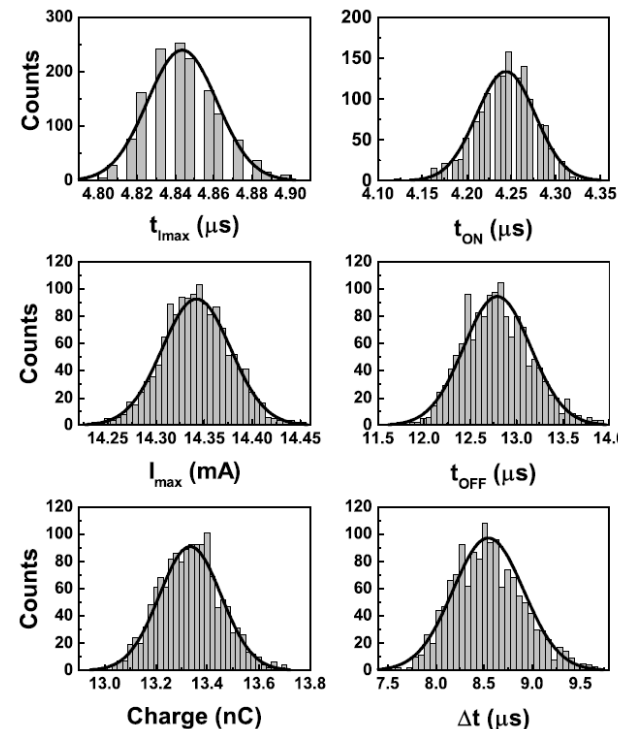
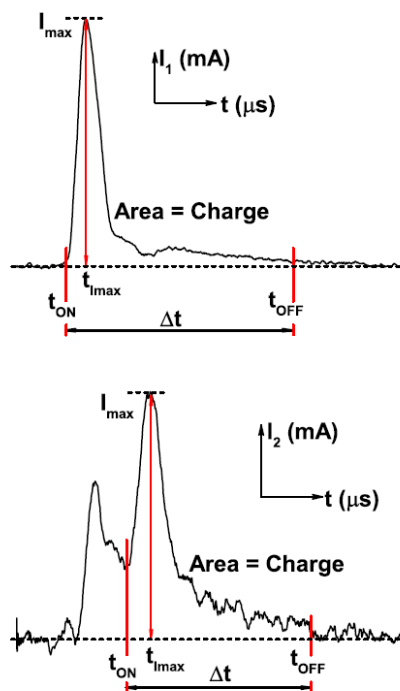
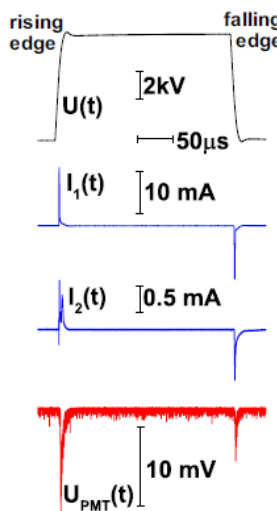
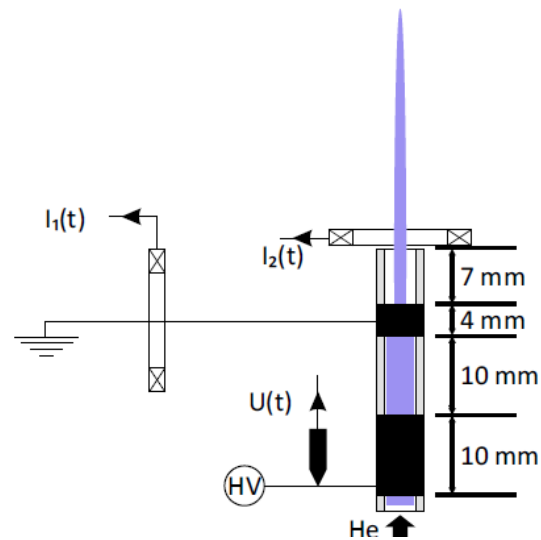
High Power Impulse Magnetron Sputtering (HiPIMS): deposition rate and peak current dependence on the external magnetic field.



<https://dx.doi.org/10.1088/0022-3727/48/49/495204>



EXAMPLE:



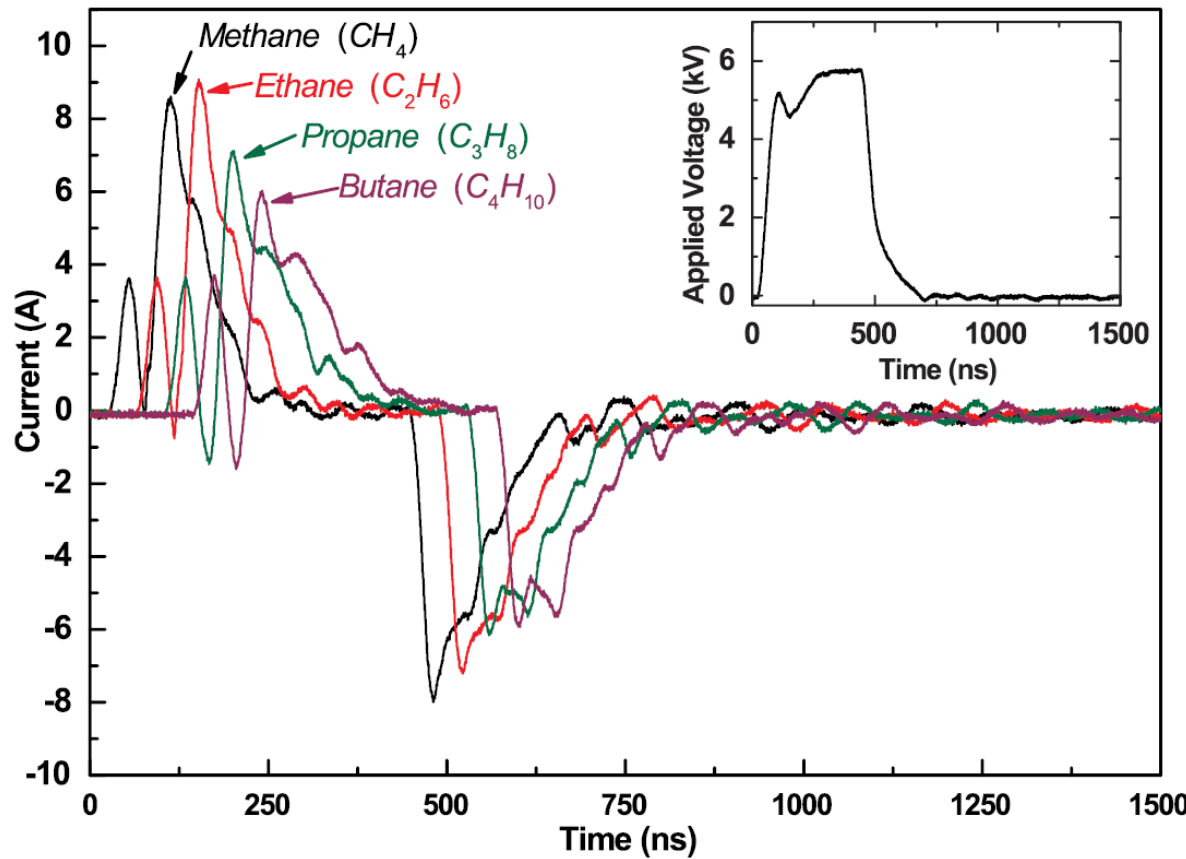
Details of estimated parameters for the currents I_1 and I_2 observed during the rising edge of the high voltage (HV) pulses (left side) for an Atmospheric Pressure Plasma Jet and typical histograms of all parameters for 1419 consecutive frames, with superimposed normal distribution curves (right side).



<https://doi.org/10.3390/app7080812>



EXAMPLE:



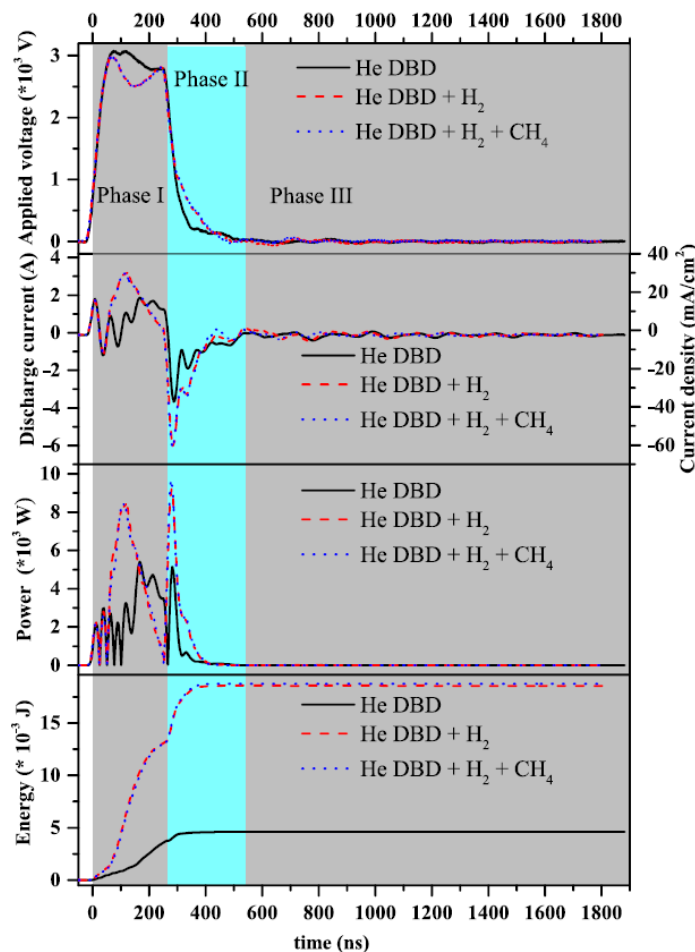
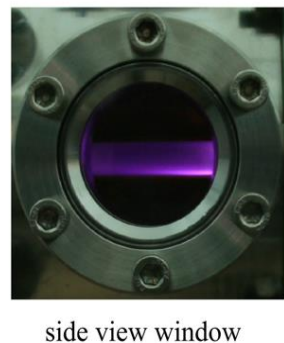
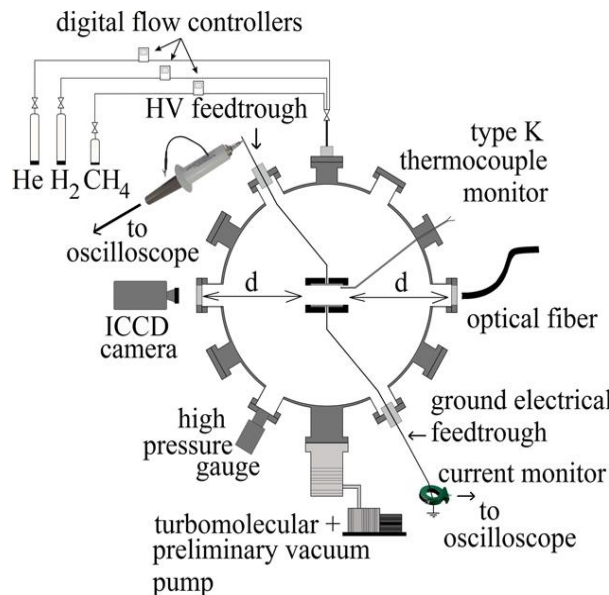
Typical current waveforms for the hydrocarbon containing high power impulse DBD for the synthesis of carbon-based materials.



<https://doi.org/10.1093/mnras/sty2497>



EXAMPLE:



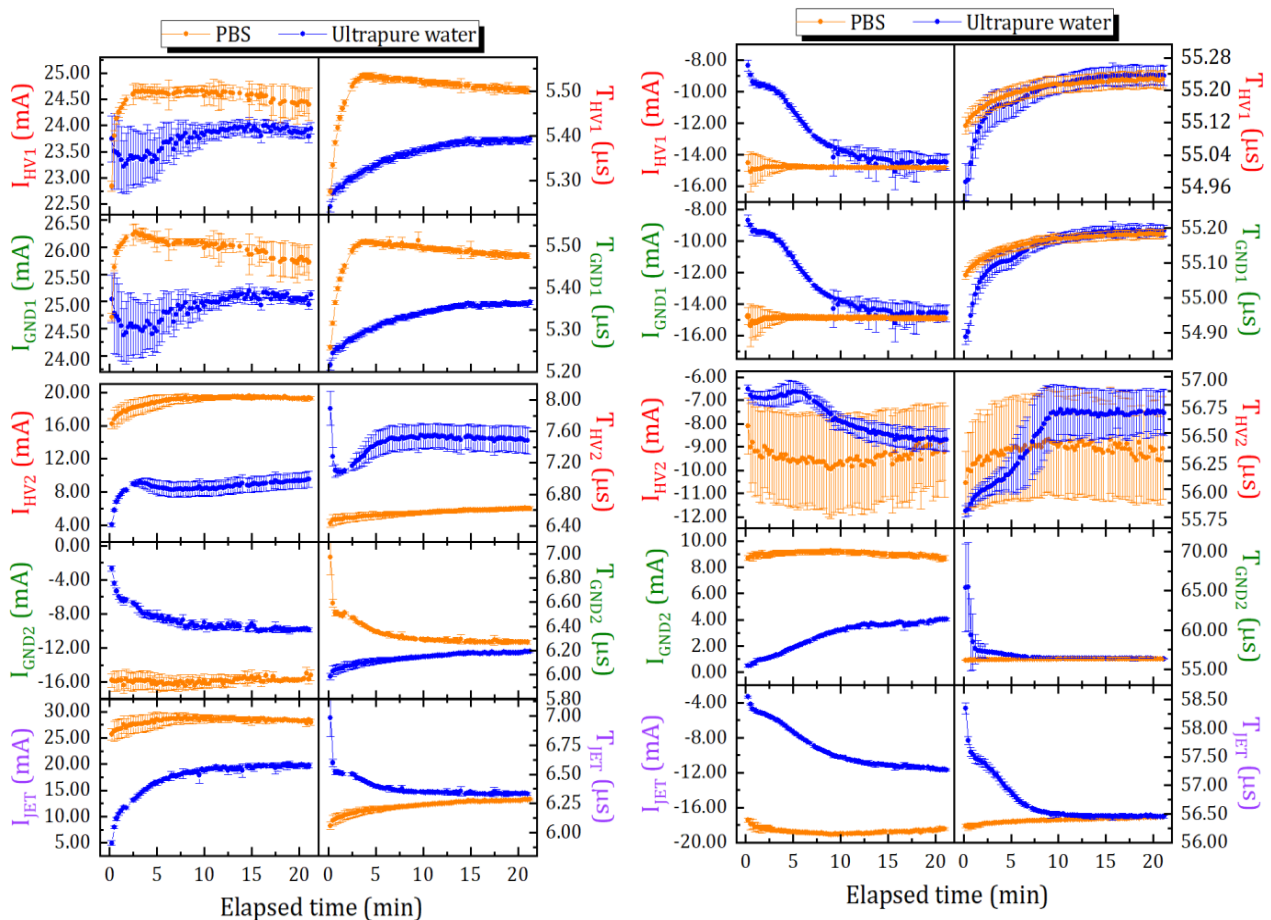
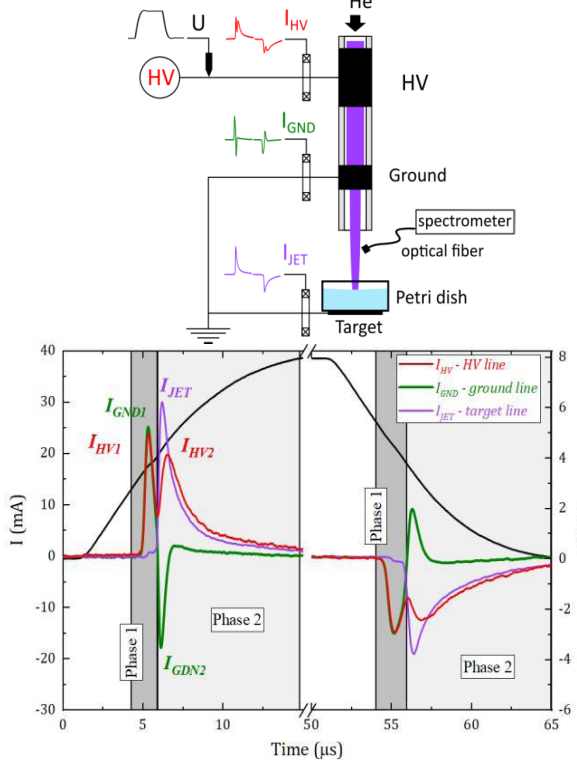
DBD plasma, in helium/helium-hydrogen/helium-hydrogen-methane gas mixture: typical voltage-current traces during primary and secondary discharges, current density, mean power, and energy for He-DBD and He-DBD with admixture of H₂, respectively, H₂-CH₄.



<https://doi.org/10.1063/1.5017097>



EXAMPLE:

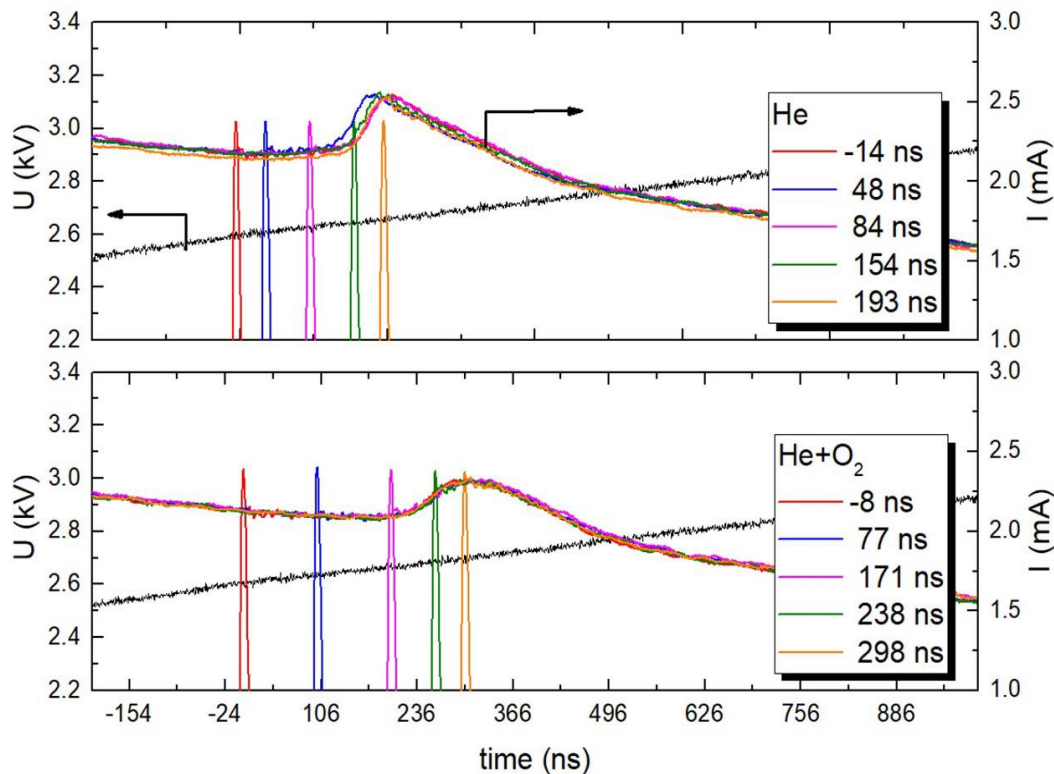
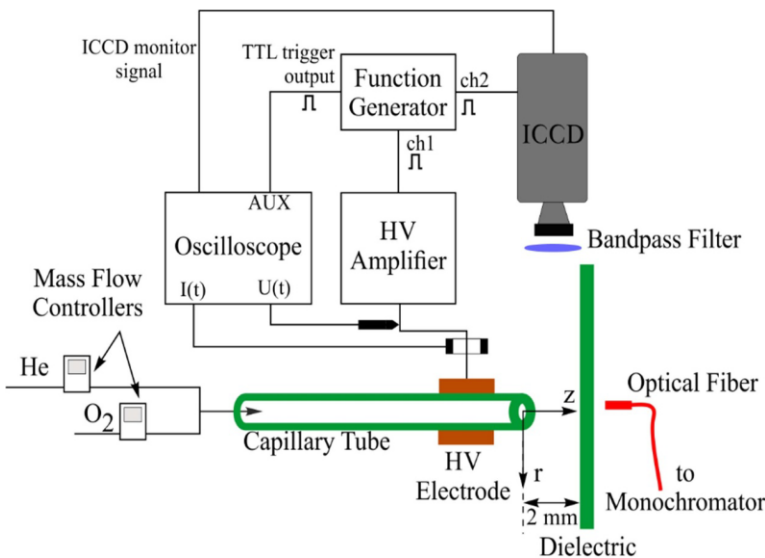


Typical current traces acquired during the rising and falling edges of the HV pulses ($I_{HV} = I_{GND} + I_{JET}$). Influence of elapsed time on peak currents and corresponding times for both PBS and ultrapure water during the rising edge and the falling edge of the HV pulse. Dots represent the mean value of all parameters, while the error bars represent the standard deviation (SD) of normal distributions.





EXAMPLE:



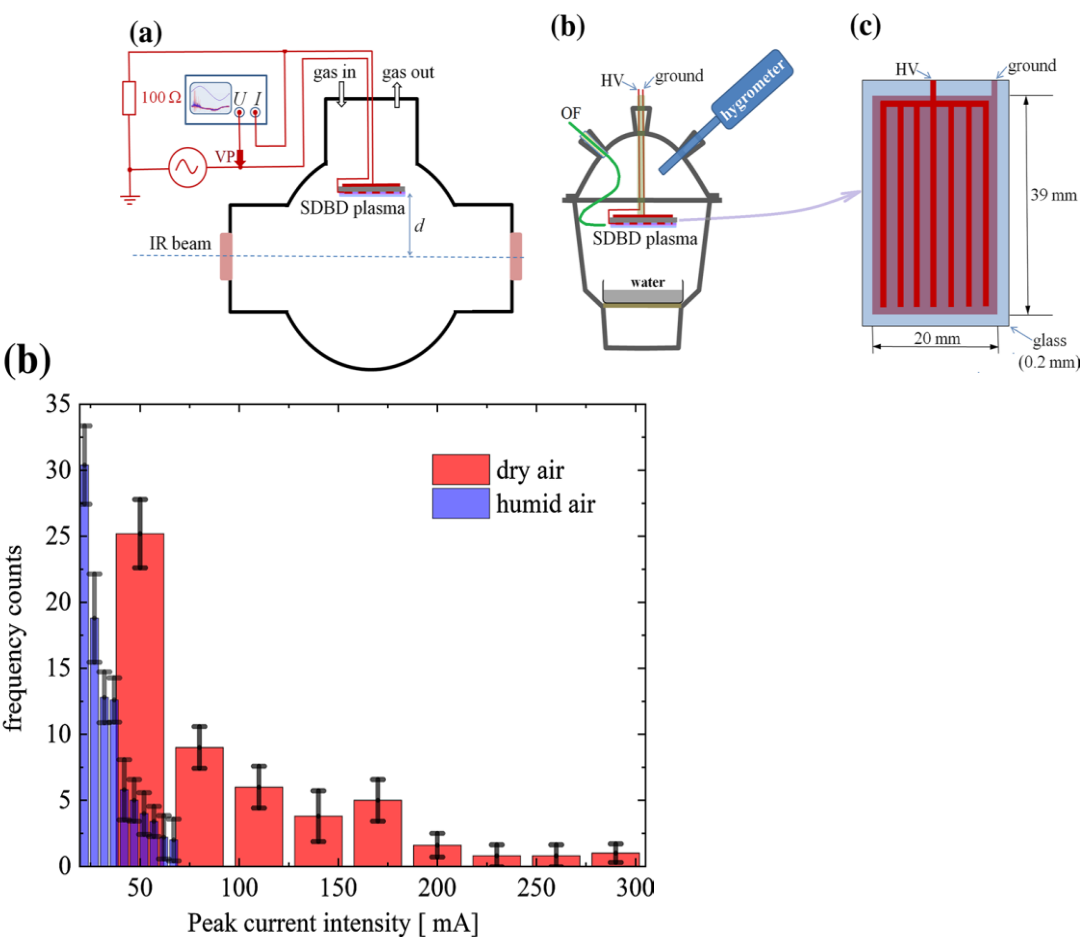
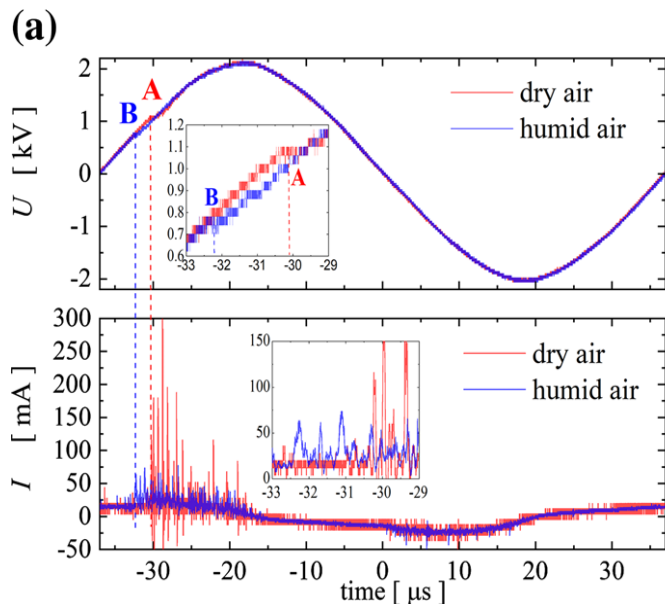
Experimental arrangement for studying He with O₂ admixtures plasma jets. Applied voltage and total current traces for He and He + O₂ (1000 ppm) plasma jets. Camera monitor signals are also included.



<https://doi.org/10.1088/1361-6463/acb1c1>



EXAMPLE:

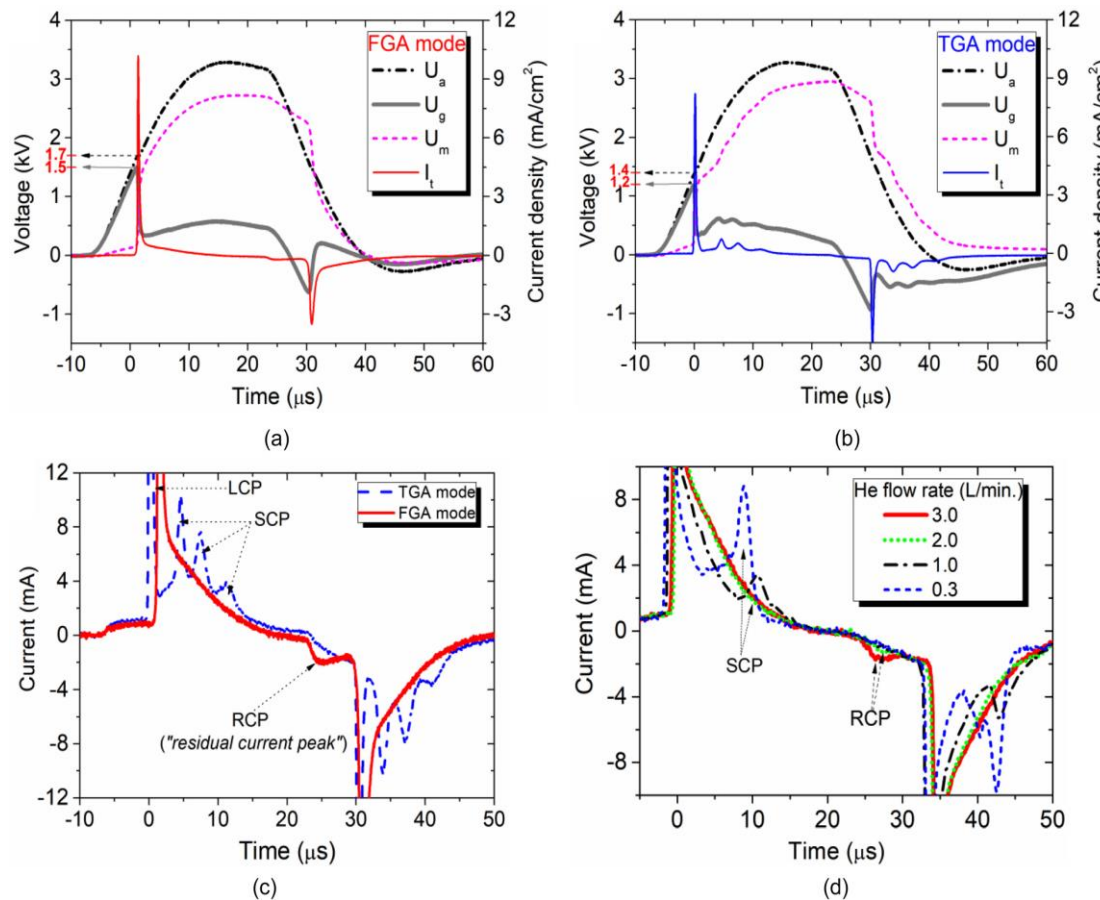


- a Time dependence of voltage and current intensity for SDBD working in dry and humid air, respectively. A and B indicate the onset of positive discharge for SDBD working in dry and humid air, respectively.
- b Histograms of peak values of intensity spikes occurring during five positive discharges for SDBD working in dry and humid air





EXAMPLE:



Typical applied voltage (U_a), gap voltage (U_g), memory voltage (U_m), and total discharge current (I_t) waveforms for He-DBD working in (a) FGA mode—with a flow rate of 3 L/min and (b) TGA mode—without gas flow, at atmospheric pressure, after pumped down to 10^{-1} Torr. Enlarge view of the current to emphasize the presence of the “residual current peak” (RCP) in FGA mode only (c) at different He flow rates (d).



<https://doi.org/10.1063/5.0043349>

Electrical diagnosis: probes



UNIVERSITATEA "ALEXANDRU IOAN CUZA" din IAŞI

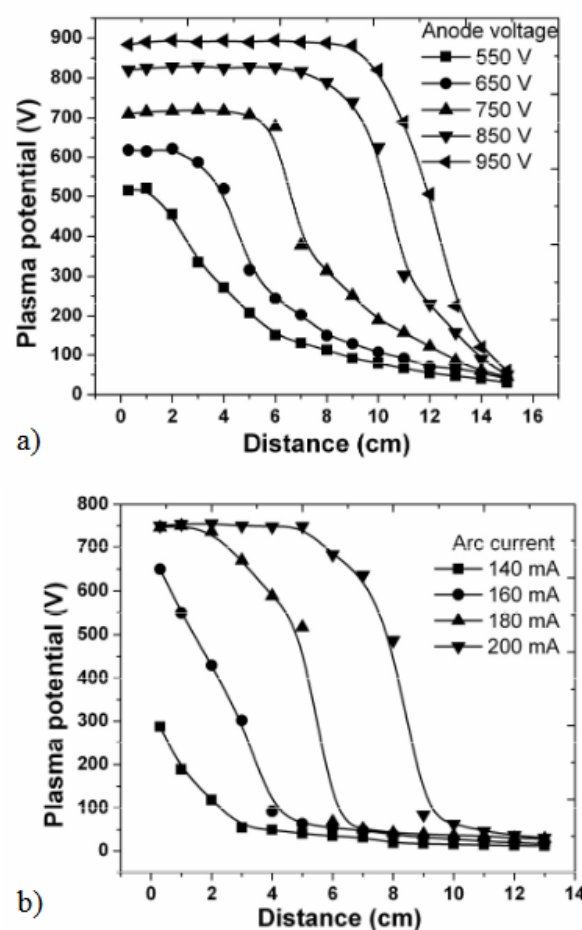
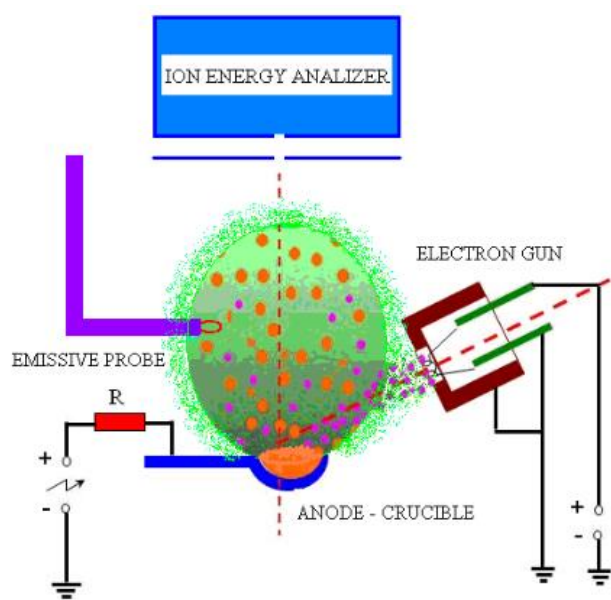
www.uaic.ro

Equipment and materials:

- probes
- electrostatic analysers
- power supply



EXAMPLE:



Thermionic vacuum arc (TVA): axial distribution of plasma potential for a constant arc current and different arc voltage values, arc current was kept constant at 180 mA (a), and for different values of arc current, arc voltage =820 V (b).

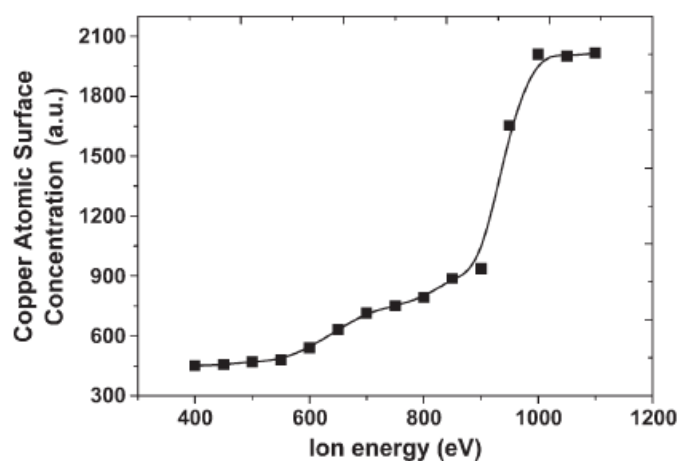
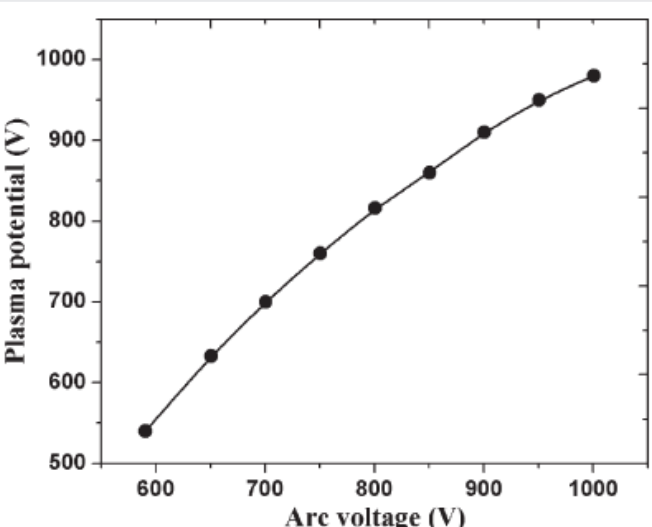
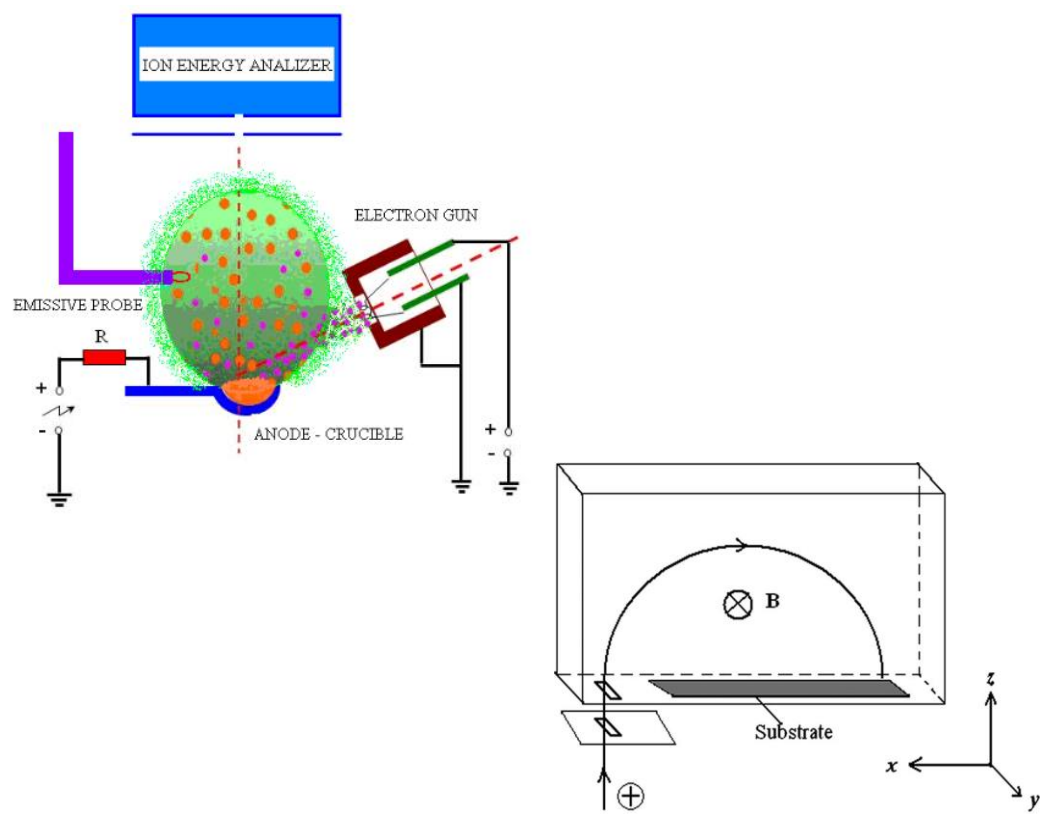


<https://doi.org/10.1109/DEIV.2010.5625866>

https://rjp.nipne.ro/2011_56_Suppl/RomJPhys.56s.p41.pdf



EXAMPLE:

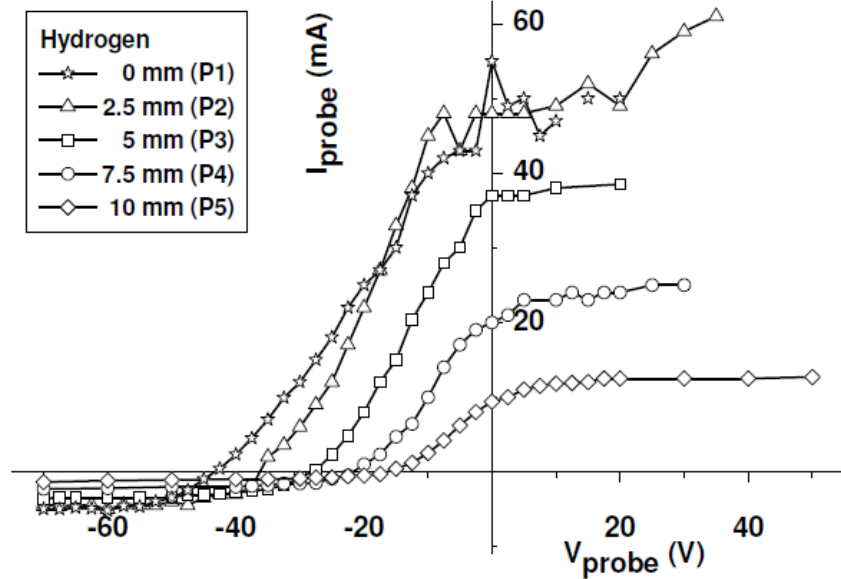
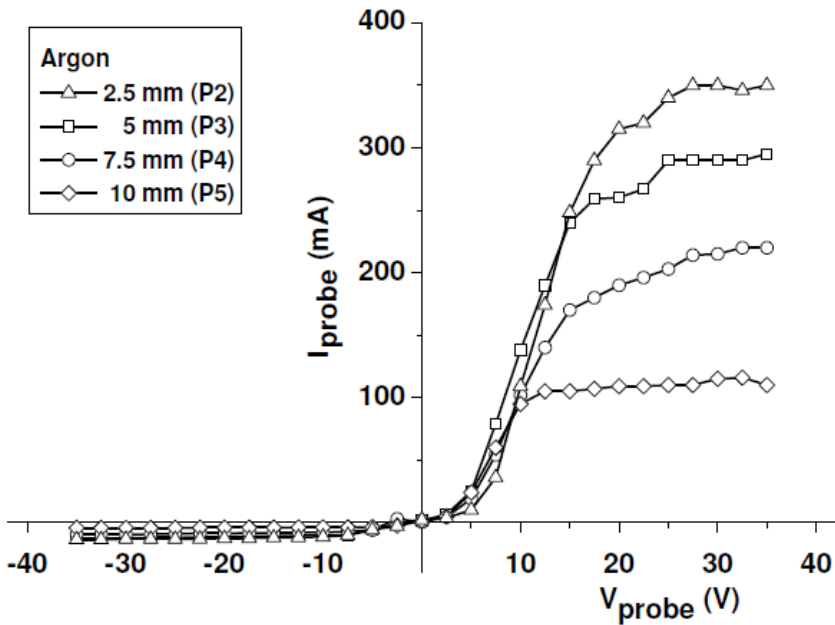


Thermionic vacuum arc (TVA): plasma potential measured at a fixed position (3 cm from the anode and inside the fireball) versus arc voltage; copper atomic surface concentration versus ion energy.





EXAMPLE:



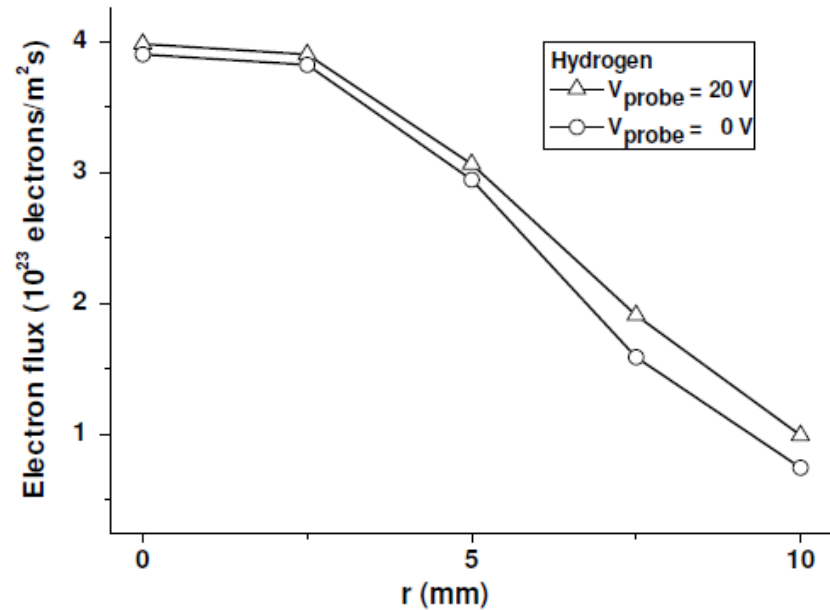
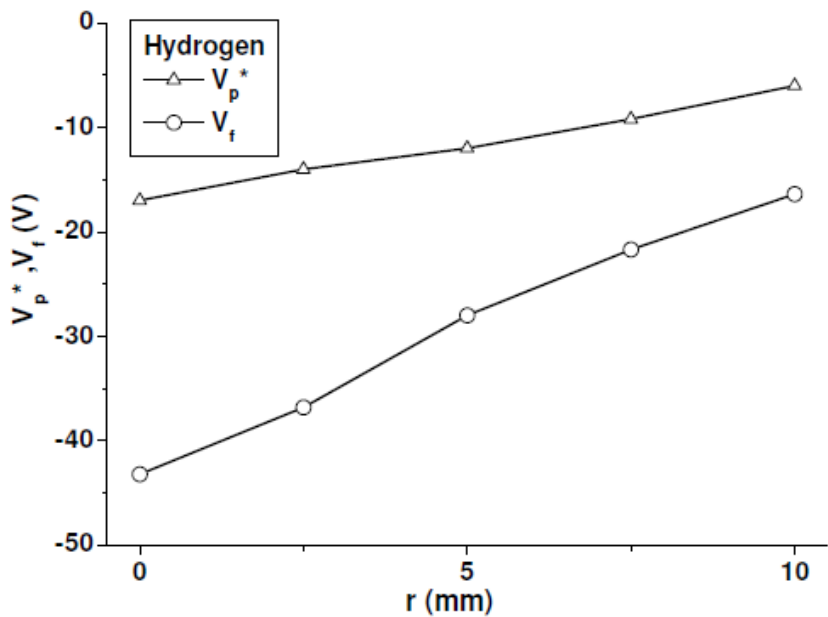
Pilot-PSI device, multi-channel analyzer used for edge plasma diagnosis: probe current-voltage characteristics measured in Ar and H_2 plasma at different radial positions.



<https://doi.org/10.1002/ctpp.201010152>



EXAMPLE:



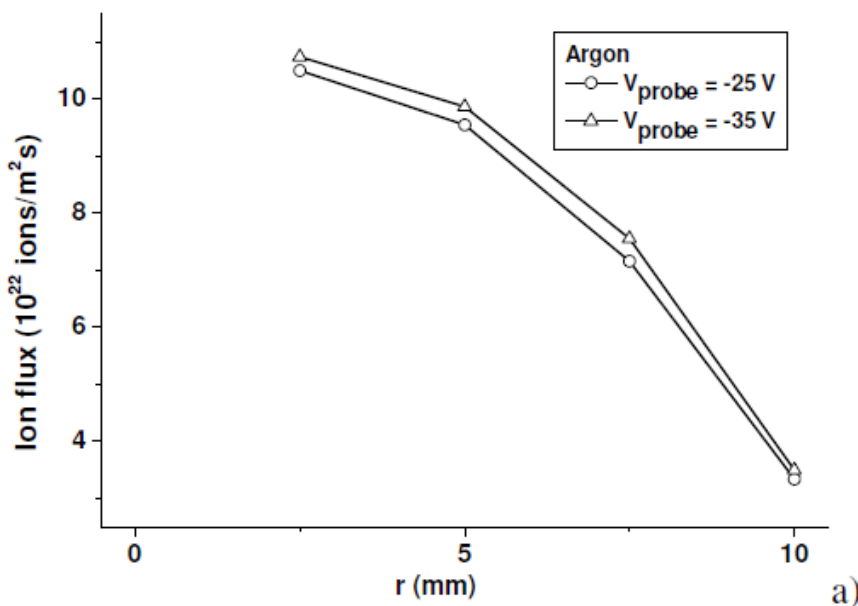
Pilot-PSI device, multi-channel analyzer used for edge plasma diagnosis: radial distribution of the floating (V_f) and "plasma potential" (V_p^*) in hydrogen plasma; radial profile of the electron flux at the target surface in hydrogen plasma, for two different target bias (0 and +20 V).



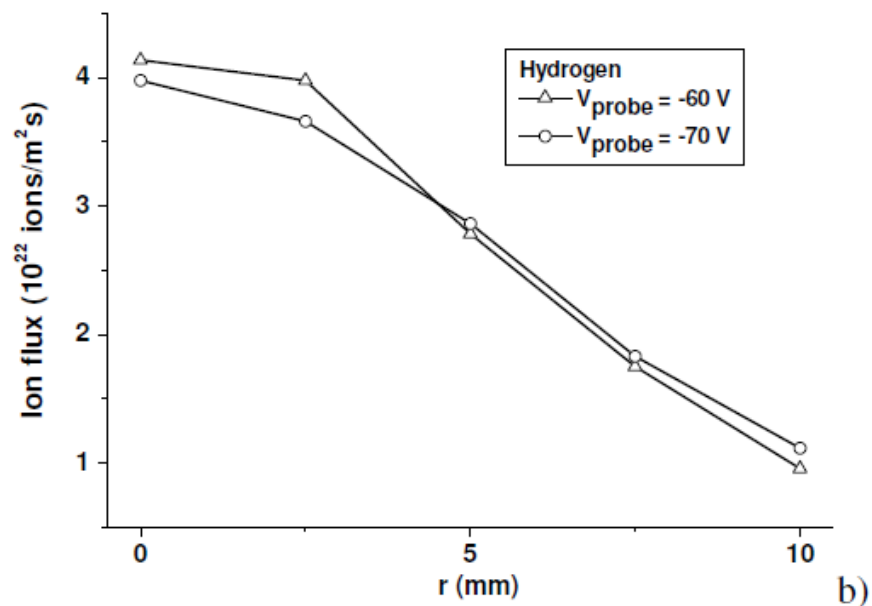
<https://doi.org/10.1002/ctpp.201010152>



EXAMPLE:



a)



b)

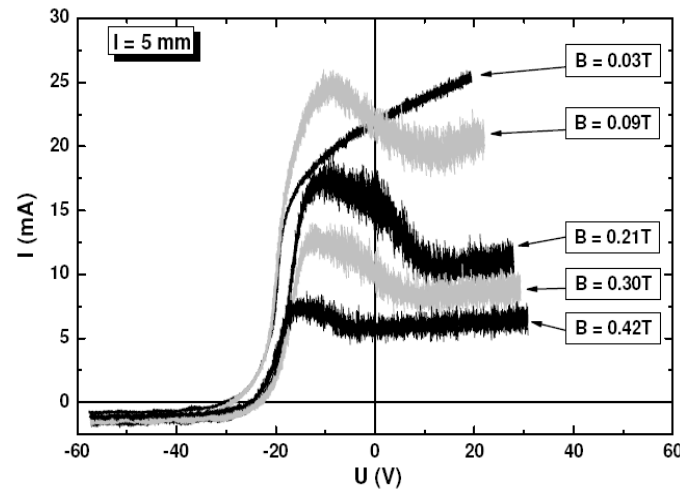
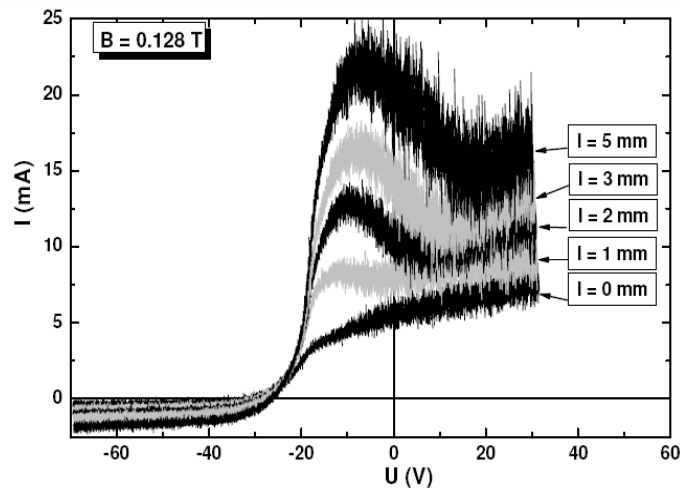
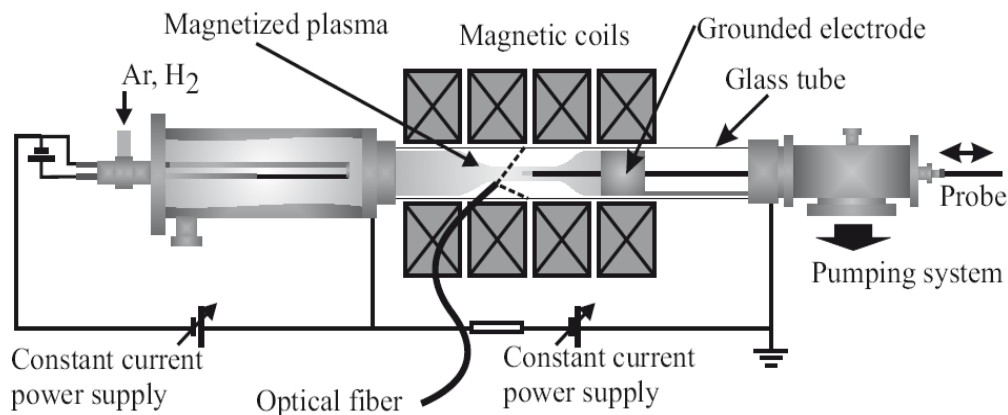
Pilot-PSI device, multi-channel analyzer used for edge plasma diagnosis: radial profile of argon (a) and hydrogen (b) ion flux at the target surface.



<https://doi.org/10.1002/ctpp.201010152>



EXAMPLE:

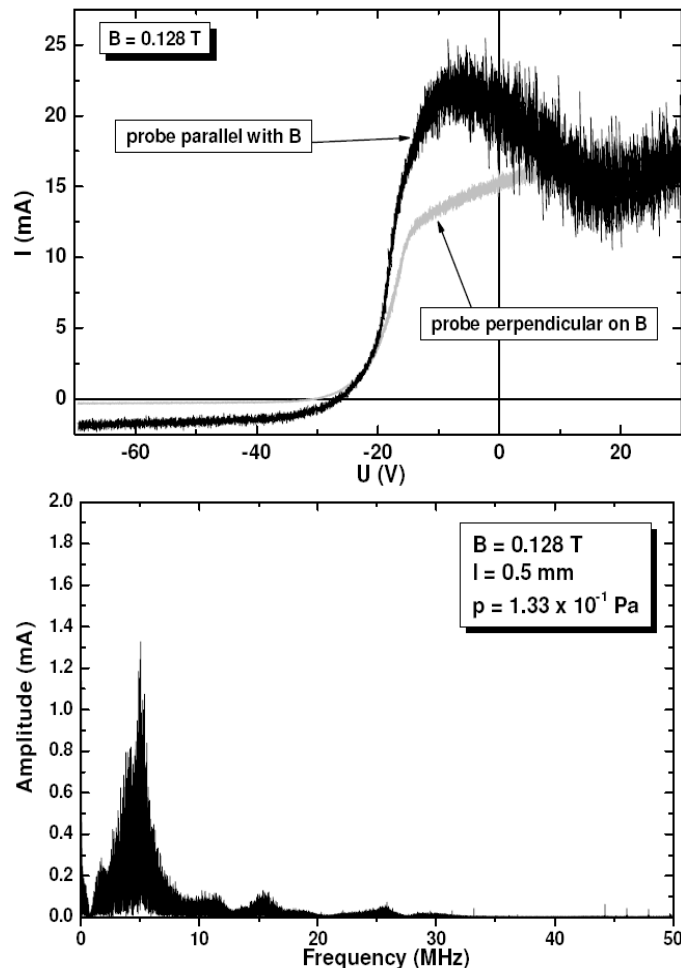
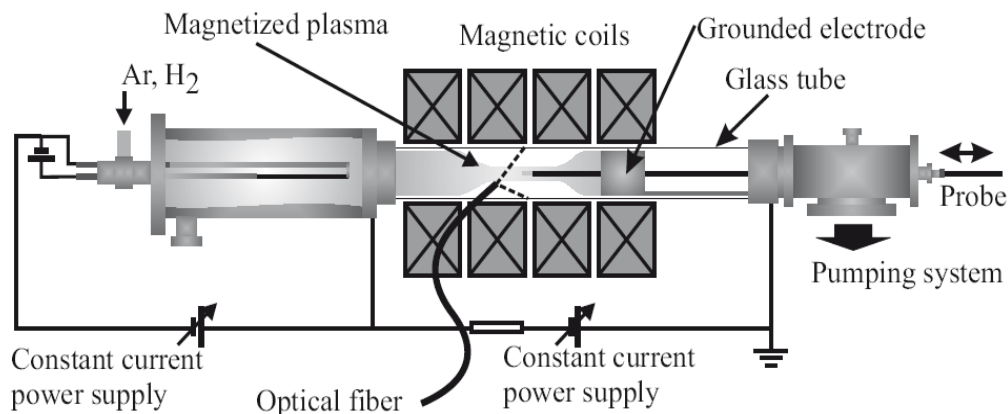


Magnetized plasma: probe I-V characteristics with negative slope obtained in argon magnetized plasma column (a) $B = 0.128 \text{ T}$ and probe length as parameter and (b) $l = 5 \text{ mm}$ and magnetic field strength as parameter, respectively, $p = 1.33 \times 10^{-1} \text{ Pa}$, probe diameter of 0.5 mm.





EXAMPLE:



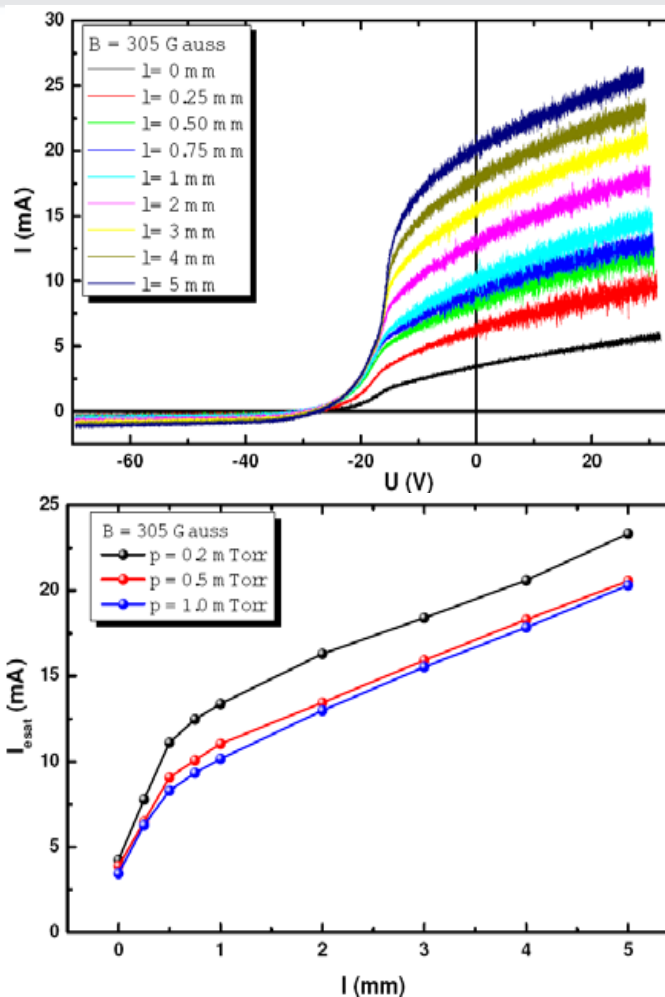
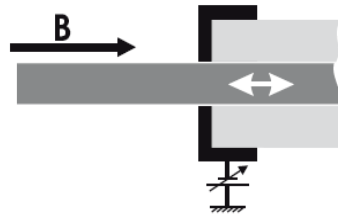
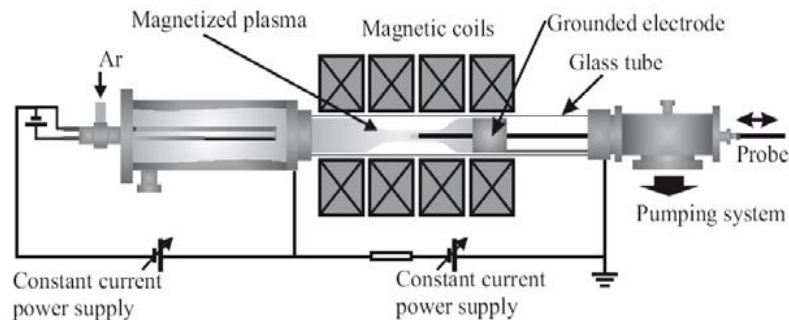
Magnetized plasma: probe I-V characteristics with negative slope obtained in argon magnetized plasma column (a) $B = 0.128 \text{ T}$ and probe length as parameter and (b) $l = 5 \text{ mm}$ and magnetic field strength as parameter, respectively, $p = 1.33 \times 10^{-1} \text{ Pa}$, probe diameter of 0.5 mm .



<https://doi.org/10.1002/ctpp.201310017>



EXAMPLE:

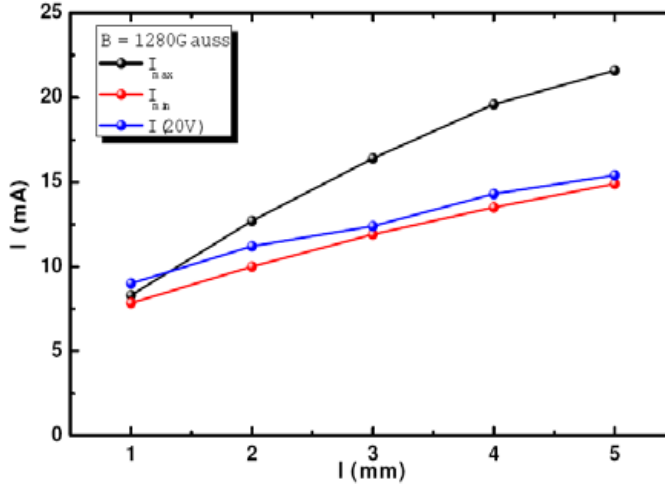
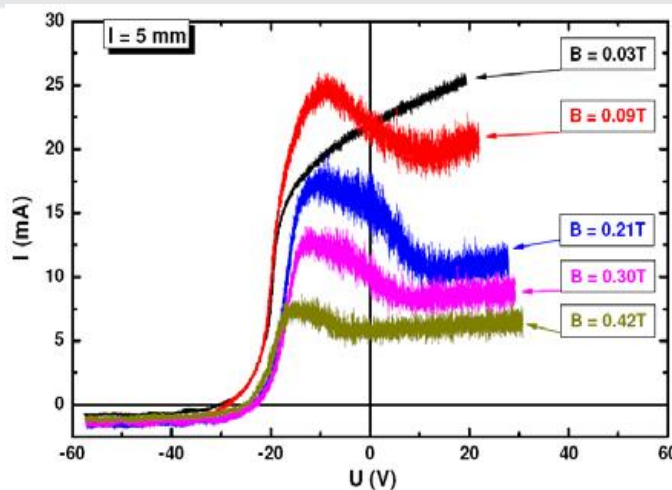
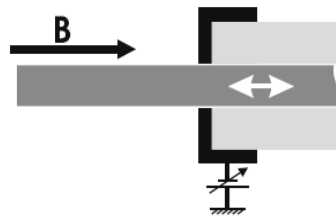
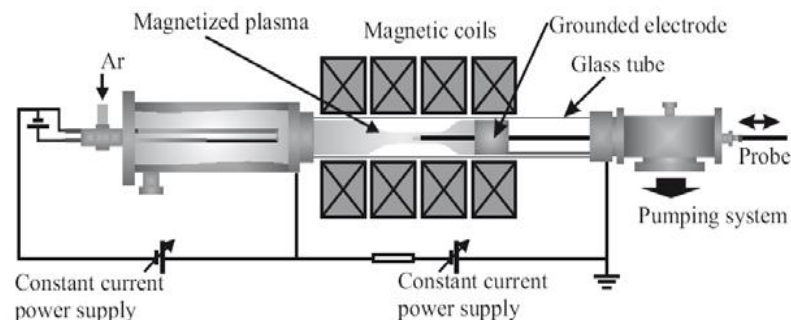


Magnetized plasma and cylindrical probe with stainless steel guard ring system: cylindrical probe characteristics at $p = 1$ mTorr argon plasma for various probe length and constant magnetic field strength ($B = 305$ Gauss) and b) electron saturation current versus cylindrical probe length at $B = 305$ Gauss, fixed probe bias (+20 V) and various argon pressure.





EXAMPLE:

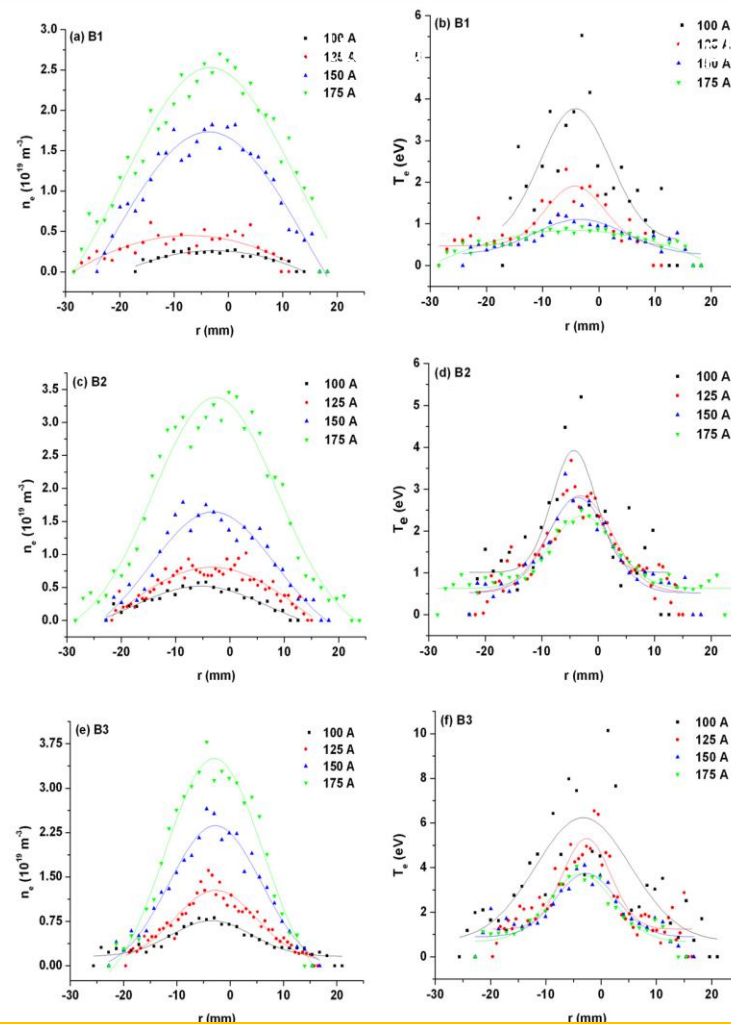
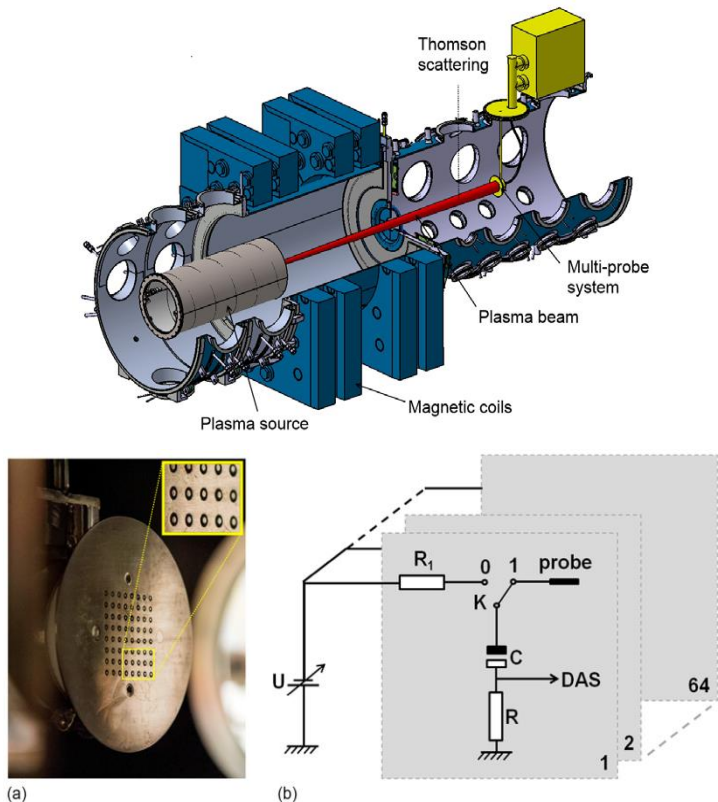


Magnetized plasma and cylindrical probe with stainless steel guard ring system: cylindrical probe characteristics at $p = 1 \text{ mTorr}$ argon plasma for various probe length and constant magnetic field strength ($B = 305 \text{ Gauss}$) and b) electron saturation current versus cylindrical probe length at $B = 305 \text{ Gauss}$, fixed probe bias (+20 V) and various argon pressure.





EXAMPLE:

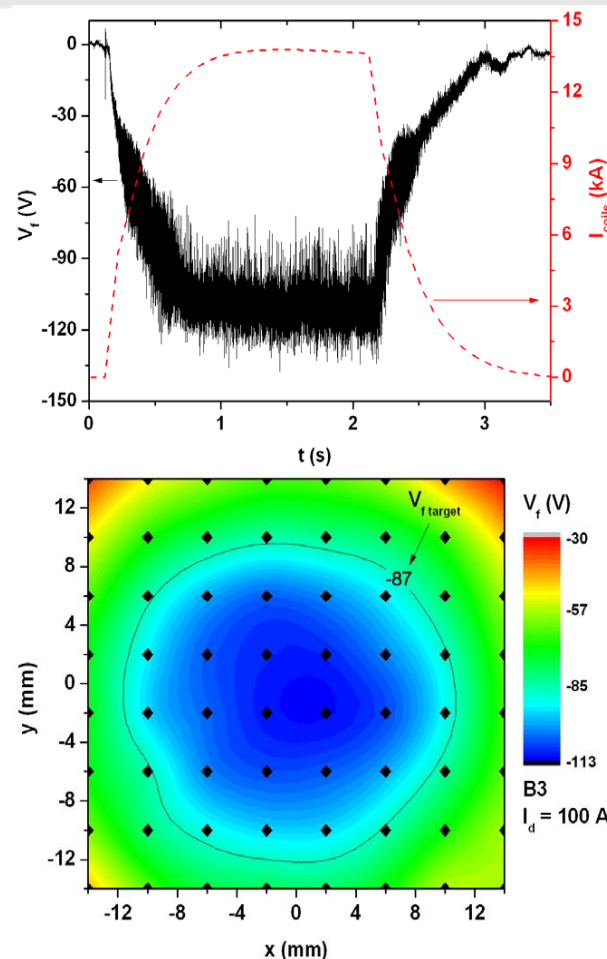
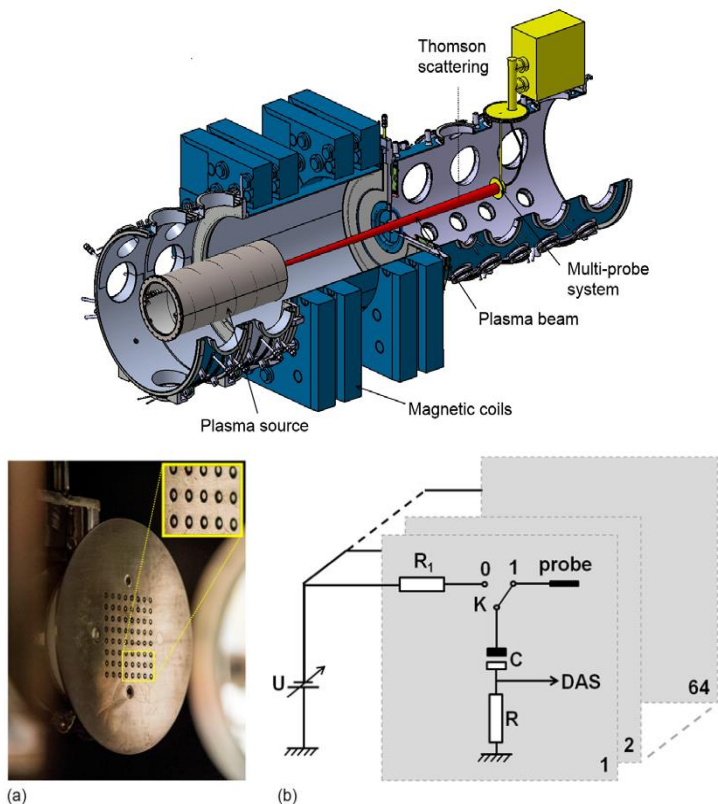


Magnum-PSI and the multi-probe system used as the target in Magnum-PSI: radial distribution of electron density and temperature obtained from TS measurements. For each graph, the magnetic field strength is constant and the discharge current varies from 100 to 175 A.





EXAMPLE:

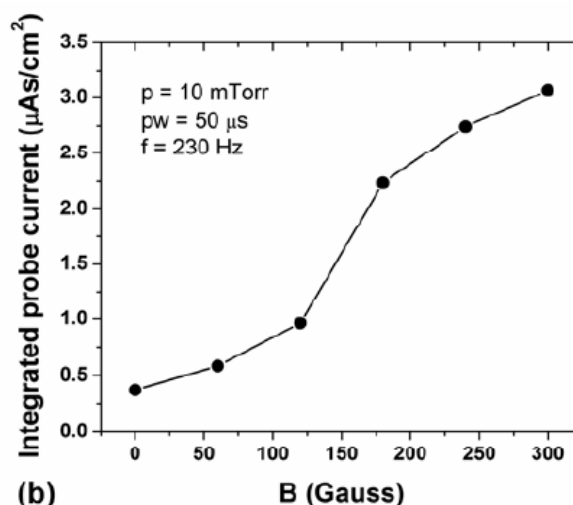
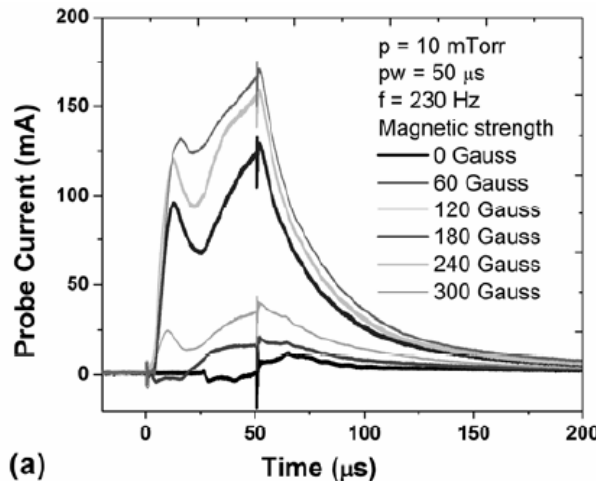
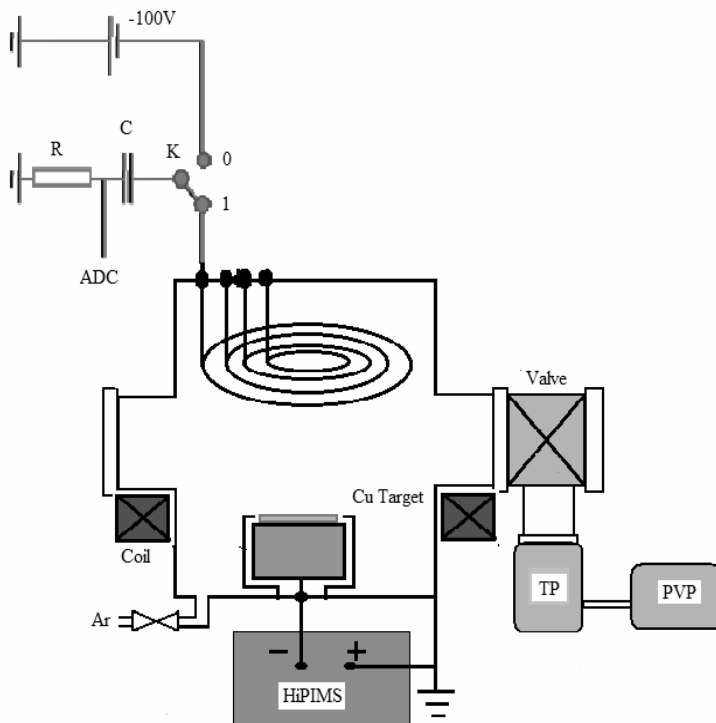


Magnum-PSI and the multi-probe system used as the target in Magnum-PSI: example of temporal evolution of the local floating potential measured with a central probe ($I_d = 100$ A, B3) (the current through the magnetic coils is also illustrated); example of a 2D distribution of the local floating potential measured with the multi-probe system ($I_d = 100$ A, B3, V_f target = -87 V).





EXAMPLE:

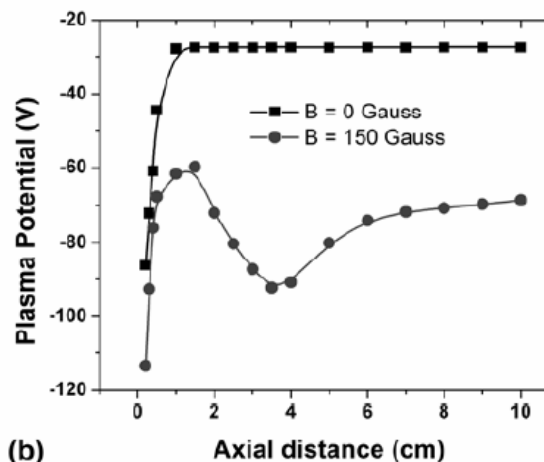
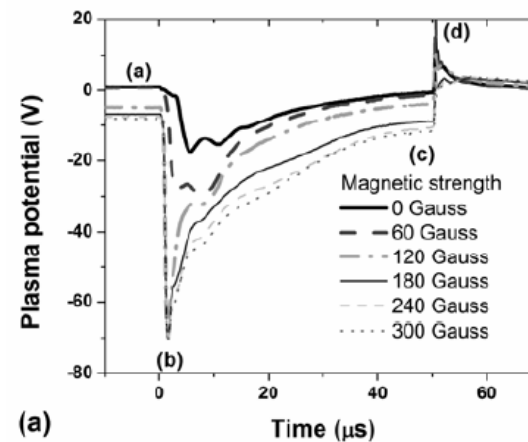
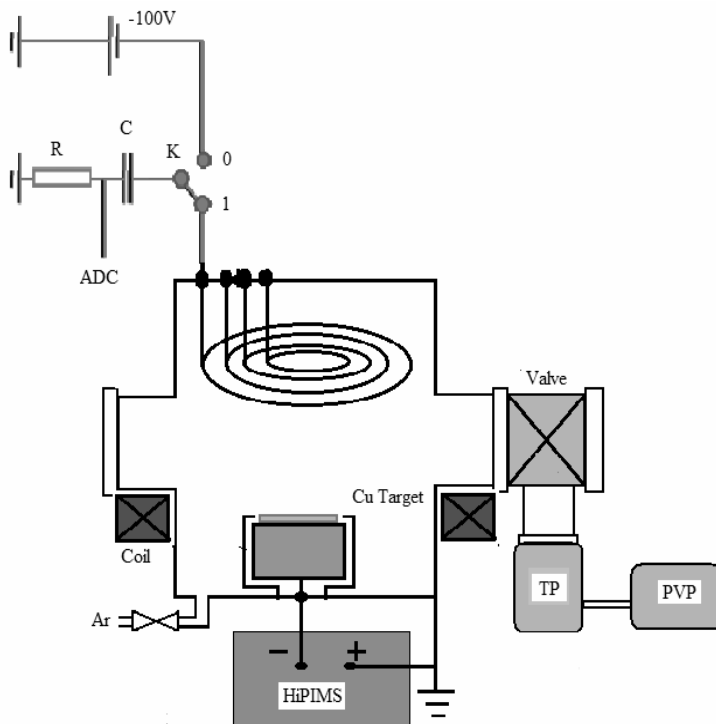


High Power Impulse Magnetron Sputtering (HIPIMS): Temporal evolution of the probe current (a) and integrated probe current vs. magnetic field strength (b).





EXAMPLE:

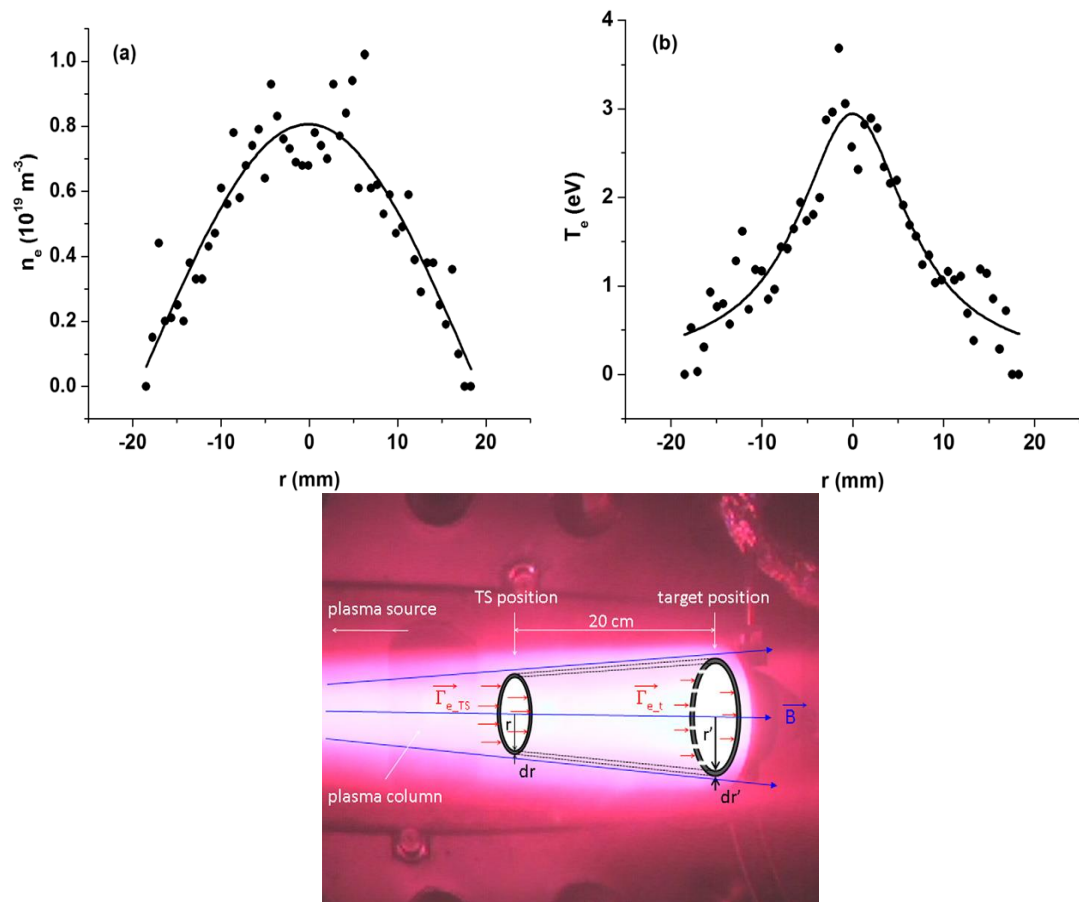
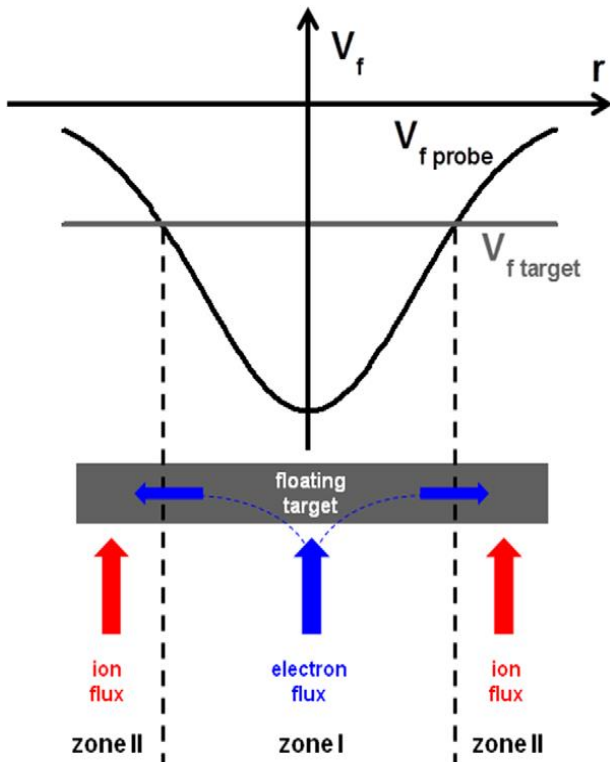


High Power Impulse Magnetron Sputtering (HIPIMS): temporal evolution of plasma potential vs. magnetic field strength (a) and axial distribution (b) of plasma potential for $B = 0$ Gauss and $B = 150$ Gauss.





EXAMPLE:

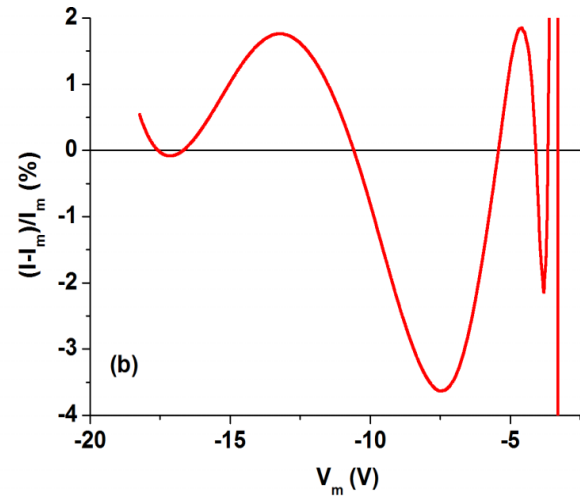
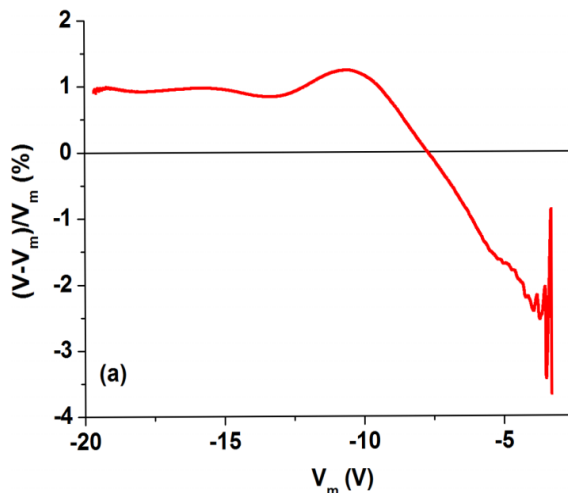
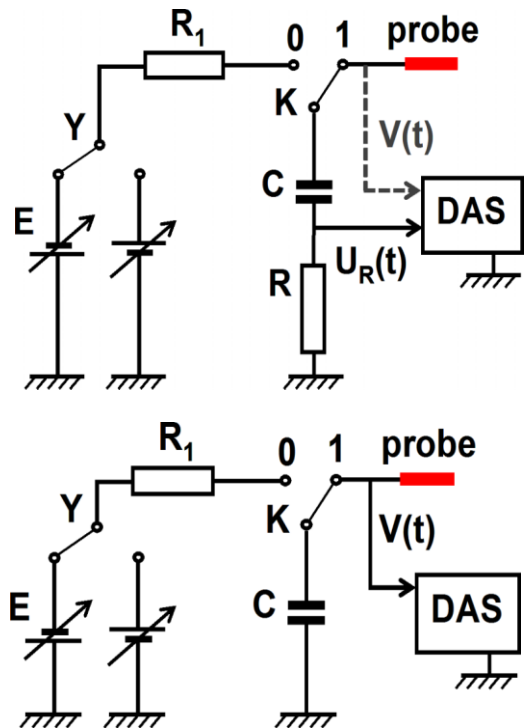


Schematic illustration of the current flow from the plasma column toward and within the floating target in Magnum-PSI. Radial distribution of electron density (a) and temperature (b) measured from Thomson scattering (H_2 gas; 0.95 T magnetic field strength; 125 A discharge current; $V_{\text{probes}} = -80$ V). Photo showing the plasma column broadening in front of the target.





EXAMPLE:



Electrical circuit designed to record the current-voltage characteristic of a probe by the integral and differential approach. The relative difference between the calculated and the measured parameters for the integral (a) and for the differential approach (b).



<http://dx.doi.org/10.1063/1.4943669>

Optical diagnosis: emission spectra



UNIVERSITATEA "ALEXANDRU IOAN CUZA" din IAŞI

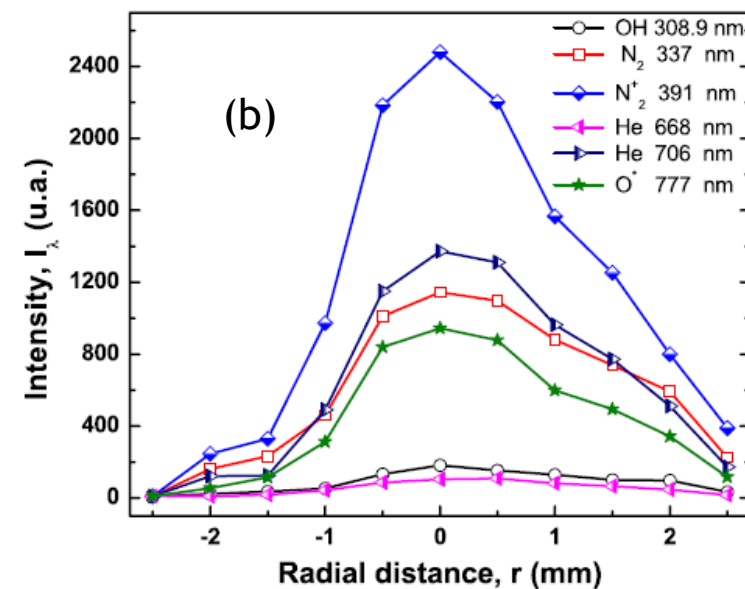
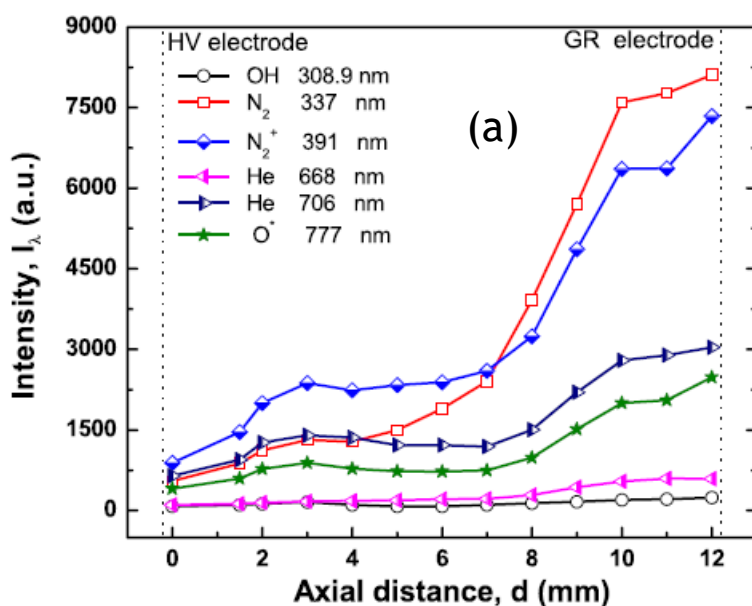
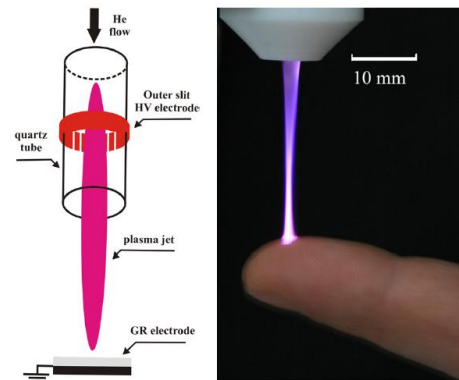
www.uaic.ro

Equipment and materials:

- Fiber optics
- Monochromators
- Computer



EXAMPLE:

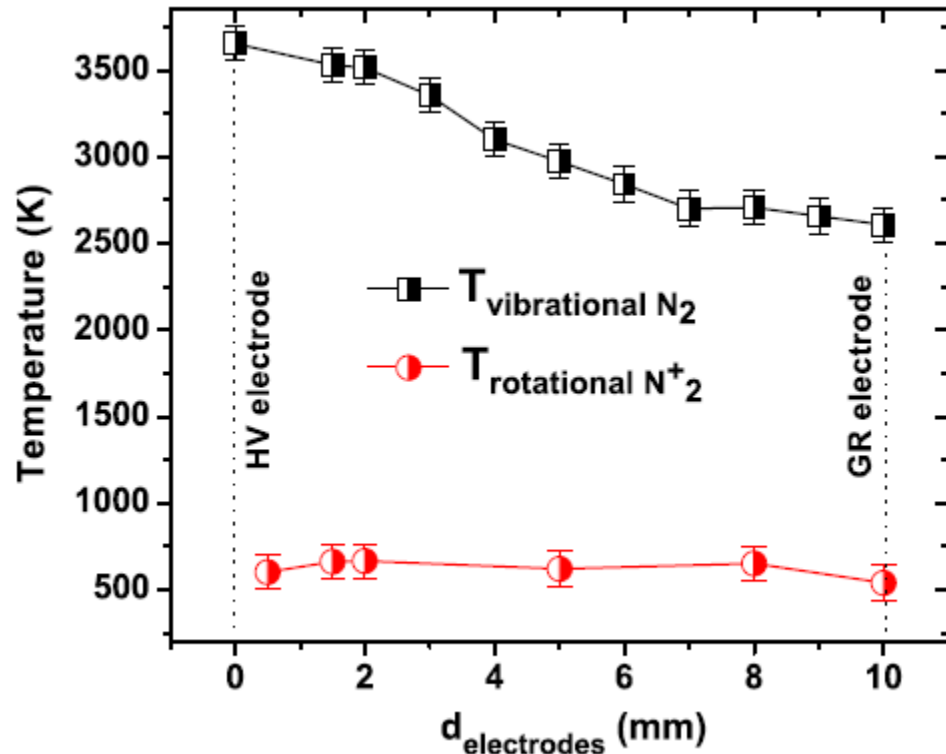
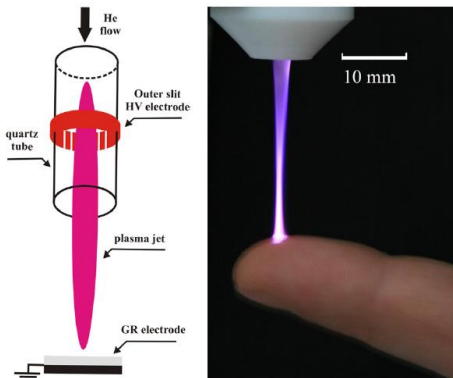


Axial profile of selected emission lines of the helium Atmospheric Pressure Plasma Jet (APPJ) in the electrode gap (a). Radial profile of selected emission lines of the APPJ at 3mm from the tube nozzle (b).





EXAMPLE:



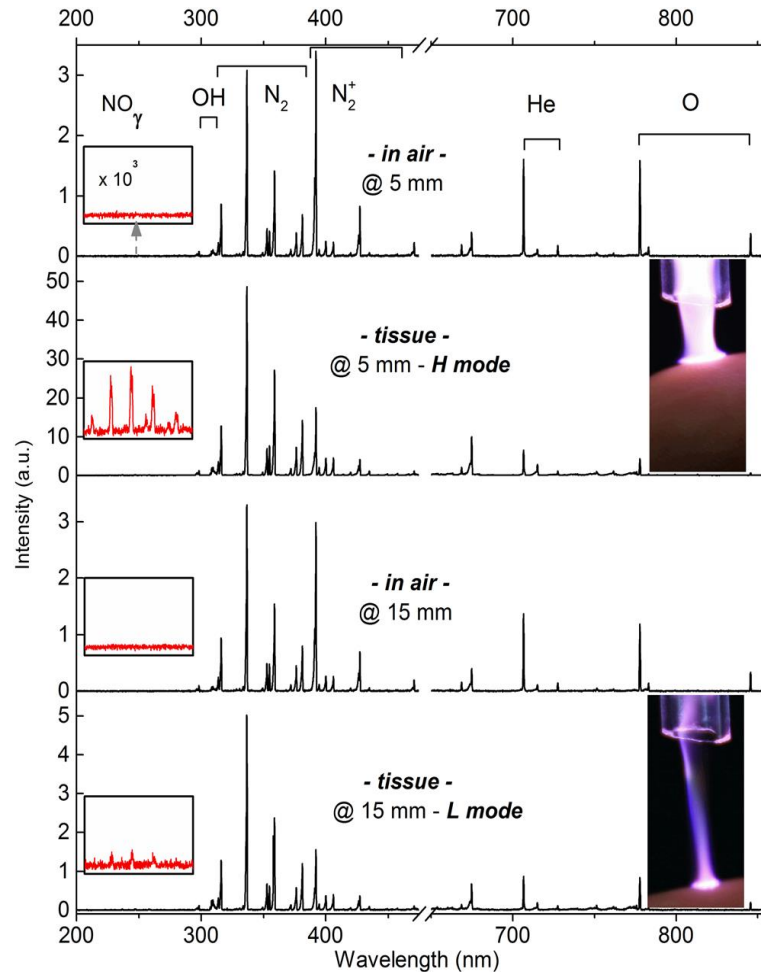
The axial distribution of the plasma temperatures of the helium for the Atmospheric Pressure Plasma Jet (APPJ) as function of electrodes gap.



<https://doi.org/10.1088/0022-3727/44/10/105204>



EXAMPLE:



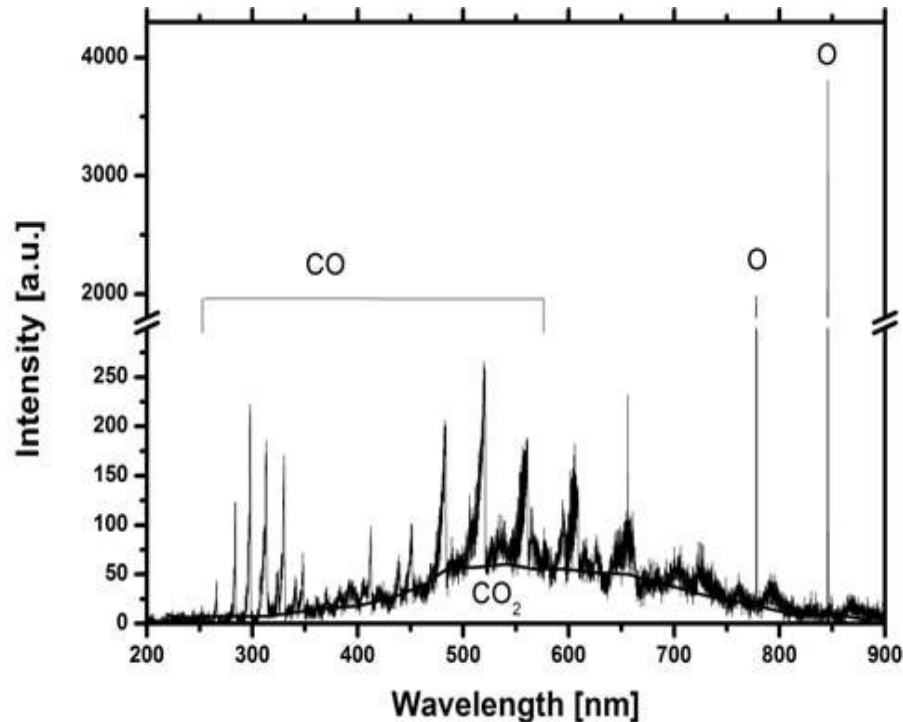
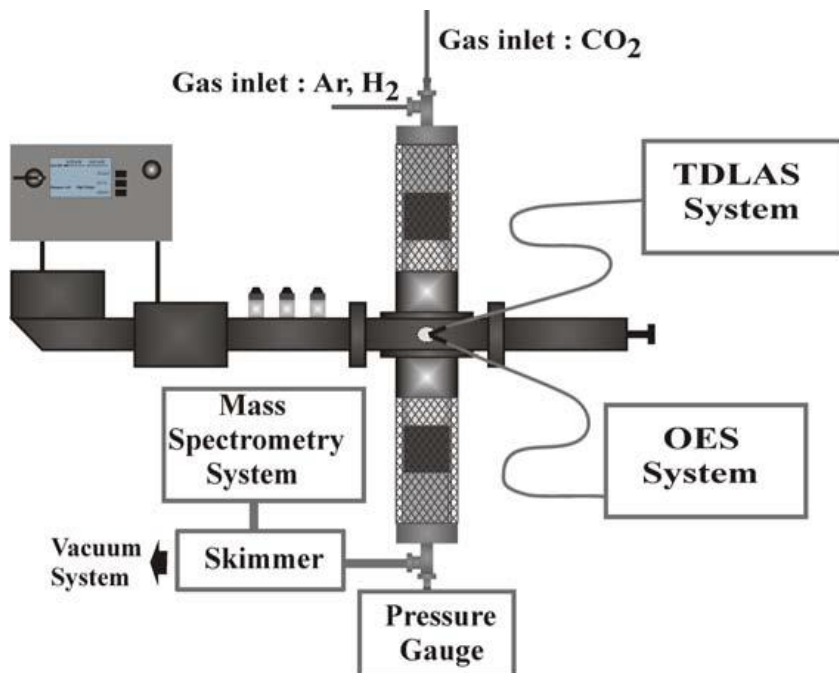
Influence of elapsed time on selected bands and lines integral intensity of a helium **Atmospheric Pressure Plasma Jet** (HV pulse parameters: 8 kV, 2 kHz, 50 μ s, positive polarity). Black dots: gas flow and HV pulses turned on simultaneously; Red dots: gas flow turned on for 10 min prior the HV pulses.



<https://dx.doi.org/10.1063/1.4804319>



EXAMPLE:

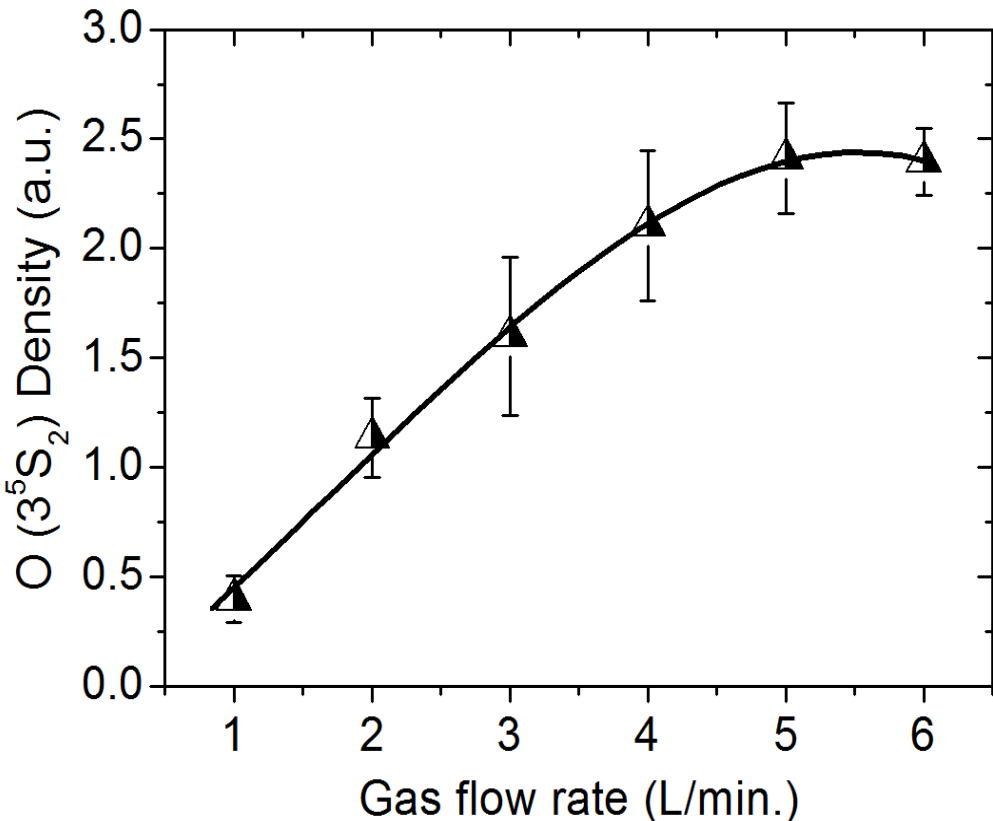
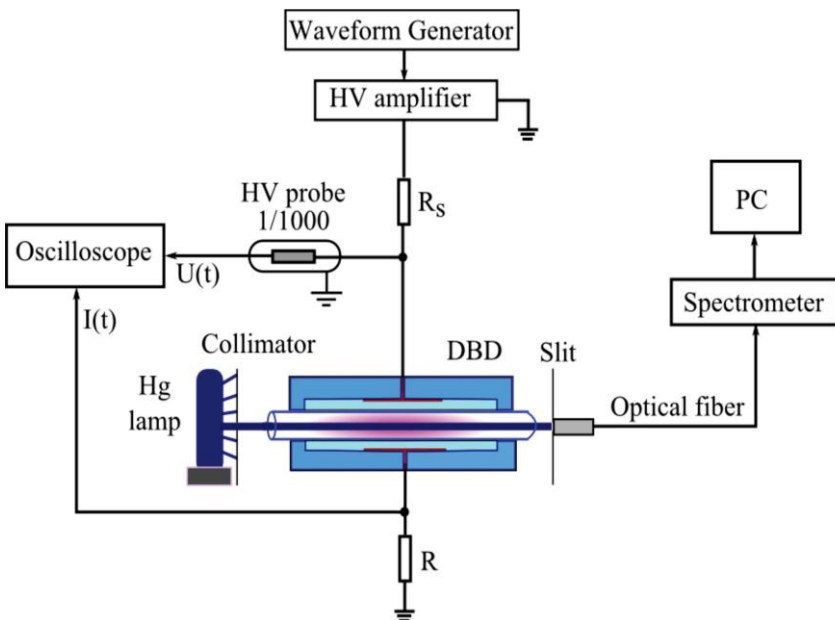


Microwave discharge: optical emission spectrum of a CO₂ microwave plasma discharge for initial pressure of 0.55 Torr and 500 W microwave radiation power





EXAMPLE:

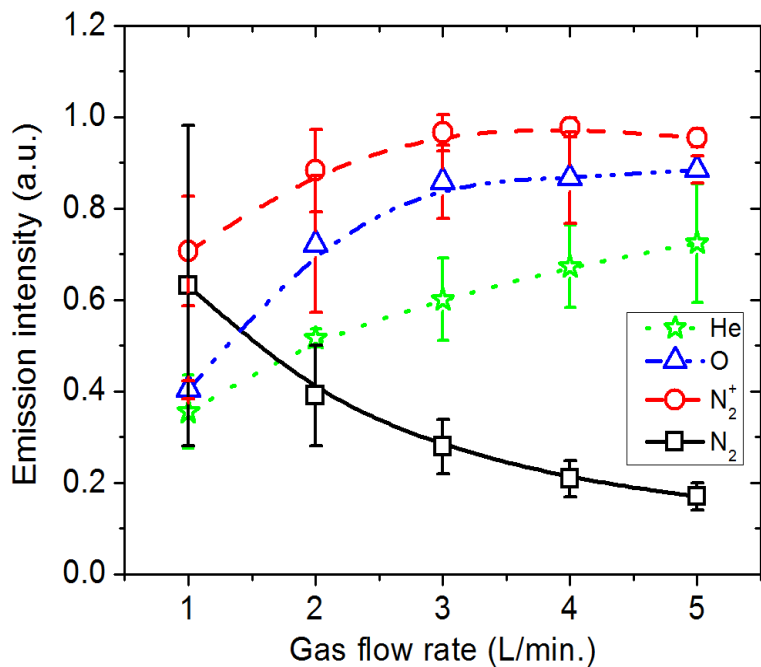


Dielectric Barrier Discharge: measured $O (3^5S_2)$ density in the He-DBD plasma as a function of the gas flow rate. Voltage pulse width and its amplitude were kept constant at 35 μ s and 5.2 kV, respectively, while its frequency was 6 kHz.

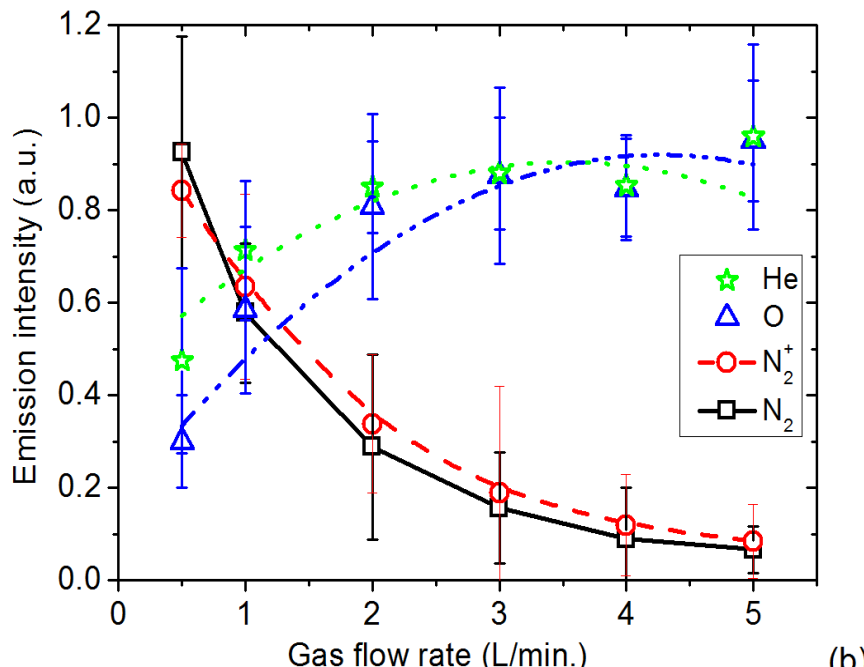




EXAMPLE:



(a)



(b)

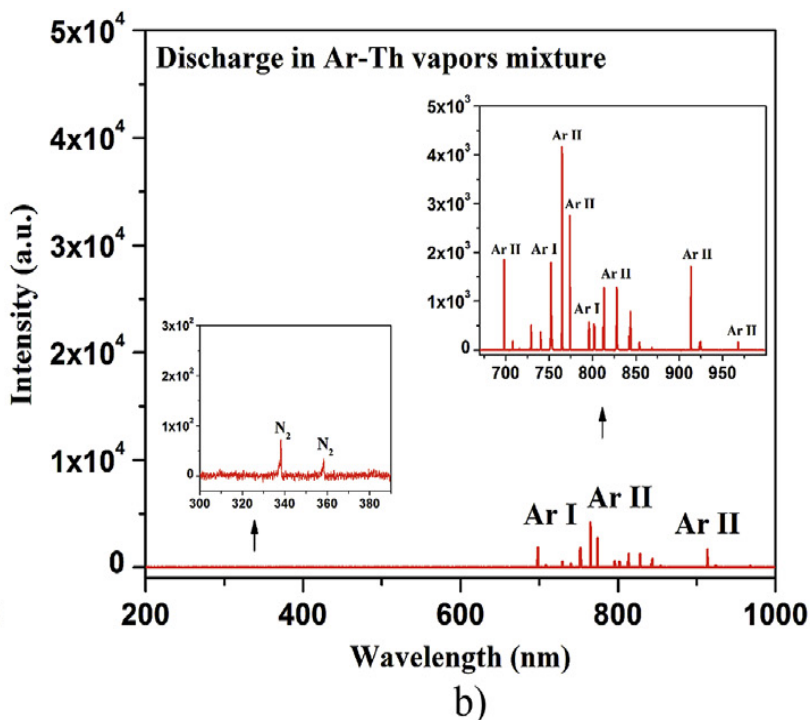
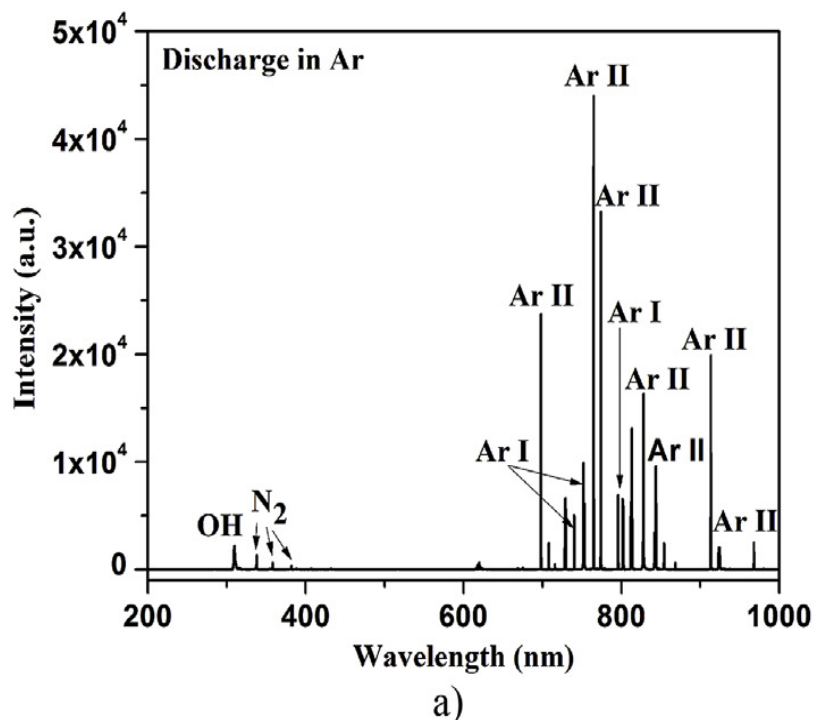
Dielectric Barrier Discharge: Relative emission intensities of He, O, N_2^+ , and N_2 versus gas flow rate for (a) He-DBD at 2 kHz and (b) He + 0.5%O₂-DBD at 6 kHz. Voltage pulse width and its amplitude were kept constant at 35 μ s and 5.2 kV, respectively.



<http://dx.doi.org/10.1109/TPS.2015.2388494>



EXAMPLE:



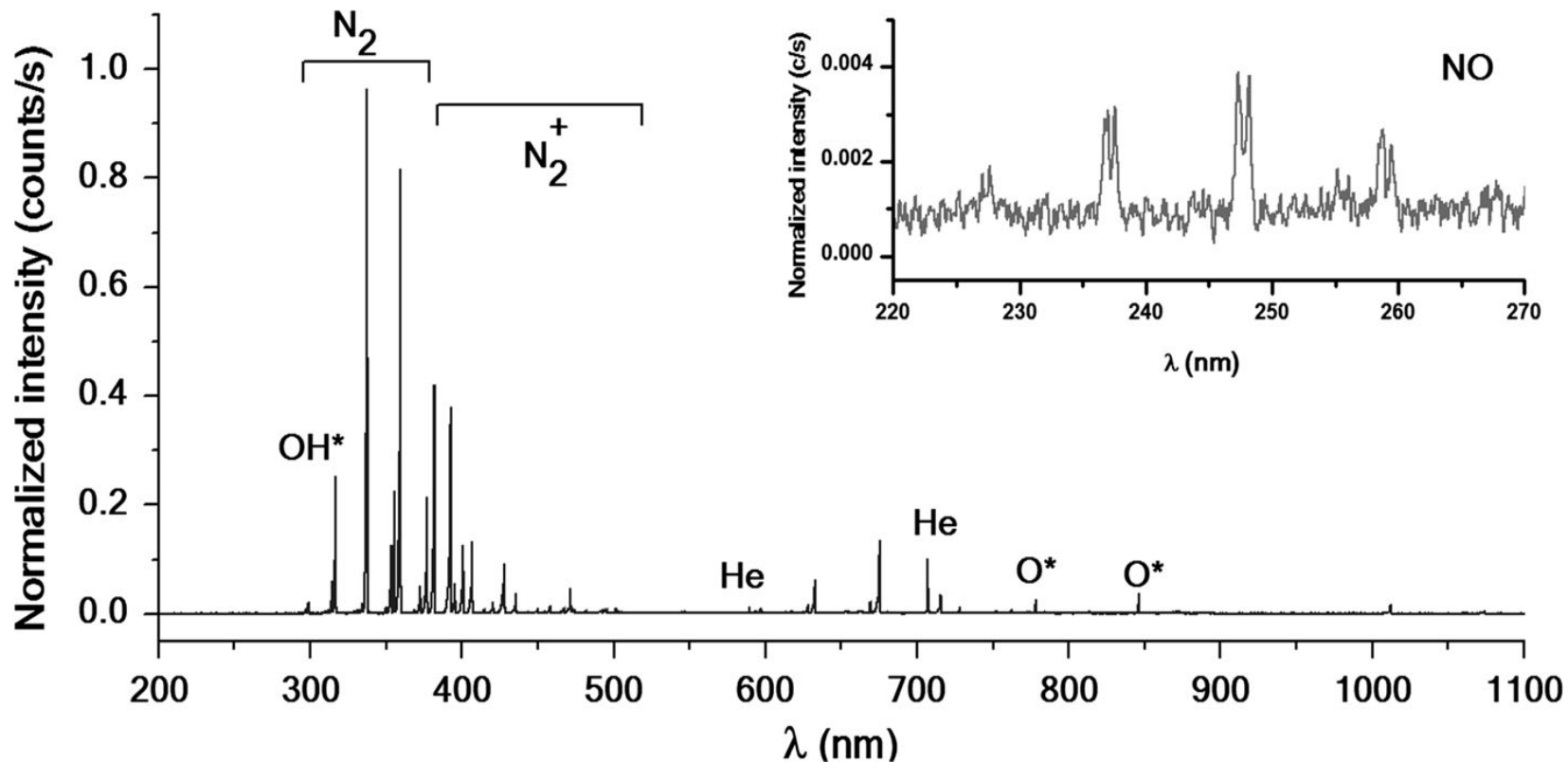
A typical emission spectrum for DBD reactor:
a) argon discharge; b) discharge in mixture of argon and thiophene vapors.



<https://dx.doi.org/10.1016/j.matchemphys.2015.11.038>



EXAMPLE:



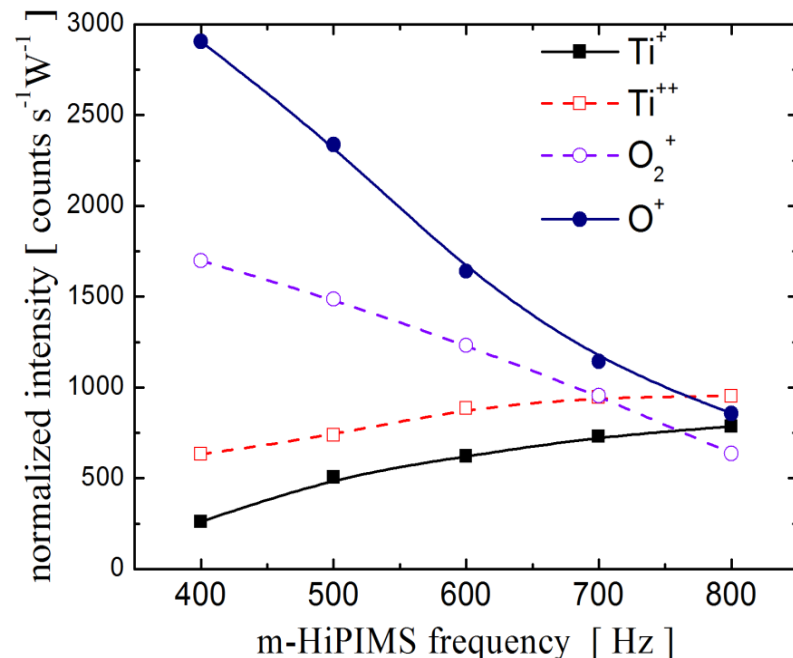
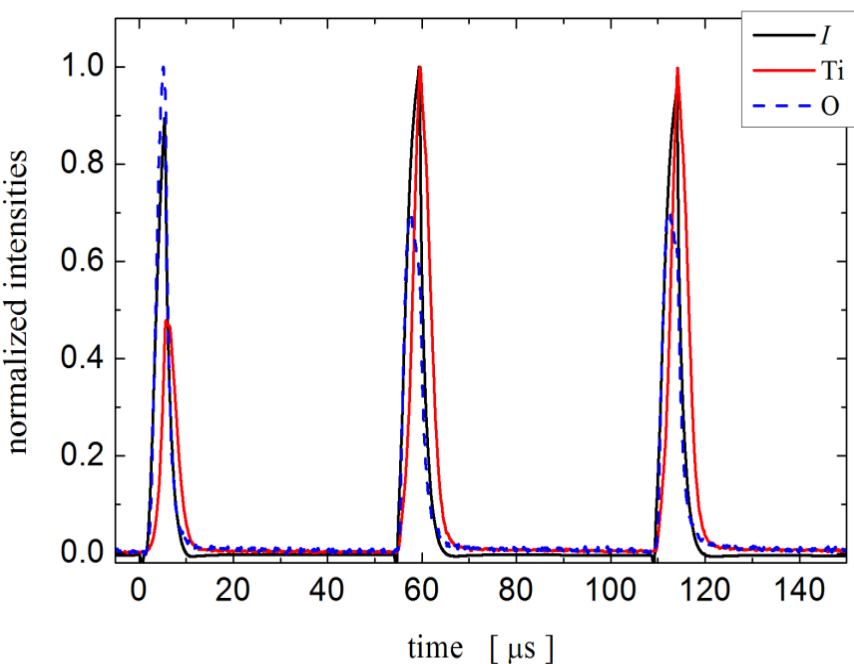
Emission spectrum of DBD for fabrics surface processing, in presence of the fabric between the electrodes.



<https://doi.org/10.1007/s11090-015-9655-4>



EXAMPLE:

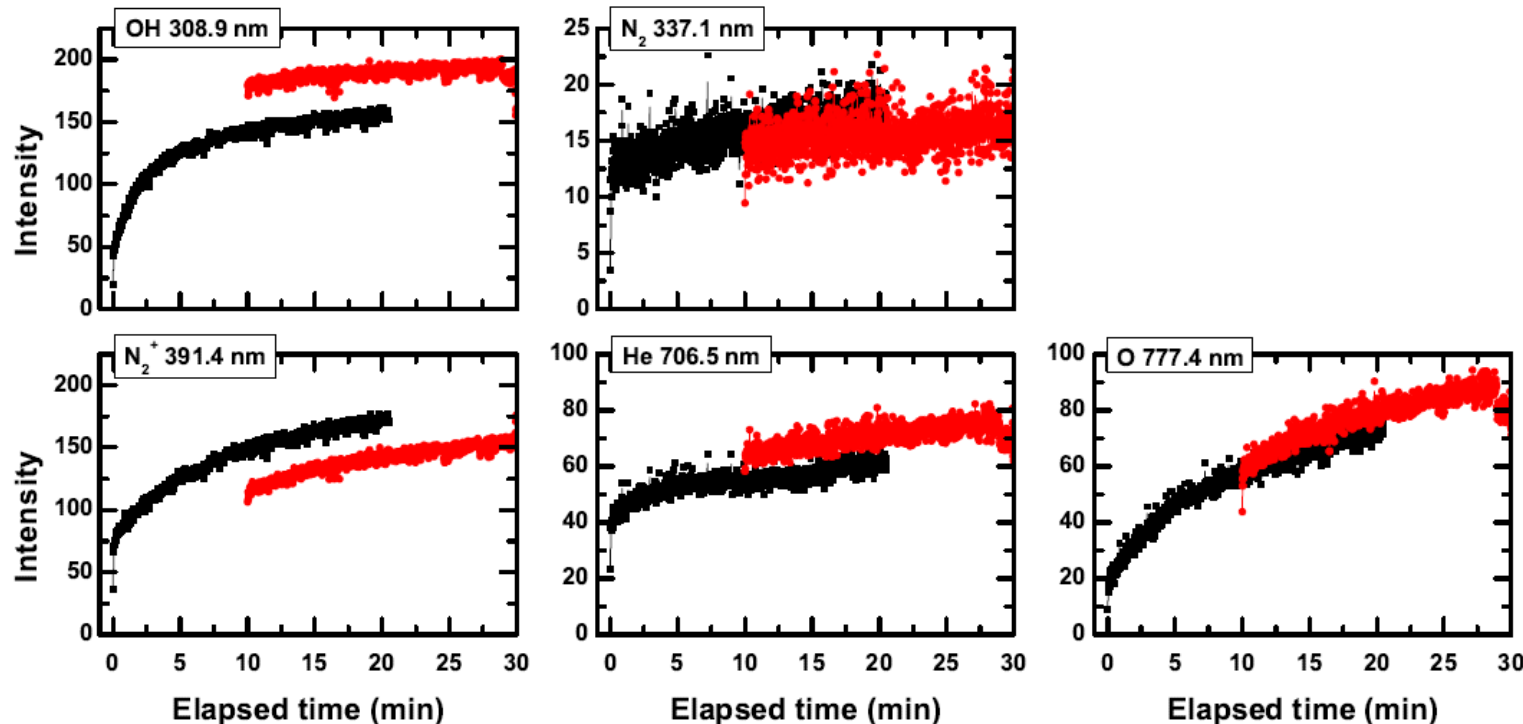


Typical time evolutions of the discharge current intensity, I , and intensities of atomic spectral lines of O ($\lambda_0 = 777.4$ nm) and Ti ions ($\lambda_{\text{Ti}} = 376.13$ nm) during a sequence of 3 micropulses (5 μ s in width with a time-off of 50 μ s) registered during the m-HiPIMS deposition of TiO_x thin films. Variation of intensities normalized to the discharge power of positively charged species by the change of m-HiPIMS repetition frequency.





EXAMPLE:



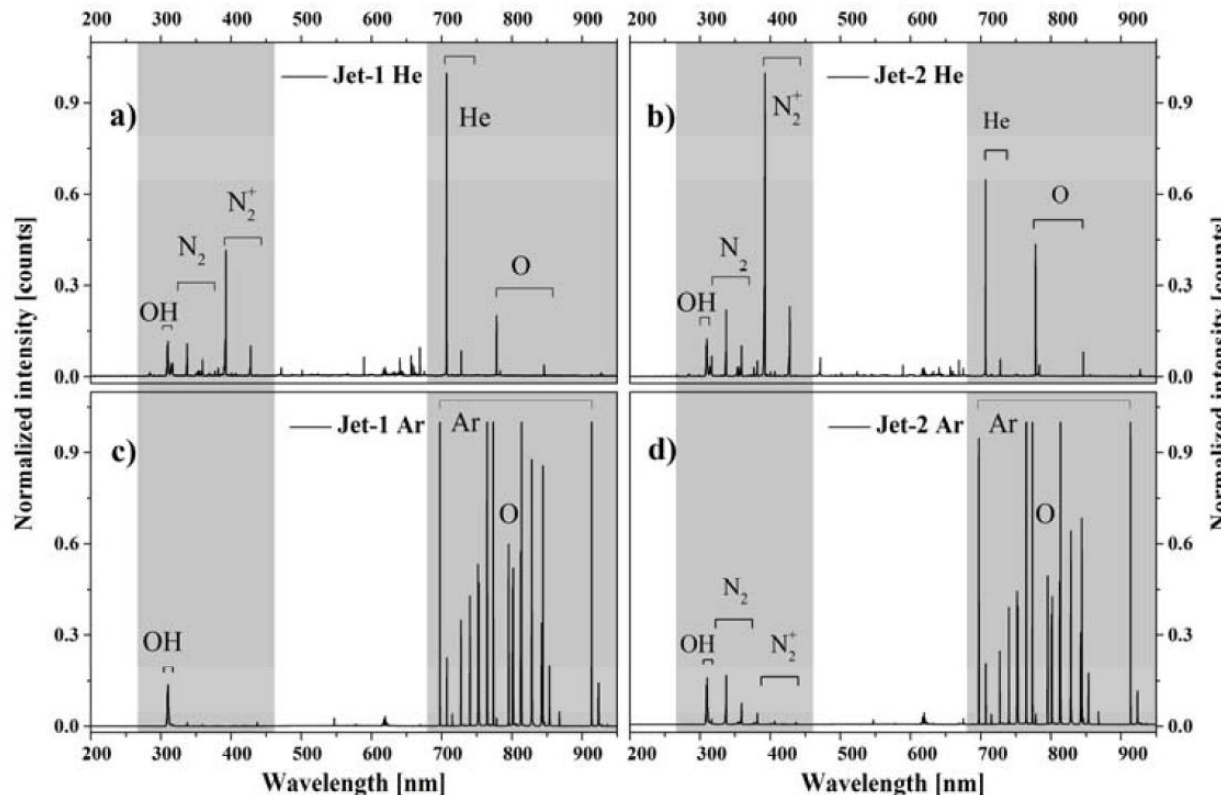
Influence of elapsed time on selected bands and lines integral intensity of a helium **Atmospheric Pressure Plasma Jet** (HV pulse parameters: 8 kV, 2 kHz, 50 μ s, positive polarity). Black dots: gas flow and HV pulses turned on simultaneously; Red dots: gas flow turned on for 10 min prior the HV pulses.



<https://doi.org/10.3390/app7080812>



EXAMPLE:



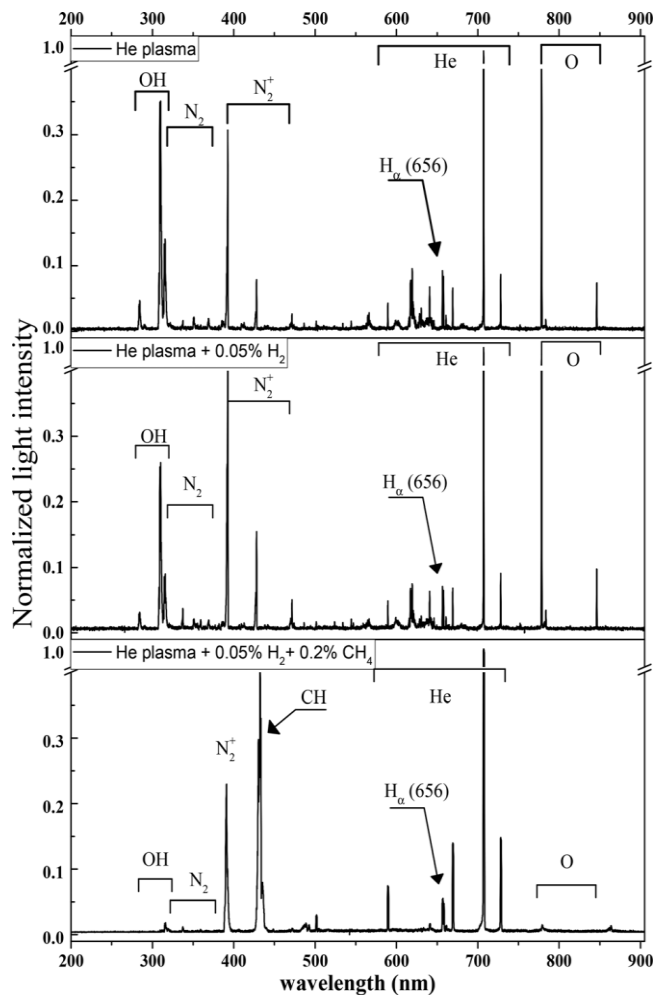
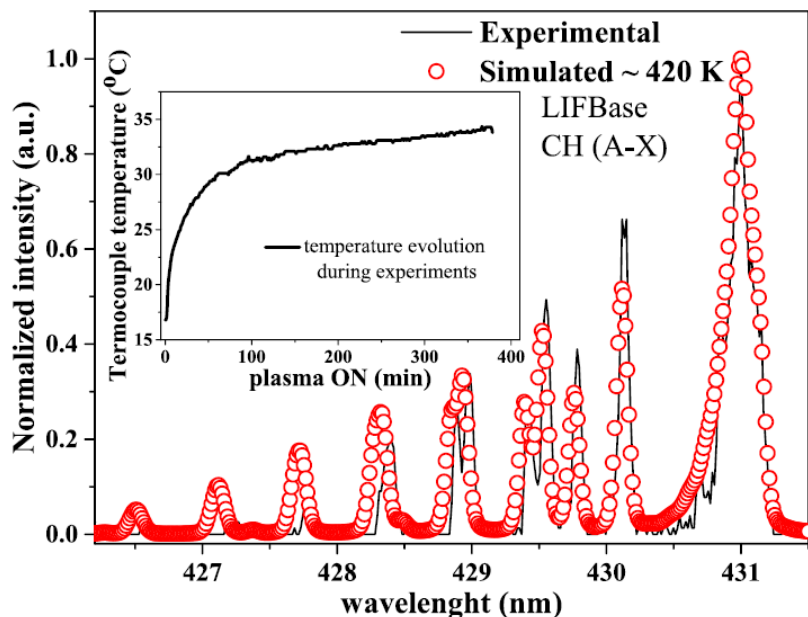
Emission spectrum for two different atmospheric pressure plasma jets (**Jet-1** and **Jet-2**)
in He (a, b) and Ar (c, d)



<https://rrp.nipne.ro/2017/AN407.pdf>



EXAMPLE:



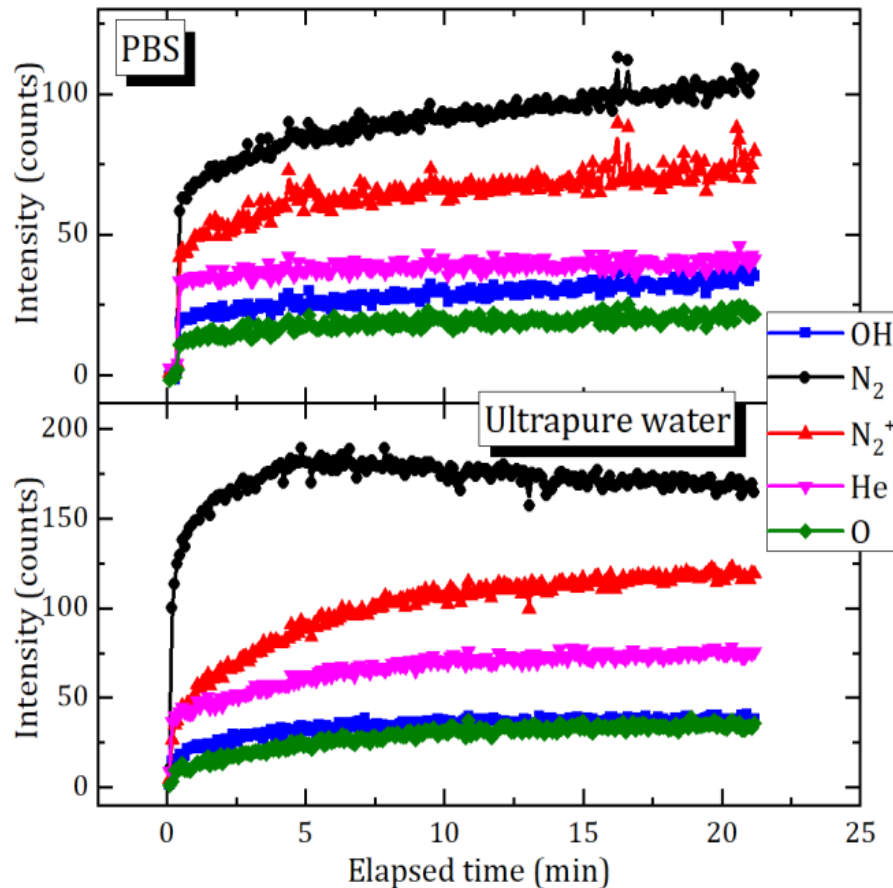
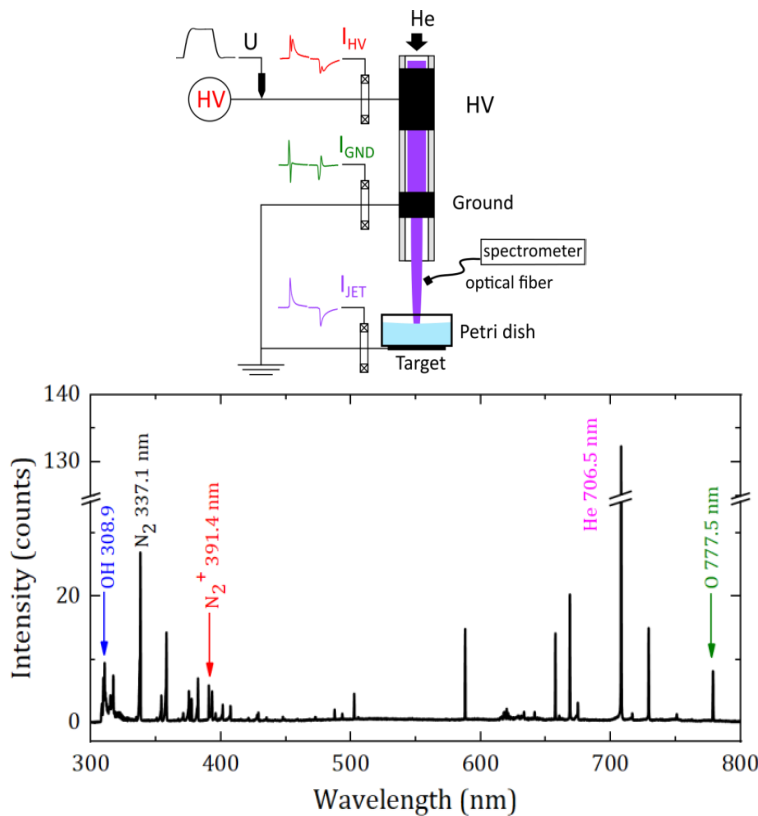
DBD plasma, in helium/helium-hydrogen/helium-hydrogen-methane gas mixture: typical spectra for He-DBD and He-DBD with admixture of H₂, respectively, H₂-CH₄; gas temperature estimation from CH(A-X) band and temperature reading (inset) from a K-type thermocouple.



<https://doi.org/10.1063/1.5017097>



EXAMPLE:



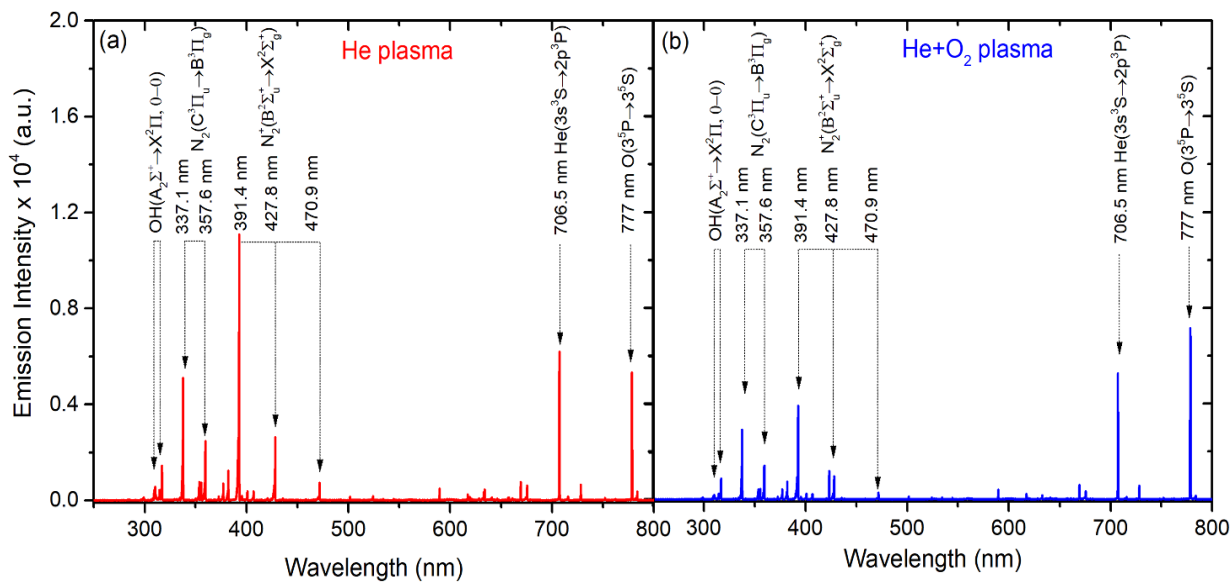
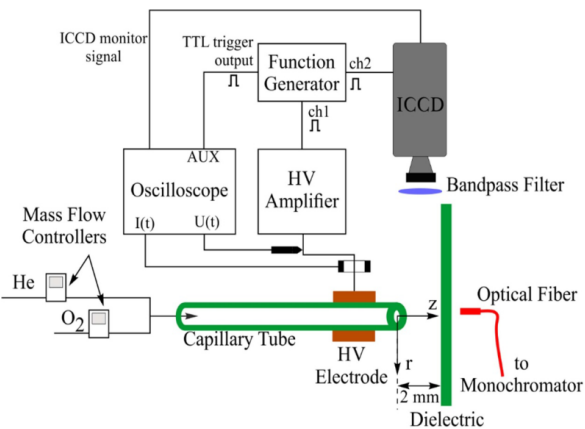
Optical emission spectrum of the helium atmospheric pressure plasma jet at the interface with the liquid target. Elapsed time dependence of selected bands and lines integral intensity.



<https://doi.org/10.1109/TPS.2020.3008967>



EXAMPLE:



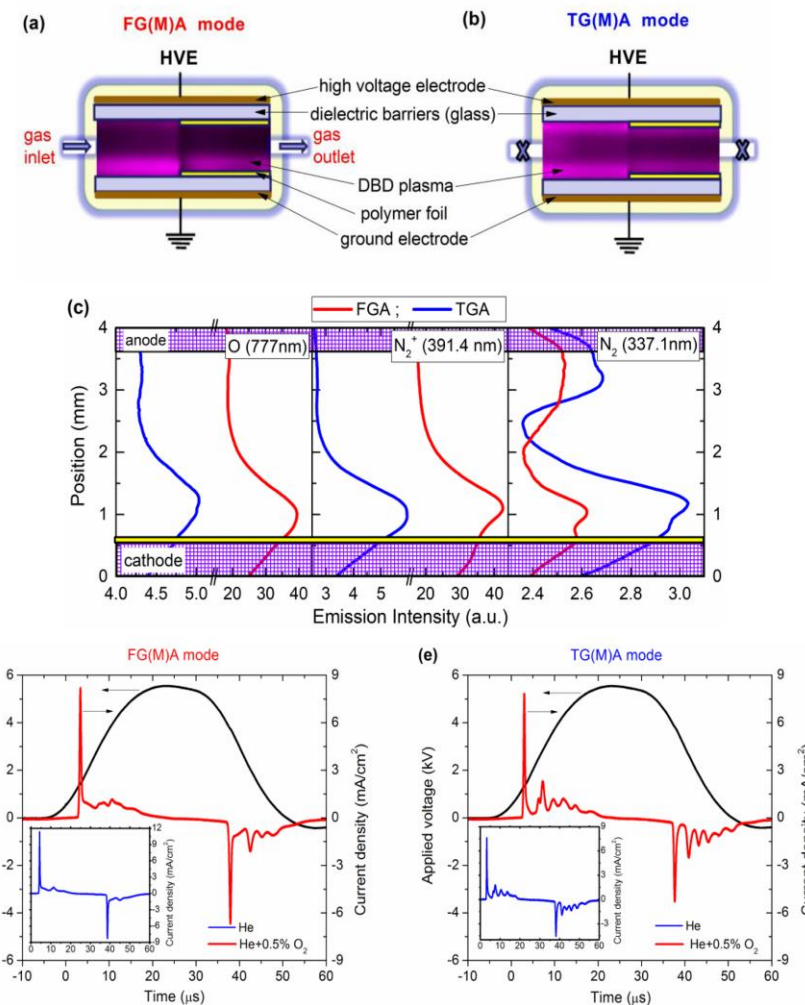
Experimental arrangement for studying He with O₂ admixtures plasma jets. Optical emission spectra for (a) pure helium plasma jet and (b) He + O₂ (1000 ppm) plasma jet.



<https://doi.org/10.1088/1361-6463/acb1c1>



EXAMPLE:



Experimental set-up (a and b), the spatial distribution of excited species (c), and typical electrical characteristics (d and e) of DBD working in different modes: FGA(M)A and TG(M)A.



<https://doi.org/10.1016/j.matlet.2021.130832>

Optical diagnosis: time resolved emission spectra



UNIVERSITATEA "ALEXANDRU IOAN CUZA" din IAȘI

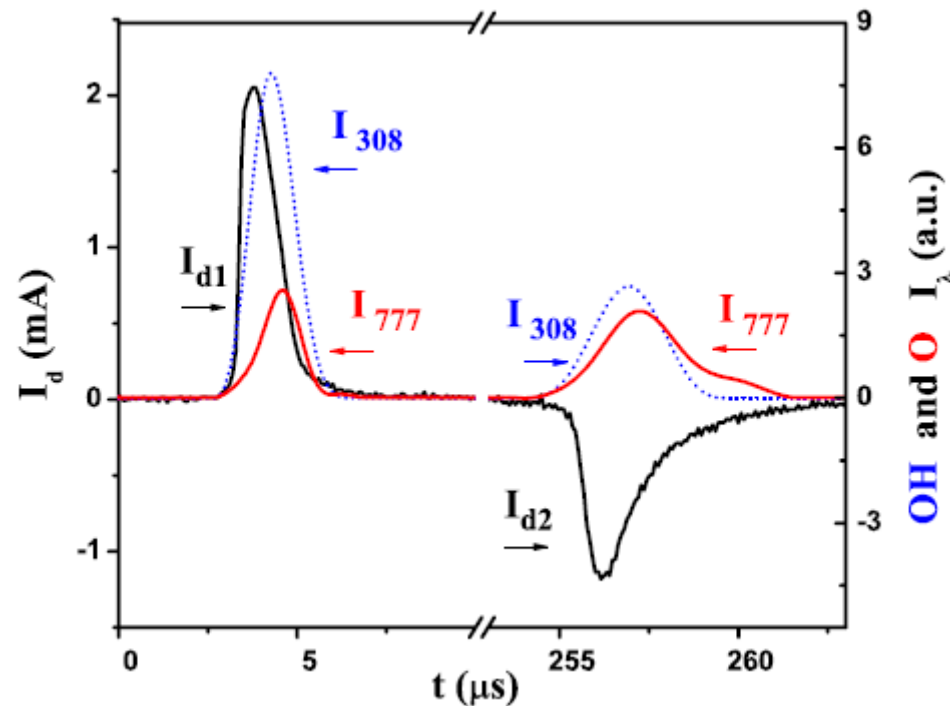
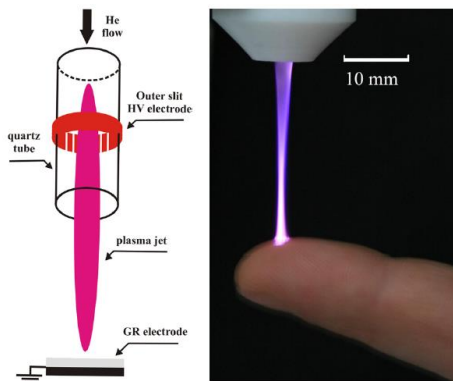
www.uaic.ro

Equipment and materials:

- Fiber optics
- Spectral filters
- Photomultipliers
- Oscilloscope



EXAMPLE:



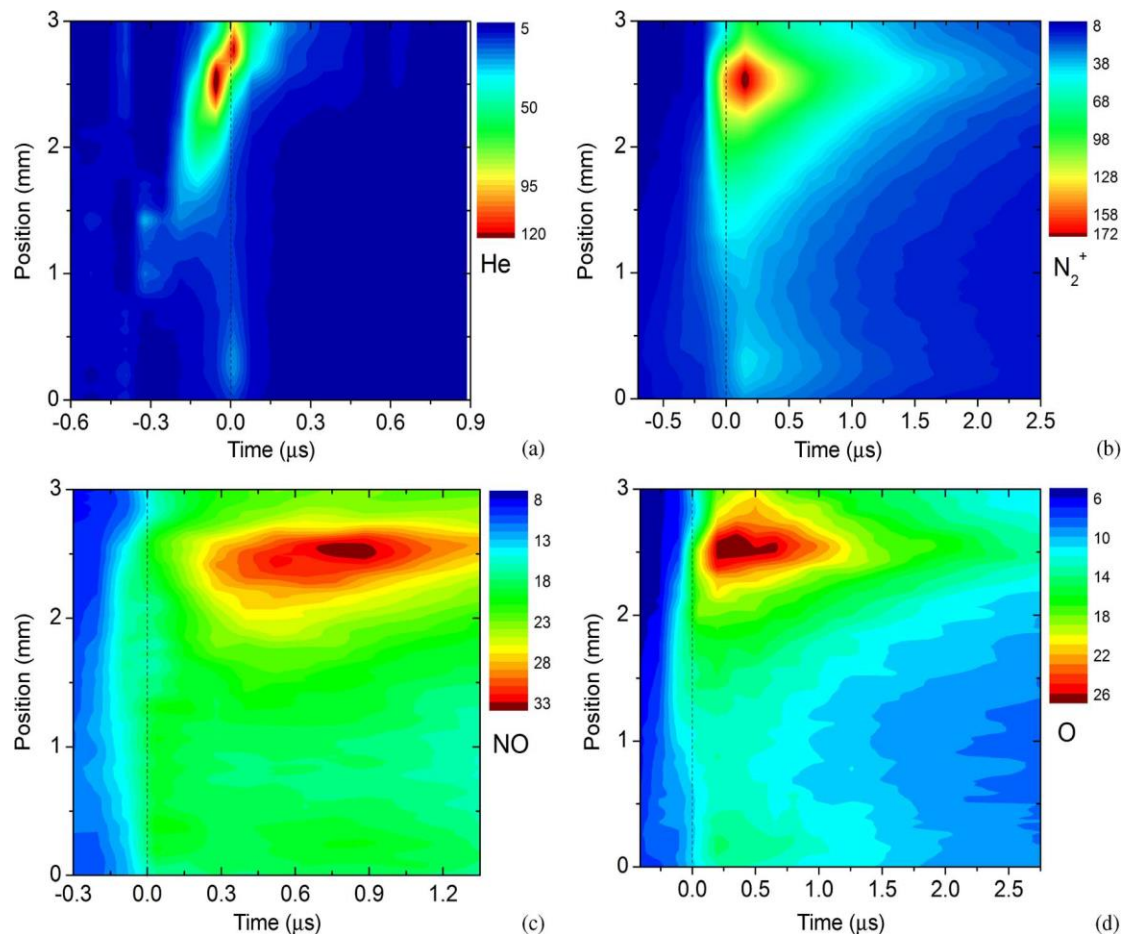
APPJ: time evolution of the emission band of the OH (at 308.9 nm) and emission line of O metastable (at 777.4 nm) with the plasma discharge current, at 2 mm from the tube nozzle.



<https://doi.org/10.1088/0022-3727/44/10/105204>



EXAMPLE:



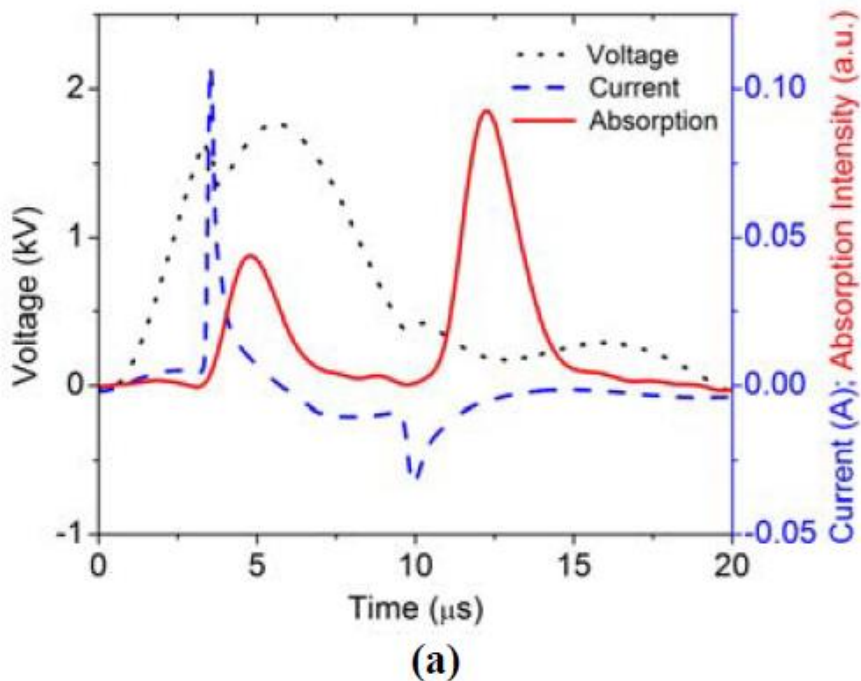
Dielectric barrier discharge (DBD): relative intensities of (a) the helium lines at 706.6 and 728.1 nm, (b) the N₂⁺ first negative system at 391.4 nm, (c) NO at 438.7 nm, and (d) the O triplet line at 777 nm are plotted versus the time and the position across the discharge gap. Position 0 mm corresponds to the anode, and position 3 mm corresponds to the cathode.



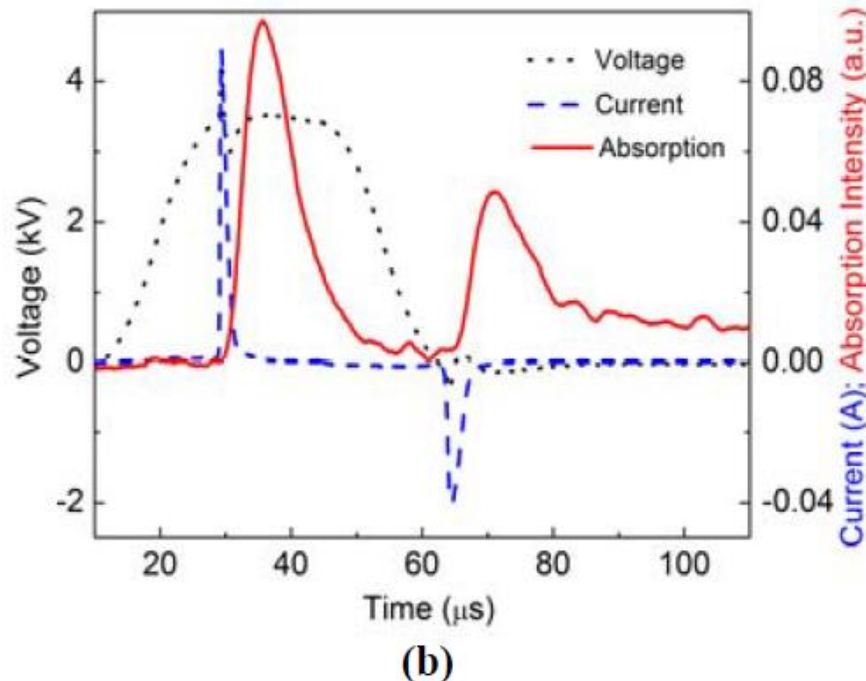
<https://doi.org/10.1109/TPS.2011.2163322>



EXAMPLE:



(a)



(b)

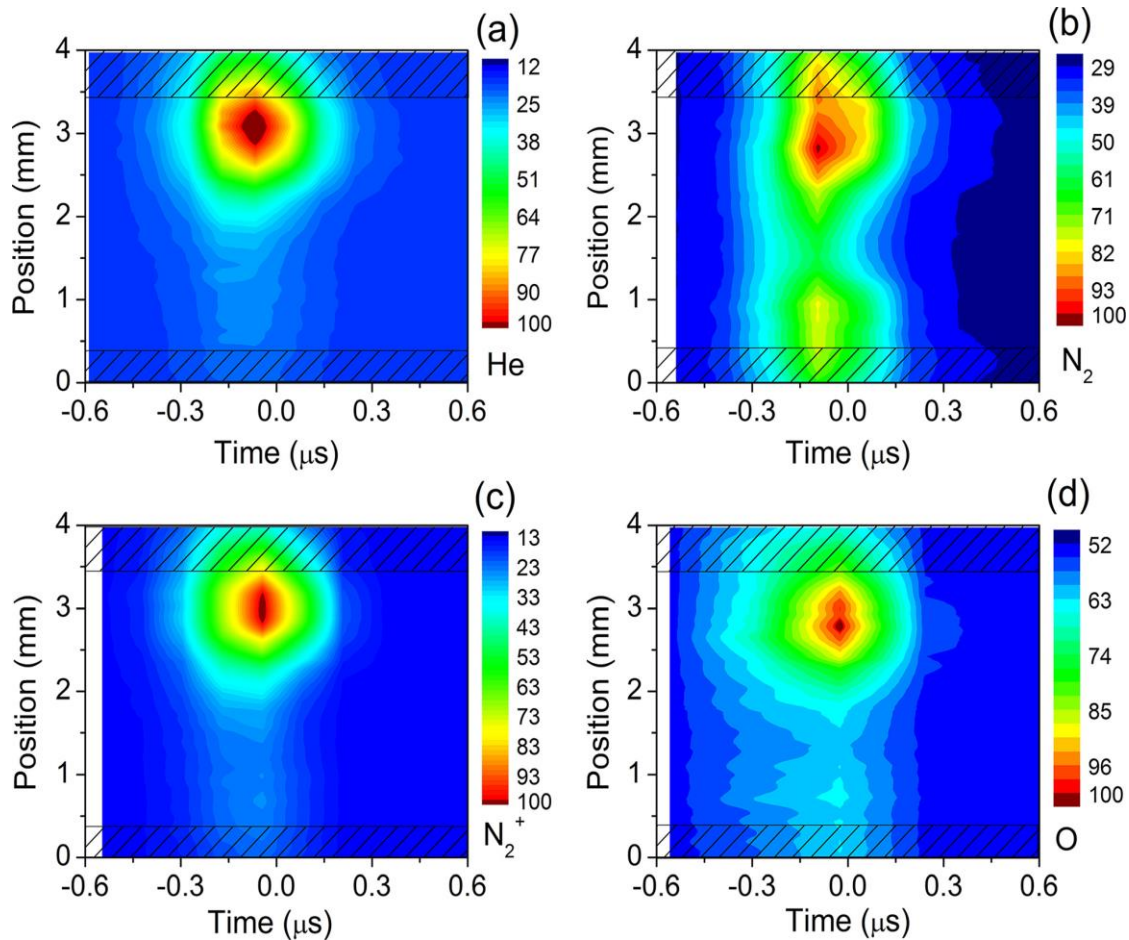
Dielectric barrier discharge (DBD): Time evolution of voltage, current and oxygen absorption intensity (777.194 nm) near the HV electrode in: (a) He - DBD and (b) Ar - DBD plasmas



https://rjp.nipne.ro/2011_56_Suppl/RomJPhys.56s.p126.pdf



EXAMPLE:

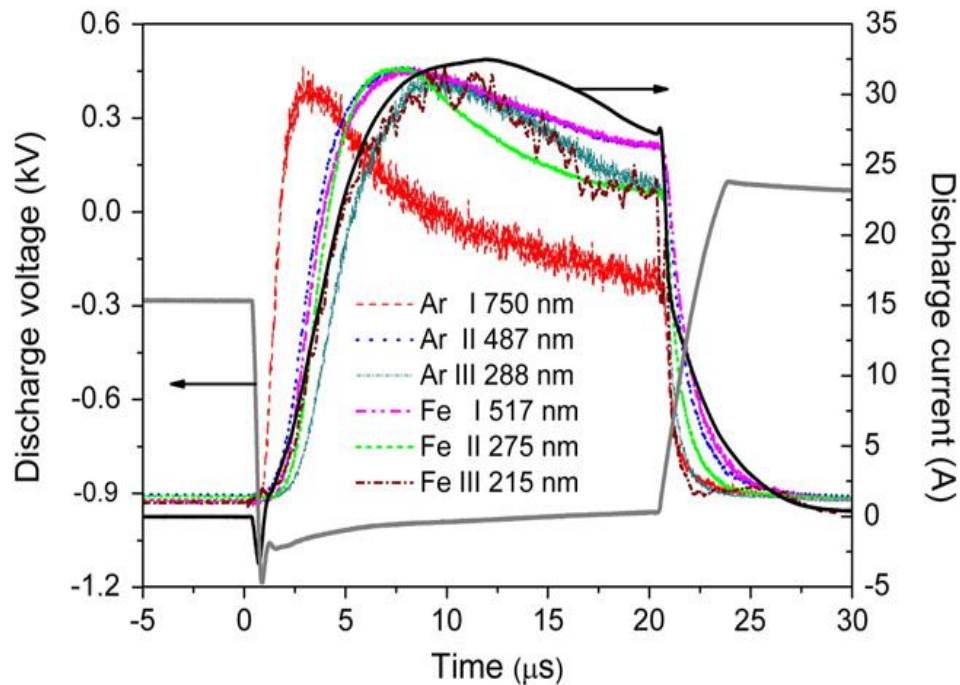
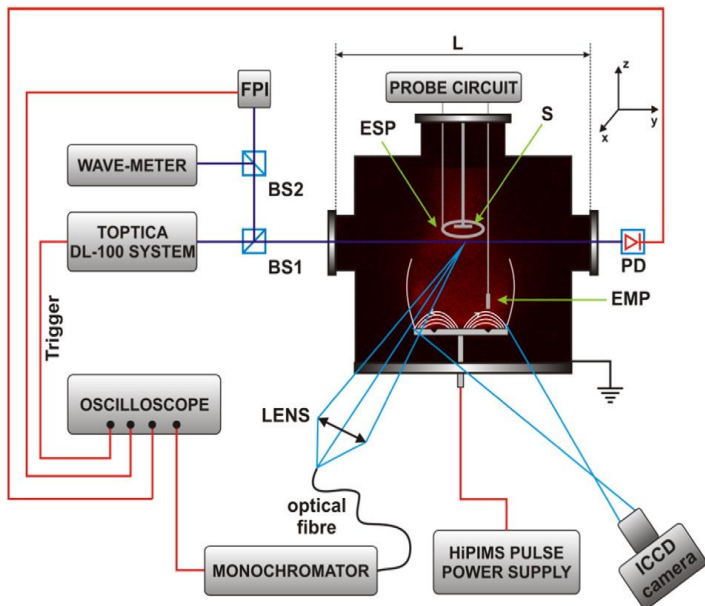


Dielectric barrier discharge (DBD): Temporally and spatially resolved imaging of (a) the He lines at 706.6 and 728.1 nm, (b) the N₂ second positive system at 337.1 nm, (c) the N₂⁺ first negative system at 391.4 nm, and (d) the O triplet line at 777 nm during the positive leading current pulse of DBD working in TGA mode at atmospheric pressure. The timescale is referenced to the maximum of the discharge current pulse.





EXAMPLE:

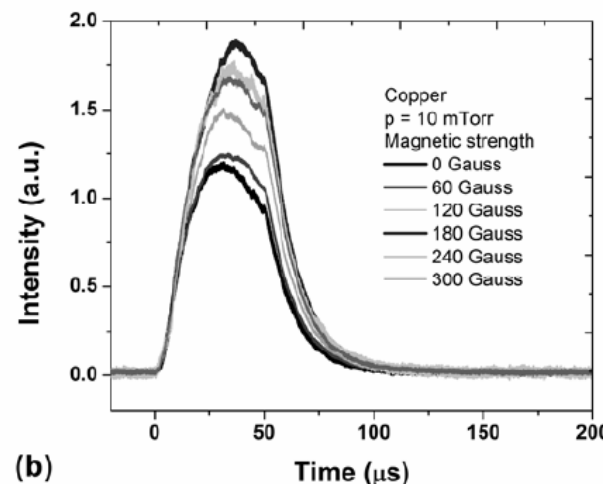
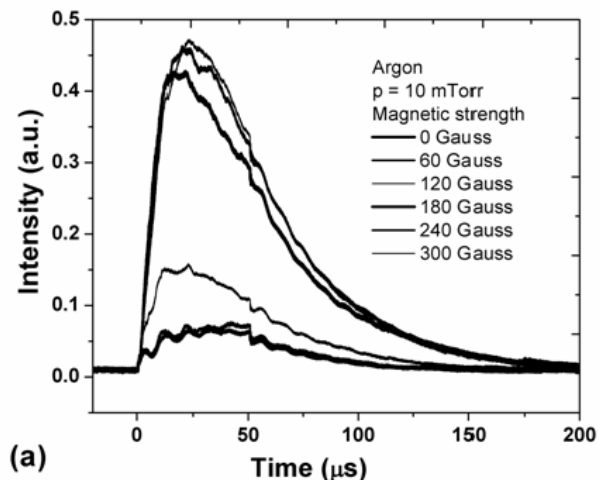
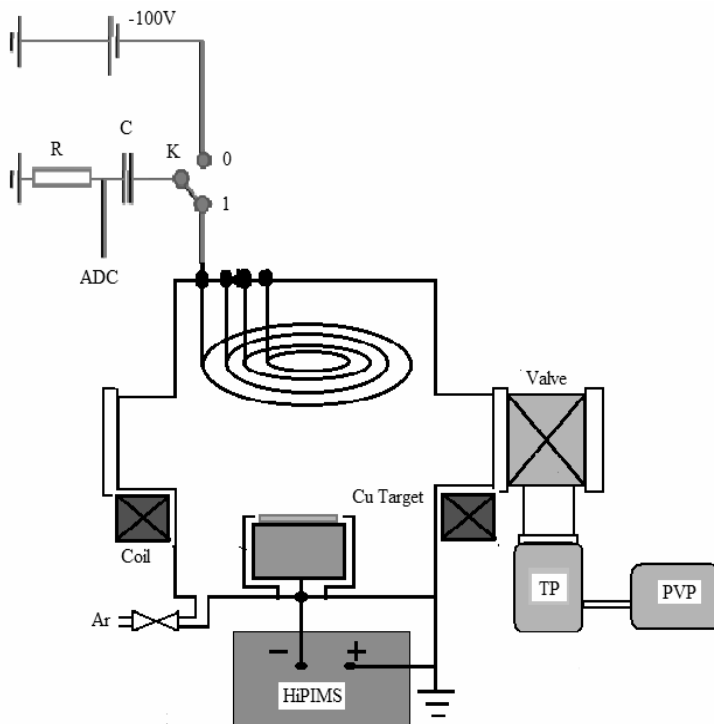


High Power Impulse Magnetron Sputtering (HIPIMS): simplified schematic of the experimental device (FPI—Fabry-Pérot interferometer, PD—photodiode, BS—beamsplitter, ESP—electrostatic probe, EMP—emissive probe, S—substrate, L—optic distance of the laser beam probing the plasma volume); Time evolution on pulse of discharge voltage, discharge current intensity and normalized spectral lines intensities of Ar and Fe species of plasma radiation at 1.33 Pa argon pressure, pulse duration of 20 μs and -1 kV cathode voltage.





EXAMPLE:

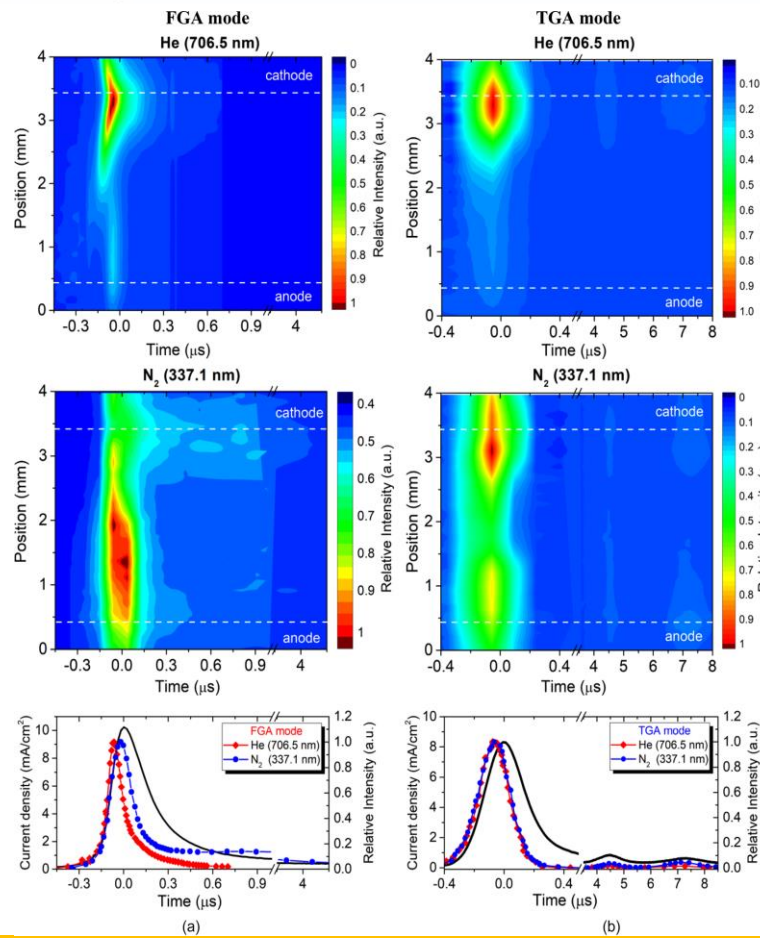


High Power Impulse Magnetron Sputtering (HIPIMS): temporal evolution on pulse of Argon ($\lambda = 750.38 \text{ nm}$) (a) and Copper ($\lambda = 521.82 \text{ nm}$) (b) spectral line vs. magnetic field strength.





EXAMPLE:



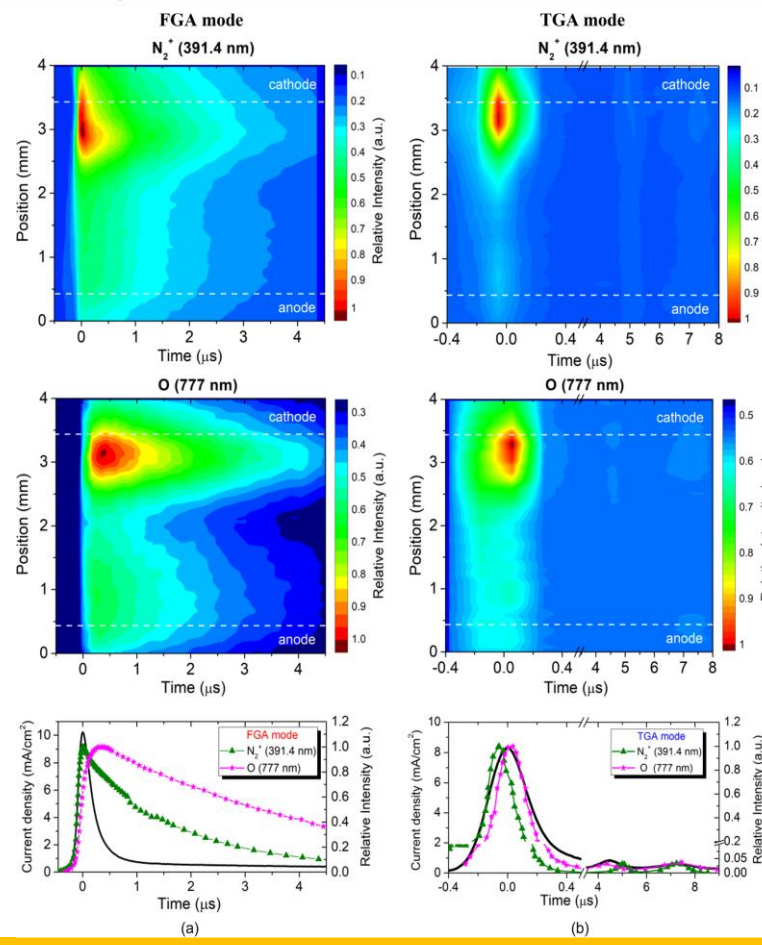
Spatio-temporally resolved emission of the N₂⁺ first negative system at 391.4 nm and the O triplet line at 777 nm during the positive current pulse(s) of He-DBD operating in FGA mode (a) and TGA mode (b). The electrodes' positions are marked by white-dashed lines. The timescale is referenced to the maximum of the discharge current pulse. Below, the temporal intensity development of corresponding emissions in comparison with the discharge current (black line).



<https://doi.org/10.1063/5.0043349>



EXAMPLE:



Spatiotemporally resolved emission of the He line at 706.5 nm and the N₂ second positive system at 337.1 nm during the positive current pulse(s) of He-DBD working in FGA mode (a) and TGA mode (b). The electrodes' positions are marked by white-dashed lines. The timescale is referenced to the maximum of the discharge current pulse. Below, the time dependence of normalized spectral intensities in comparison with the discharge current (black line).



<https://doi.org/10.1063/5.0043349>

Optical diagnosis: high speed imaging



UNIVERSITATEA "ALEXANDRU IOAN CUZA" din IAŞI

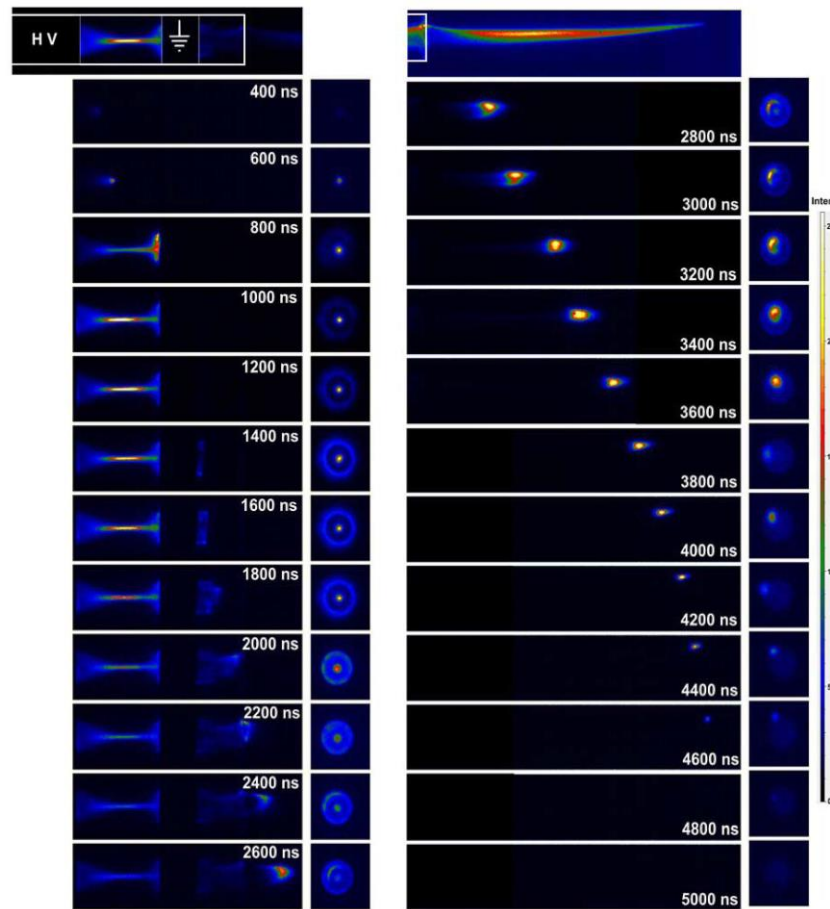
www.uaic.ro

Equipment and materials:

- High speed camera
- Computer



EXAMPLE:



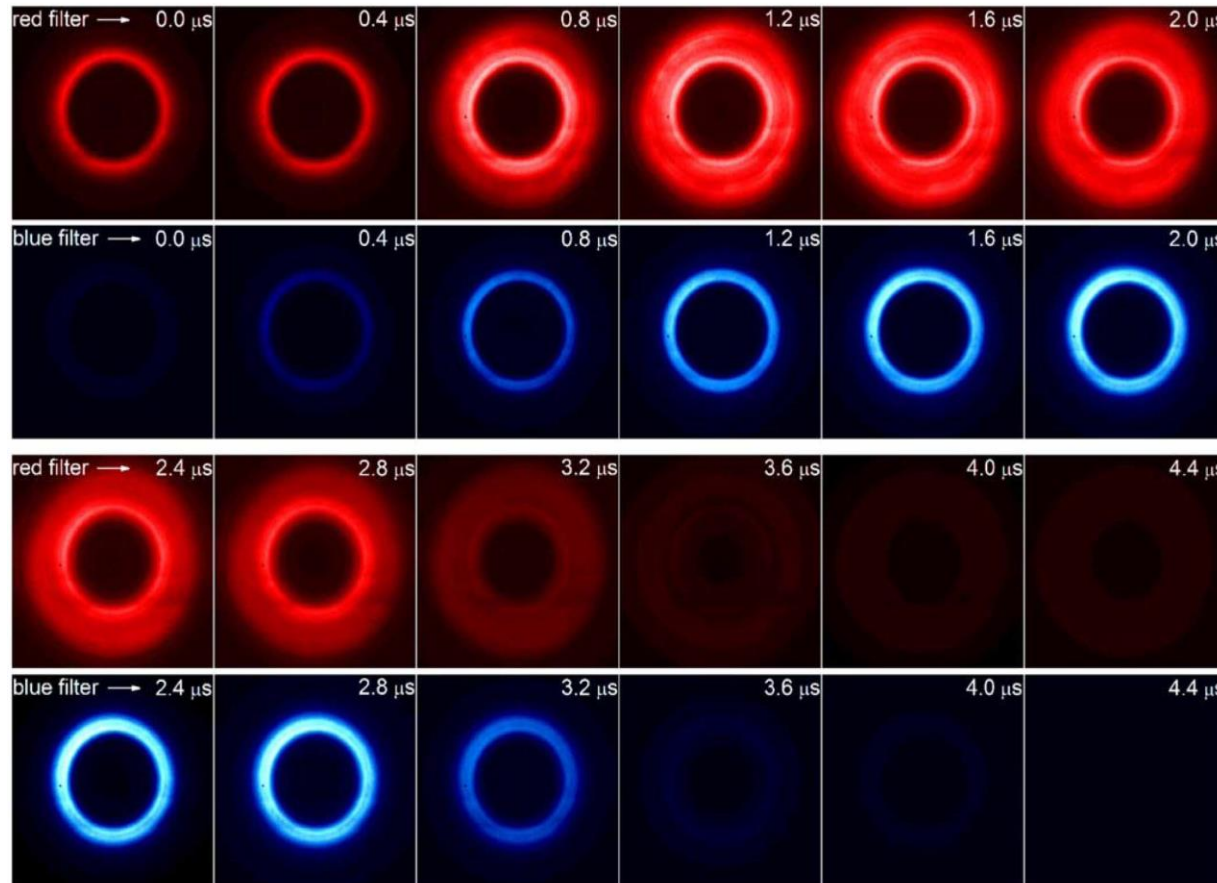
Photographs of bullets in helium of the helium **Atmospheric Pressure Plasma Jet (APPJ)** (30-ns exposure time) inside the quartz tube and in air, observed from side view and on-axis view (white lines in the top images are used to mark the position of the quartz tube, the ground electrode, and the power electrode; on the left side, the color intensity scale is shown).



<https://doi.org/10.1109/TPS.2011.2147805>



EXAMPLE:



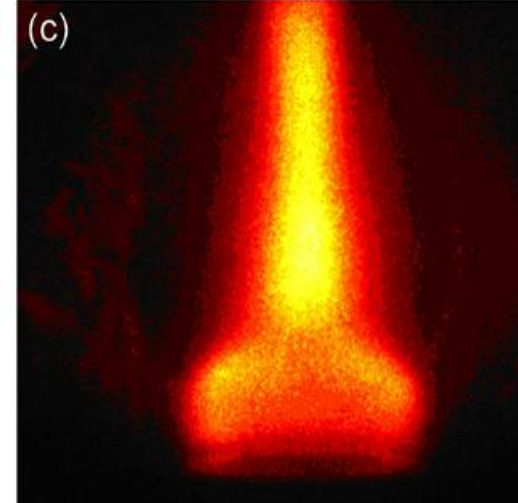
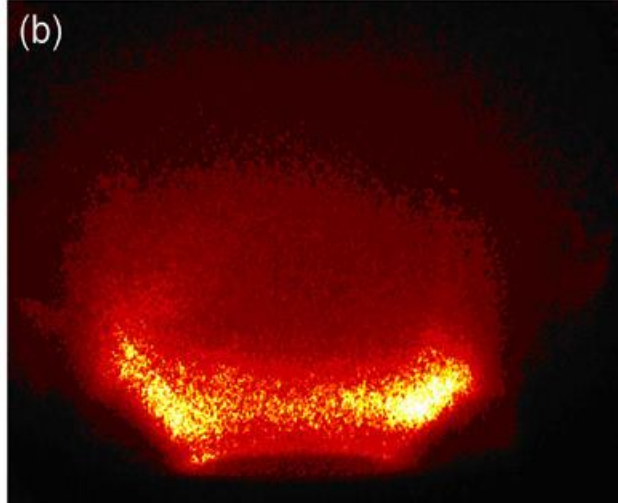
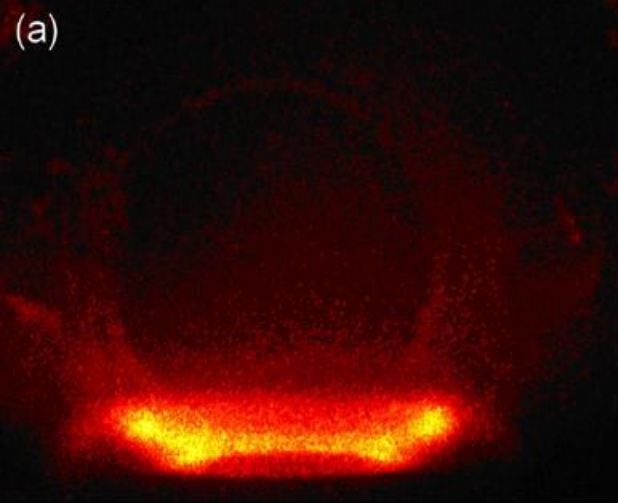
Pulsed Magnetron Discharge: on-pulse fast ICCD images taken with (Ar) red and (Al) blue filters (top view).



<https://doi.org/10.1109/TPS.2011.2145005>



EXAMPLE:



High Power Impulse Magnetron Sputtering (HIPIMS): ICCD images taken during the tungsten target sputtering, using a red (Ar) optical filter and different magnetic configurations:

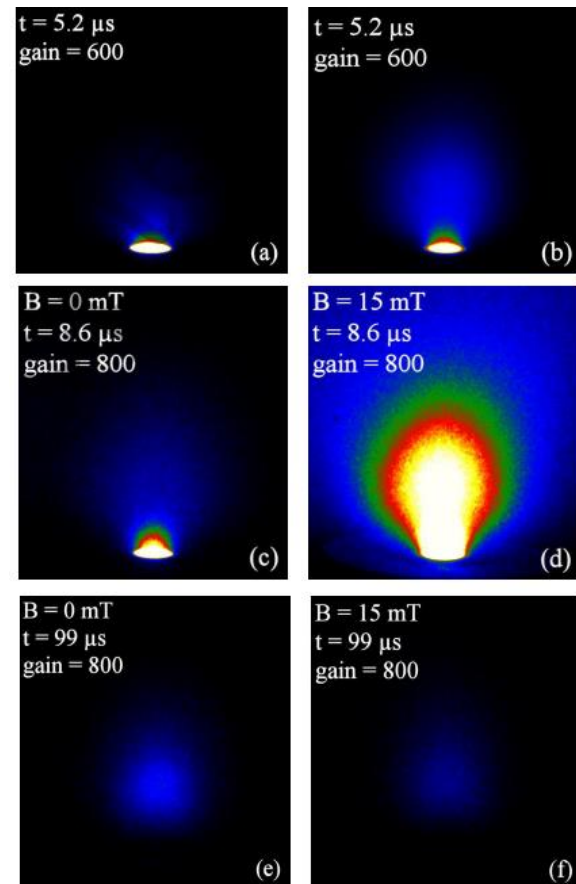
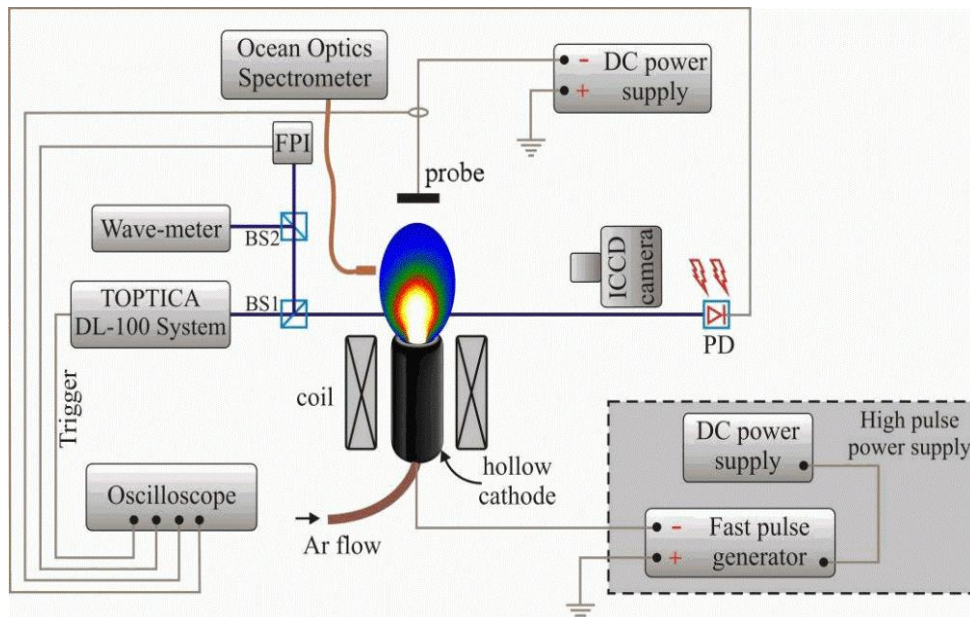
(a) unbalanced magnetron of type I, (b) balanced magnetron, and (c) unbalanced magnetron of type II.



<https://dx.doi.org/10.1088/0022-3727/48/49/495204>



EXAMPLE:

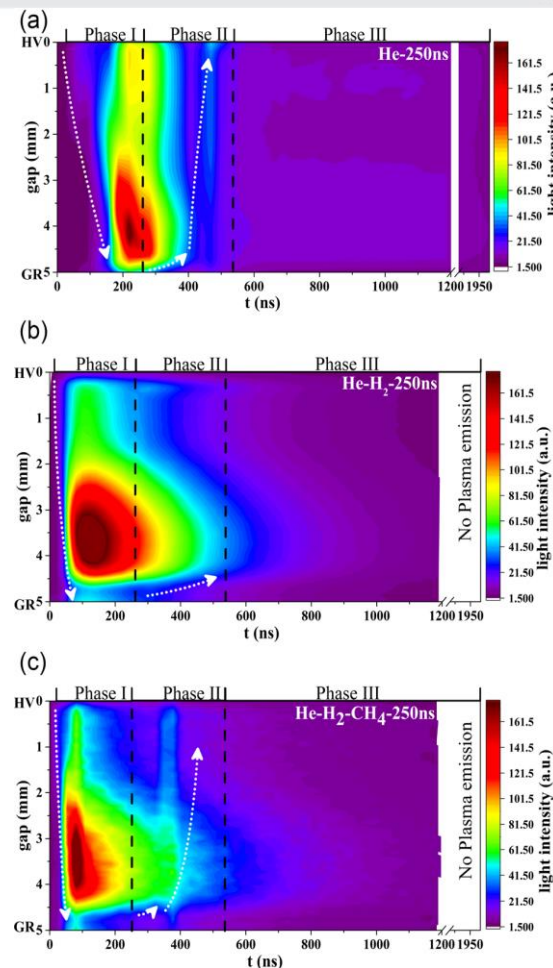
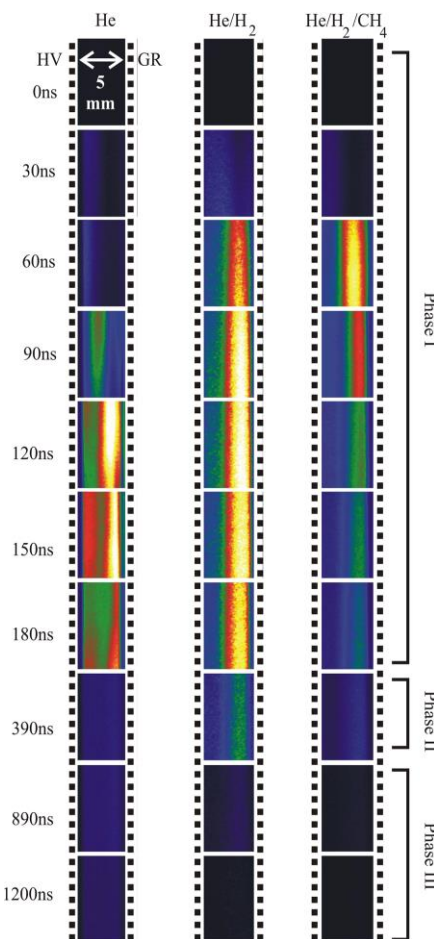


Fast ICCD images recorded during the pulse-on phase ($t = 5.2 \mu\text{s}$, gain = 600) and during the pulse-off phase ($t = 8.6 \mu\text{s}$ and $t = 99 \mu\text{s}$, gain = 800), for two magnetic flux densities of 0 and 15 mT. The average power was 110 W for $B = 0 \text{ mT}$ and 120 W for $B = 15 \text{ mT}$.





EXAMPLE:

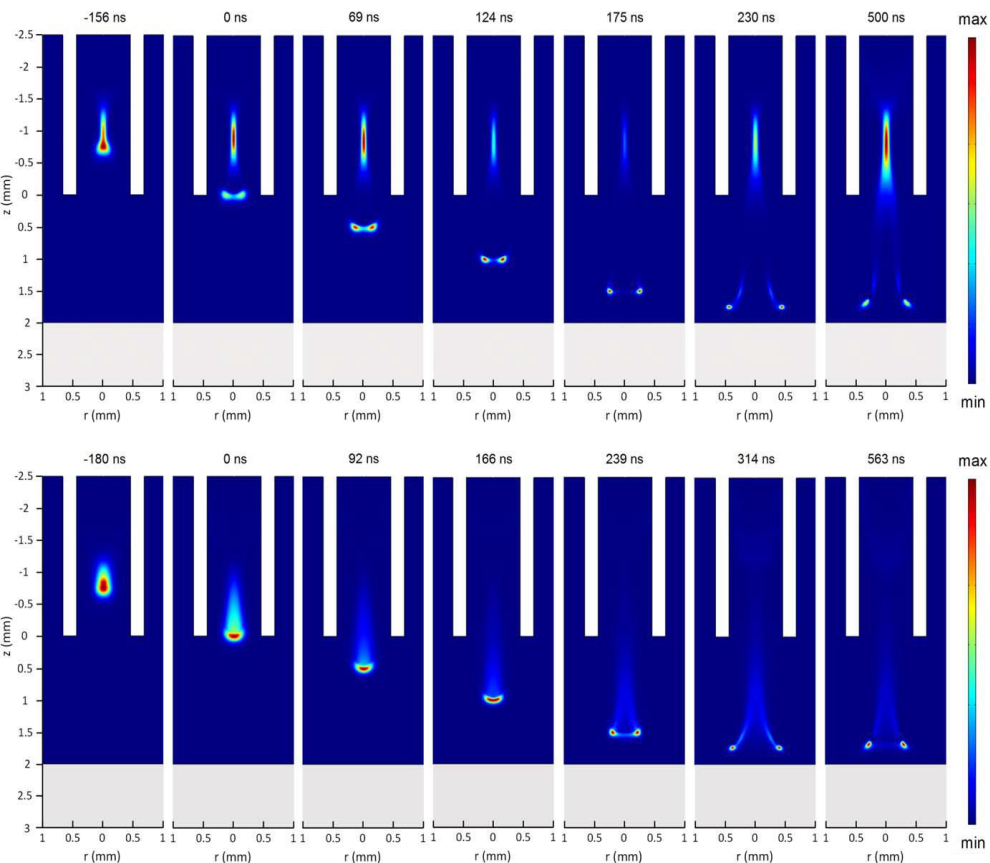
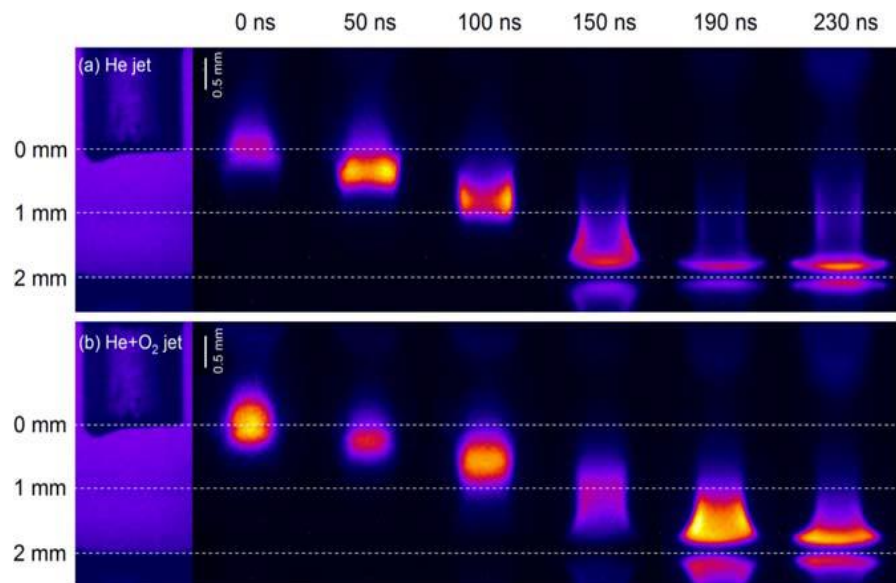


Time resolved image sequences (artificially colored) of atmospheric pressure plasma ignited in helium, helium-hydrogen, and helium-hydrogen-methane. The time axis represents the delay from the rise of the current pulses; dotted lines represent the electrode/dielectric surface. The spatial and temporal evolution of plasma emitted light observed from DBD source, for one voltage pulse.





EXAMPLE:



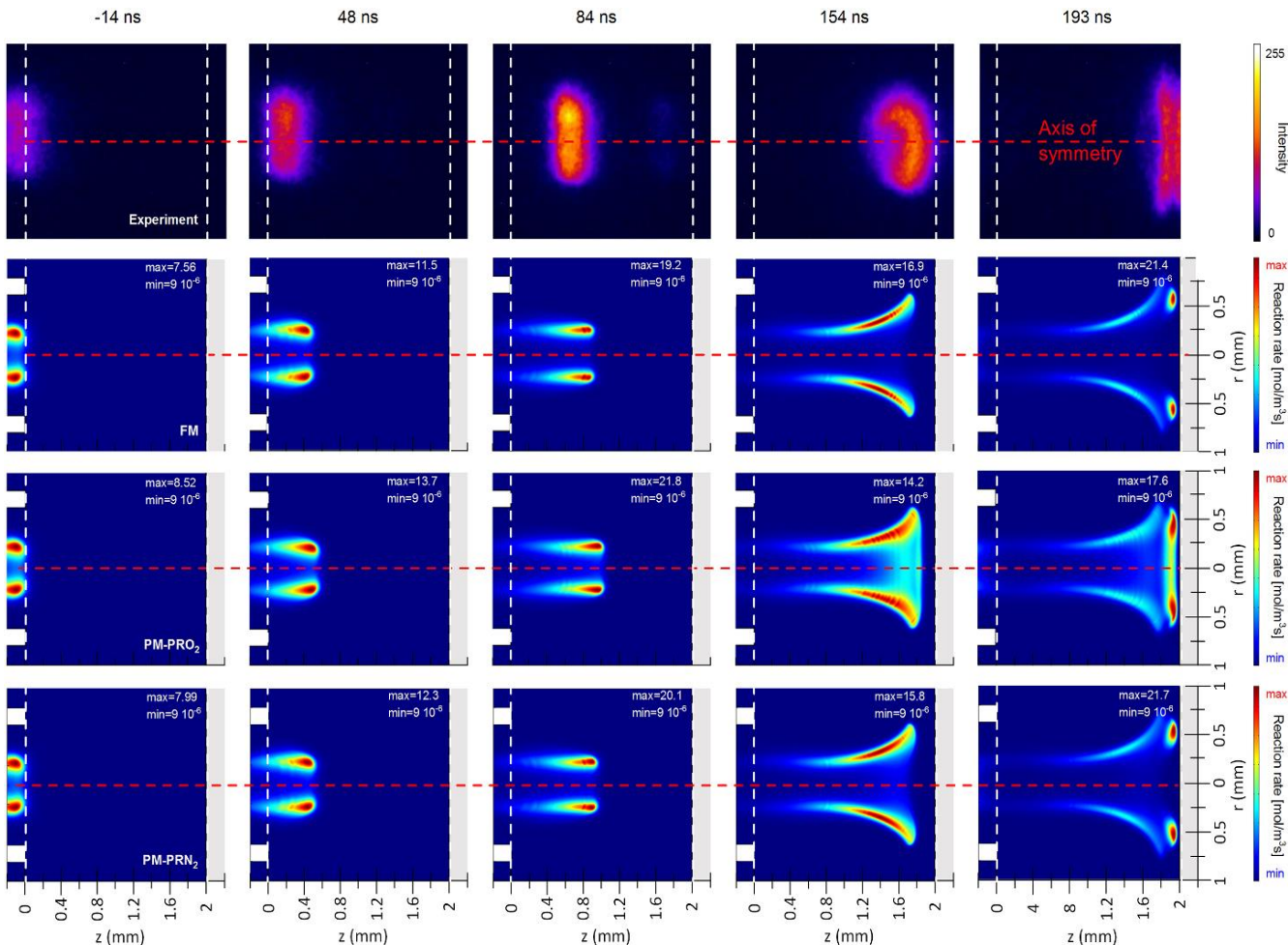
Spatio-temporal evolution of the plasma bullet for (a) He and (b) He+O₂ (1000 ppm) plasma jet. Time 0 ns corresponds to the plasma bullet just about the exit of the tube. The three dashed lines indicate the axial distance from the tube nozzle for z= 0, 1 and 2 mm. Simulation results of the spatio-temporal evolution of the total ionization rate for He and He+O₂ (1000 ppm) plasma jet where the secondary electron emission coefficient is set to zero.



<https://doi.org/10.1088/1361-6595/aadeb8>



EXAMPLE:



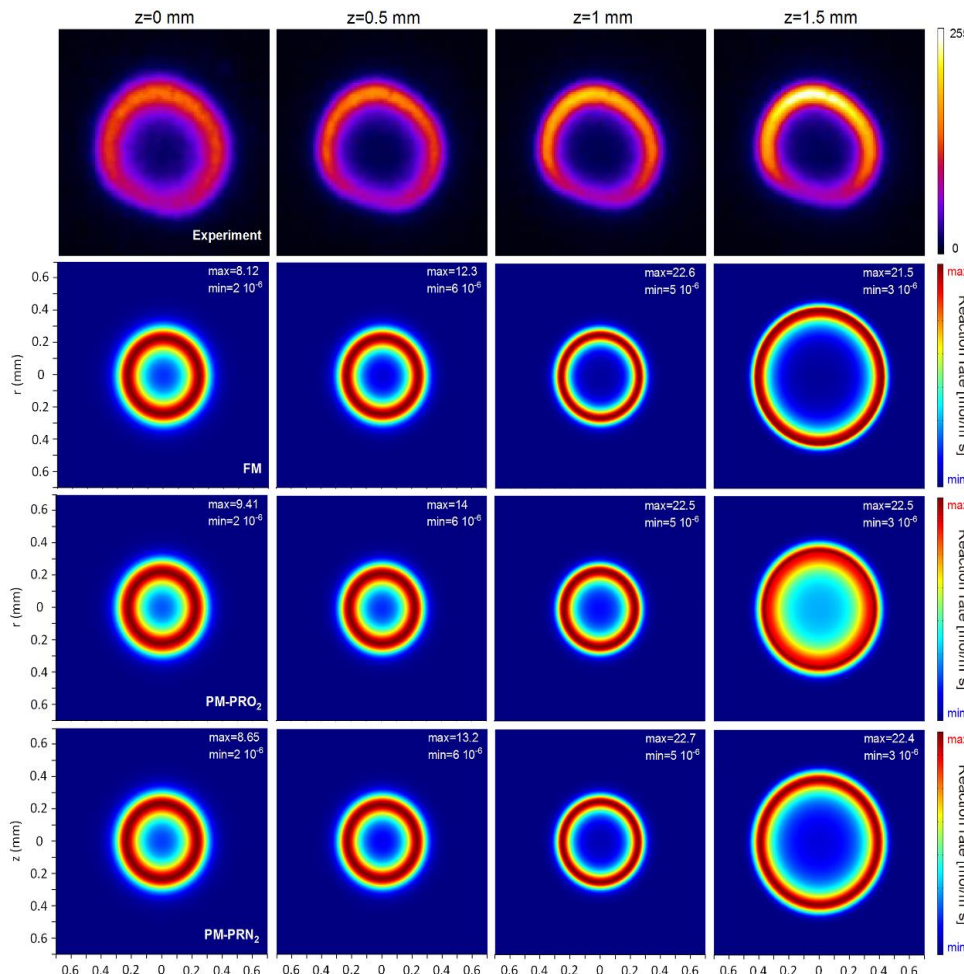
Axial view for a He plasma jet. Experimental measured relative intensity distributions of He line at 706.5 nm (first row), compared with the calculated reaction rate for the transition of $\text{He}(3s^3S) \rightarrow \text{He}(2p^3P)$.



<https://doi.org/10.1088/1361-6463/acb1c1>



EXAMPLE:



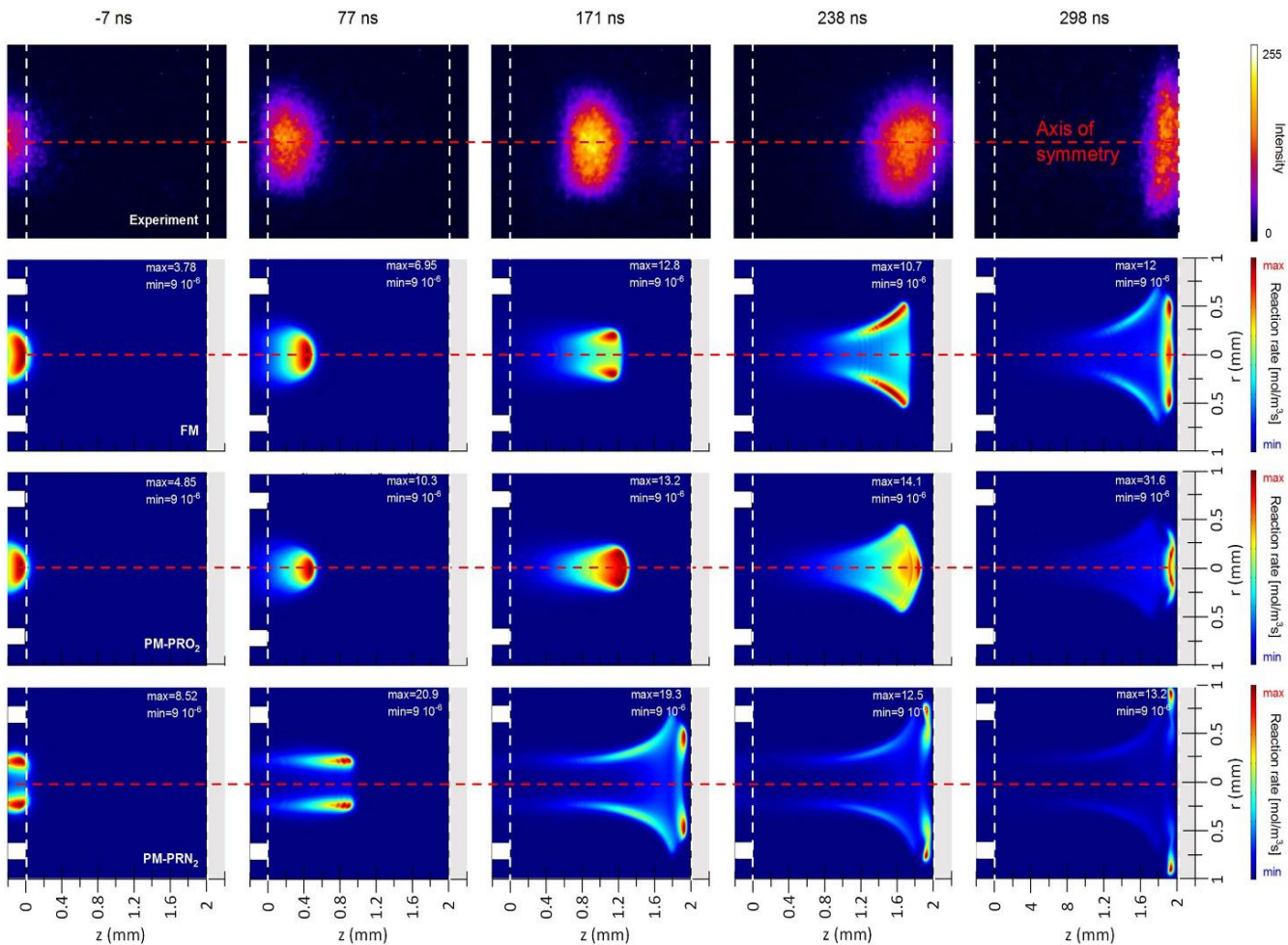
Radial view for a He plasma jet. Experimental measured relative intensity distributions of He line at 706.5 nm (first row), compared with the calculated reaction rate for the transition of $\text{He}(3s^3S) \rightarrow \text{He}(2p^3P)$.



<https://doi.org/10.1088/1361-6463/acb1c1>



EXAMPLE:



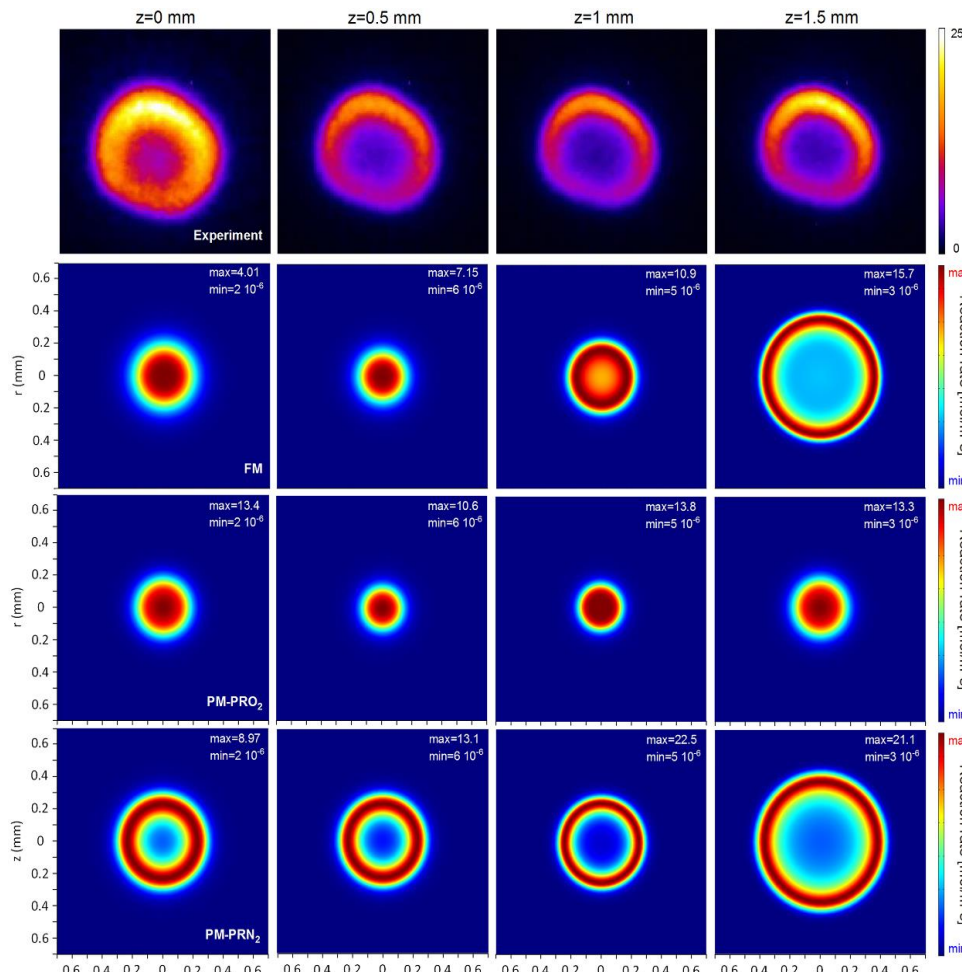
Axial view for a He + O₂ (1000 ppm) plasma jet. Experimental measured relative intensity distributions of He line at 706.5 nm (first row), compared with the calculated reaction rate for the transition of $\text{He}(3s^3S) \rightarrow \text{He}(2p^3P)$.



<https://doi.org/10.1088/1361-6463/acb1c1>



EXAMPLE:



Radial view for a He + O₂ (1000 ppm) plasma jet. Experimental measured relative intensity distributions of He line at 706.5 nm (first row), compared with the calculated reaction rate for the transition of He(3s³S)→He(2p³P).



<https://doi.org/10.1088/1361-6463/acb1c1>

Optical diagnosis: absorption spectroscopy



UNIVERSITATEA "ALEXANDRU IOAN CUZA" din IAŞI

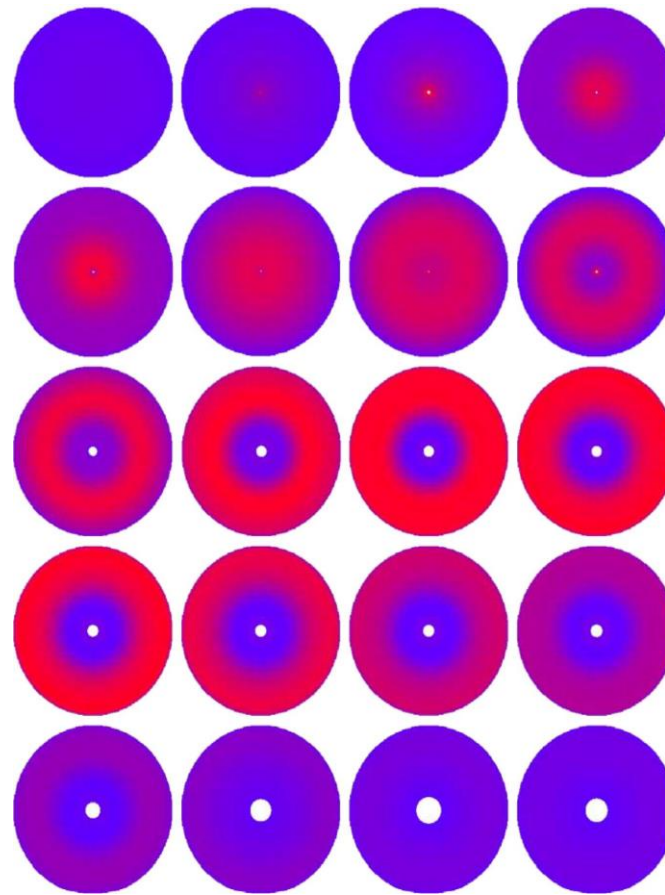
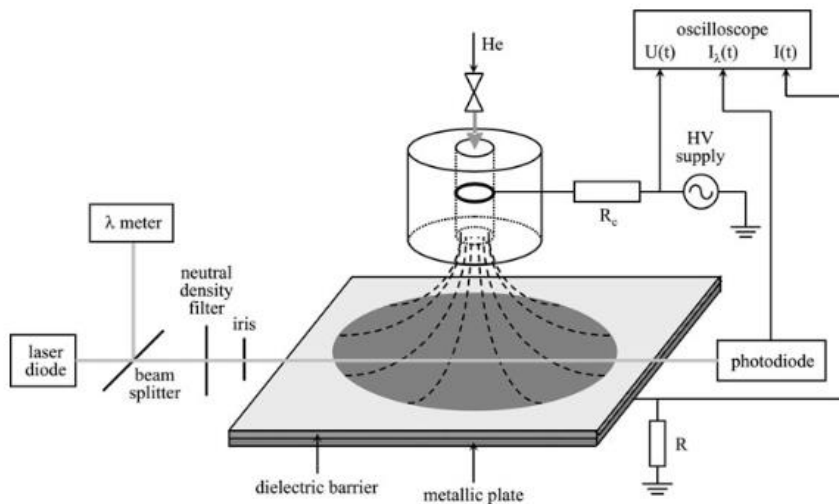
www.uaic.ro

Equipment and materials:

- tunable laser diodes
- control unit for diode temperature and current
- beam optics
- computer



EXAMPLE:



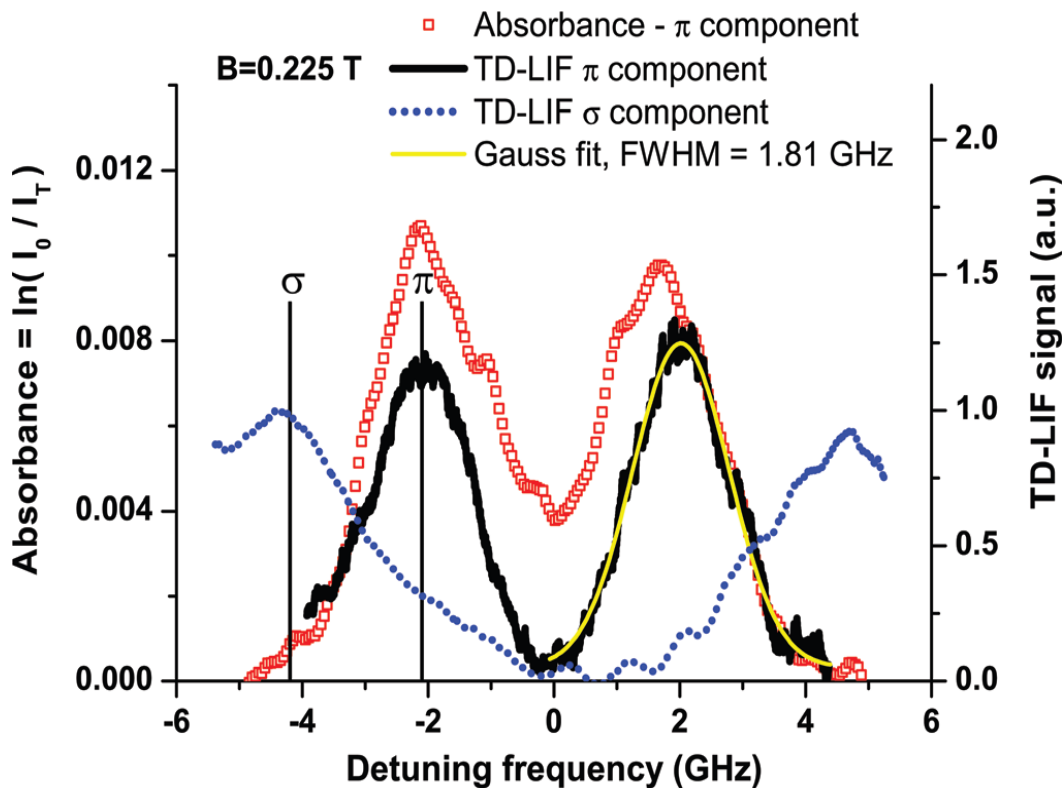
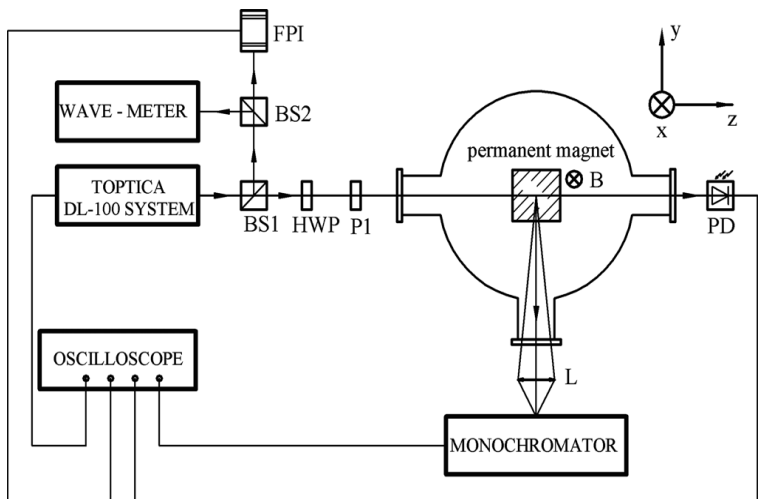
Dielectric Barrier Discharge: time evolution of the spatial distribution of 3^5S_2 oxygen metastable atoms, within the time interval 0.2-4.0 μ s (reported to ignition moment), in 0.2- μ s steps.



<https://doi.org/10.1109/TPS.2011.2145005>
<https://doi.org/10.1007/s11090-011-9314-3>



EXAMPLE:

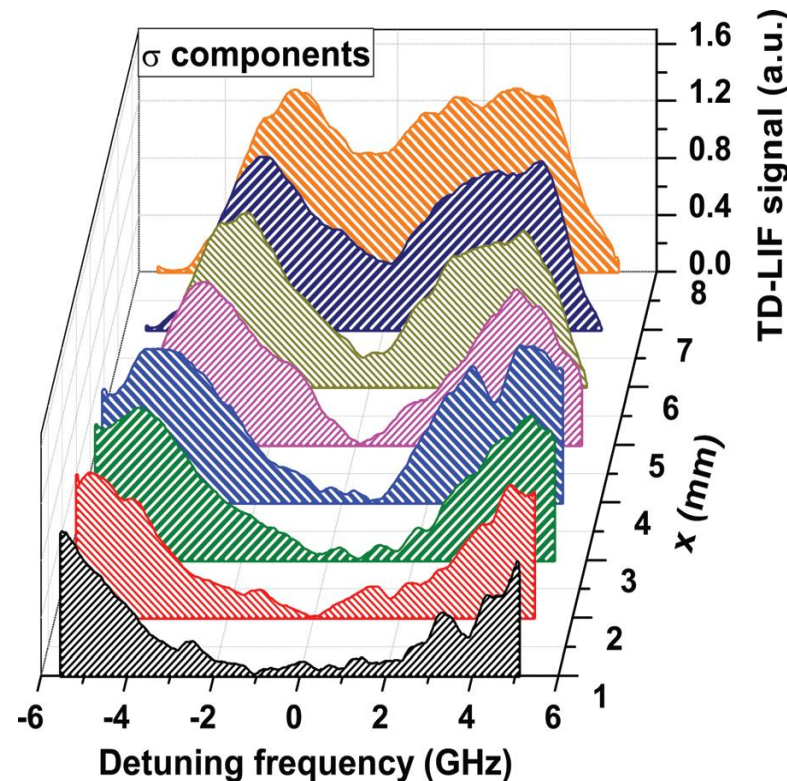
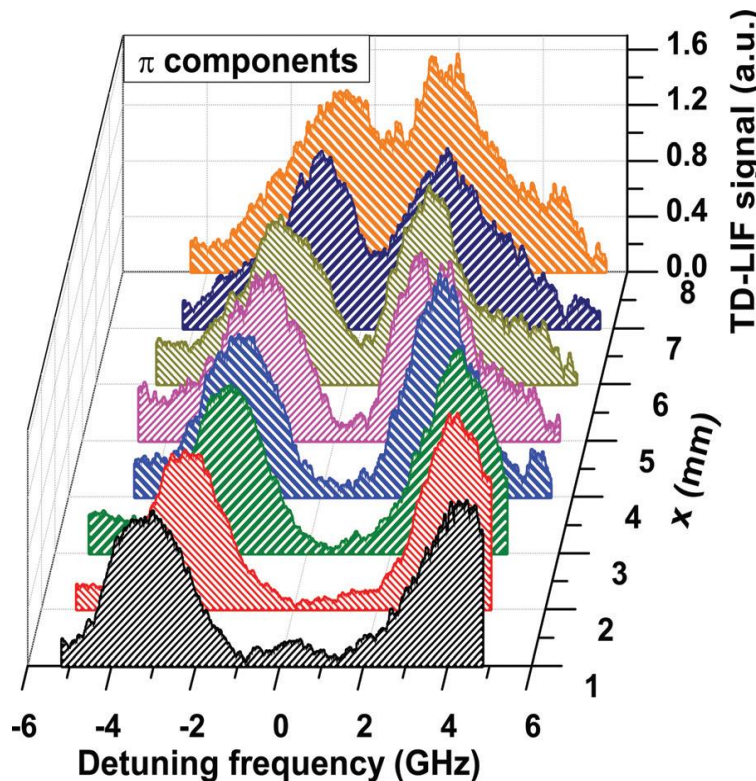


Magnetron plasma: Aluminum absorption profile (394.401 nm) of the π components (open squares); TD-LIF signal (396.15 nm) corresponding to π (full line) and σ (dotted line) components; The theoretical positions of the π ($g_{eff-\pi}^{394} \pm 2/3$) and σ ($g_{eff-\sigma}^{394} \pm 4/3$) components, corresponding to the measured magnetic field strength of $B = 0.225$ T are marked with vertical black lines. The Gaussian fit of one experimental TD-LIF π component is also plotted.





EXAMPLE:



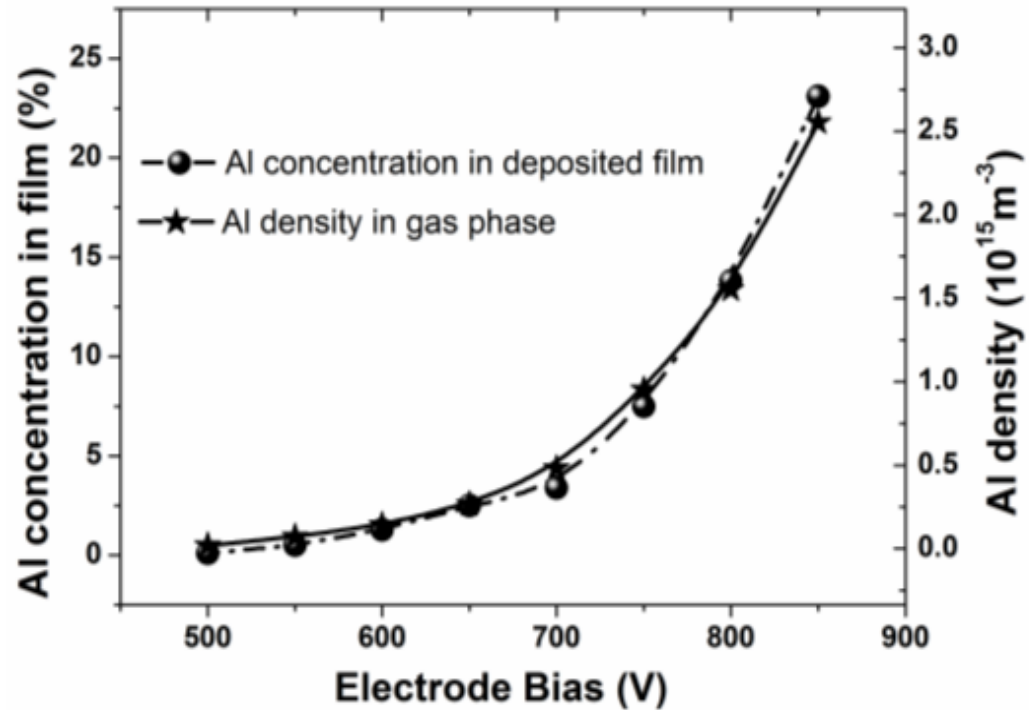
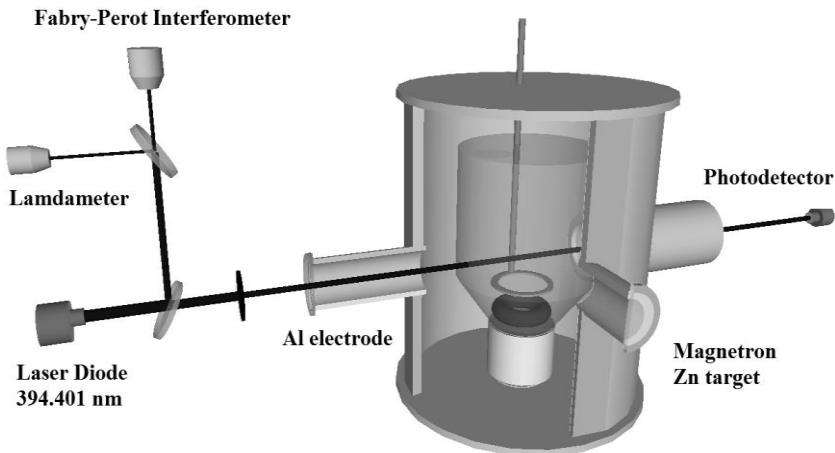
Magnetron plasma: Experimental TD-LIF profiles of the π and σ components corresponding to the aluminum $^2S_{1/2} \longleftrightarrow ^2P_{1/2}$ transition at different distances from an additional magnet surface corresponding to different magnetic field strengths.



<http://dx.doi.org/10.1063/1.3579446>



EXAMPLE:



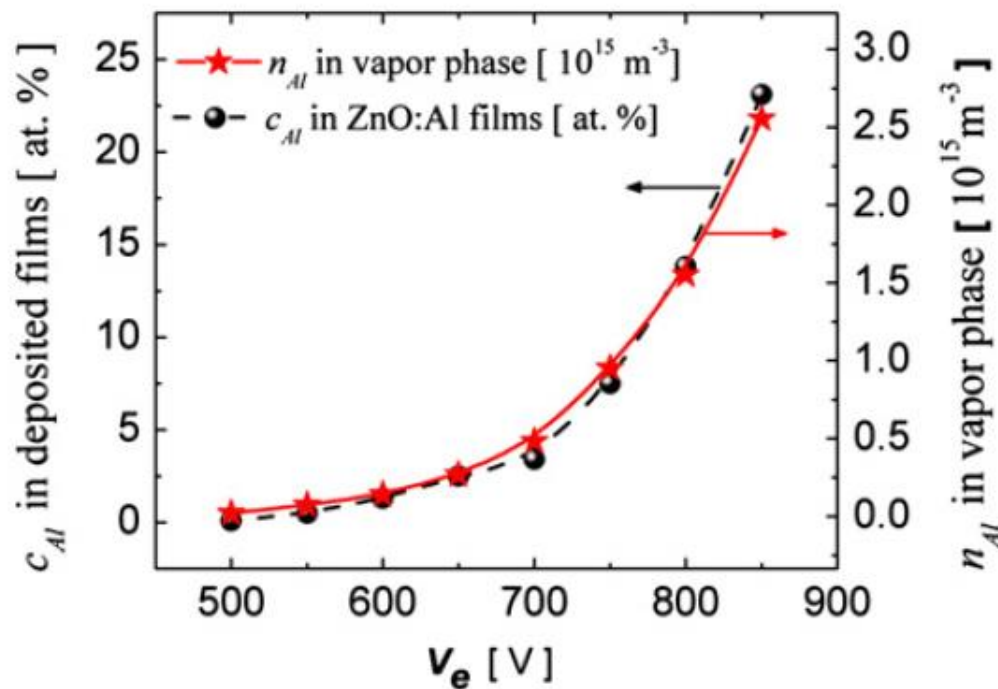
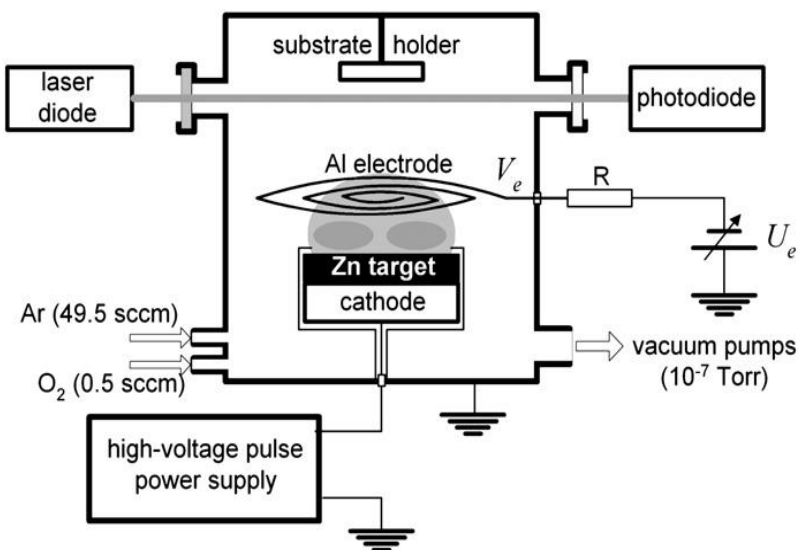
High Power Impulse Magnetron Sputtering (HIPIMS): Aluminum atom concentration measured in gas phase and aluminum atom concentration in the deposited films ((gas pressure = 50 mTorr, $\text{O}_2/\text{Ar} = 1\%$, pulse repetition frequency = 1 kHz, pulse width = 6 μs).



<http://dx.doi.org/10.1088/1757-899X/39/1/012010>



EXAMPLE:

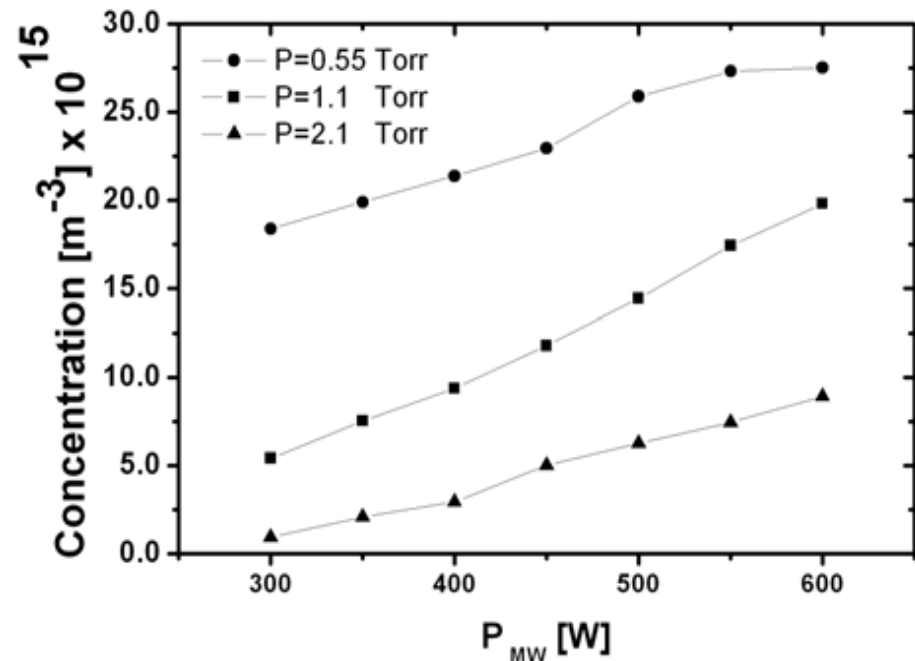
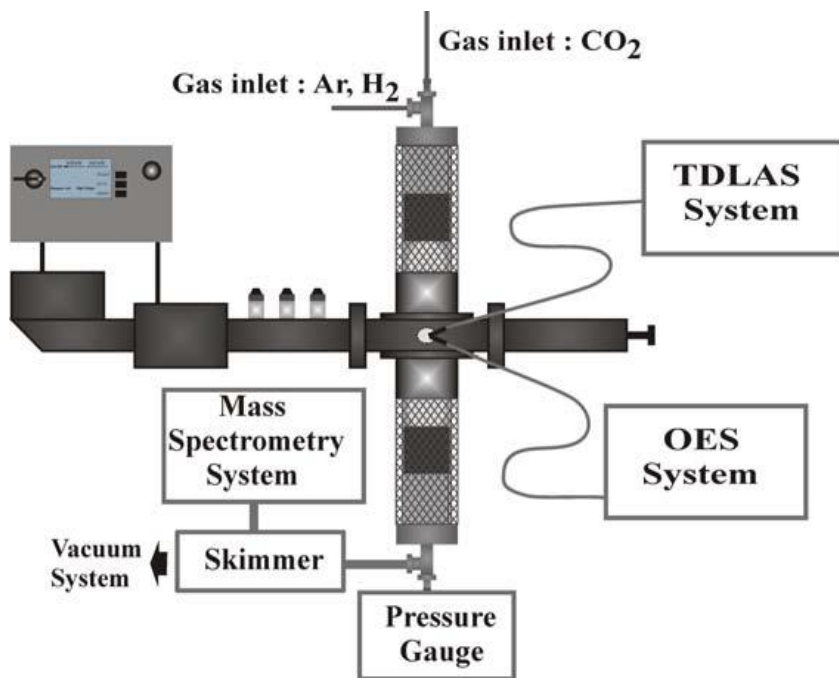


High Power Impulse Magnetron Sputtering (HIPIMS): Dependence of Al concentration in vapor phase, n_{AL} (m^{-3}), and in deposited films, c_{AL} (at.%), on the electrode biasing potential, V_e .





EXAMPLE:

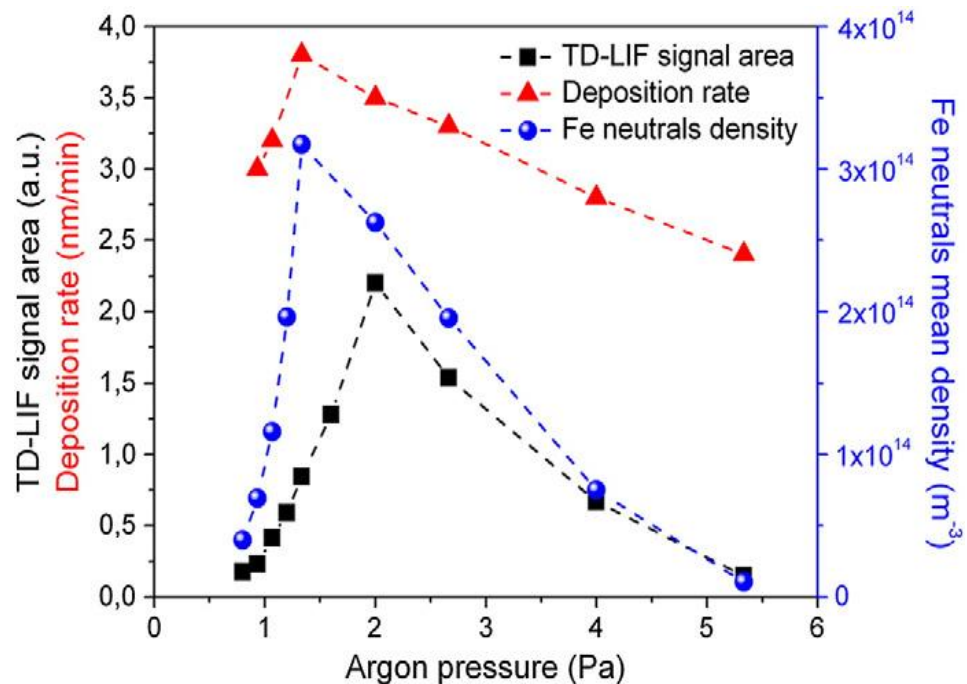
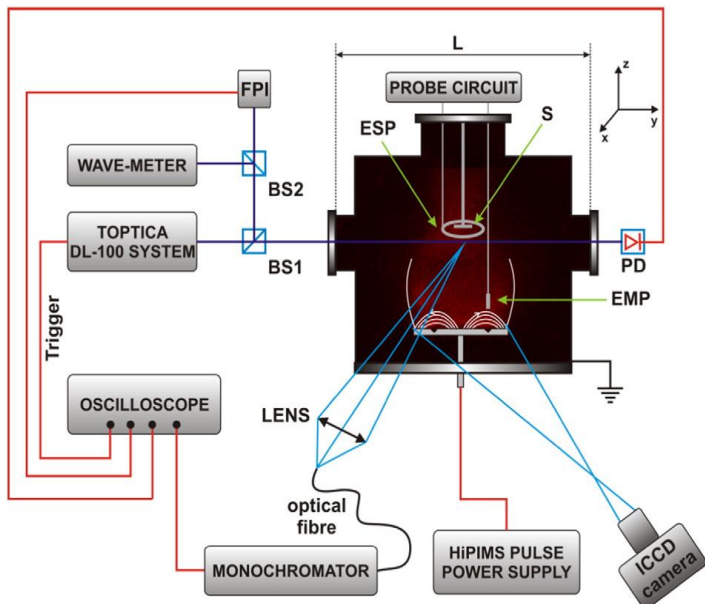


Microwave discharge: the evolution of oxygen metastables density with microwave discharge power and with increasing of the carbon dioxide pressure.





EXAMPLE:

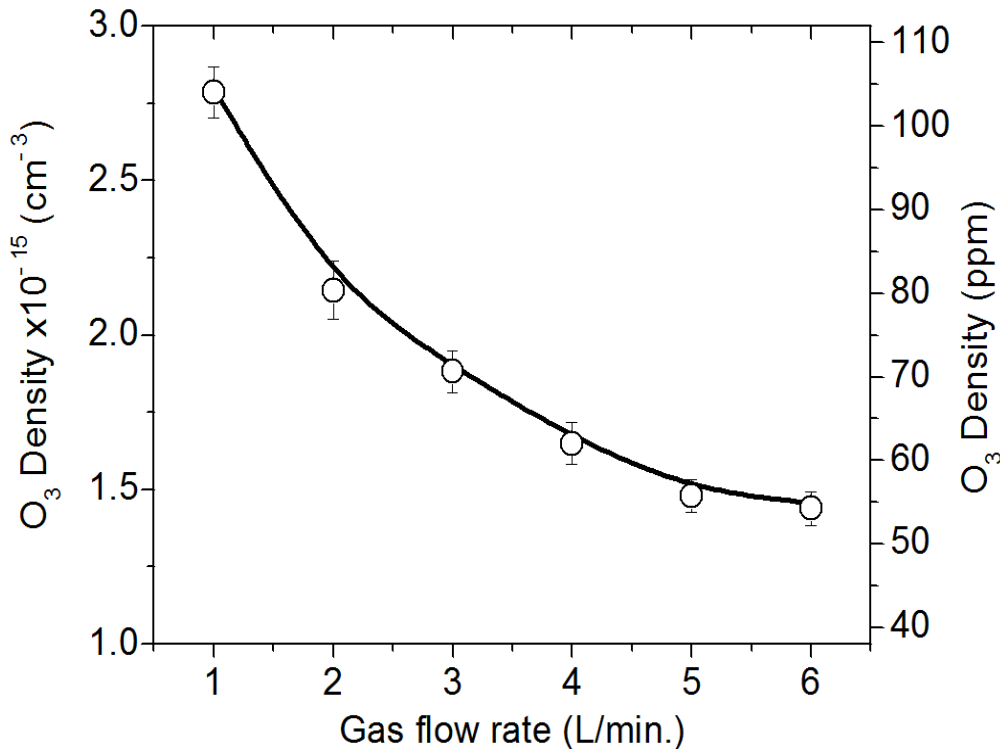
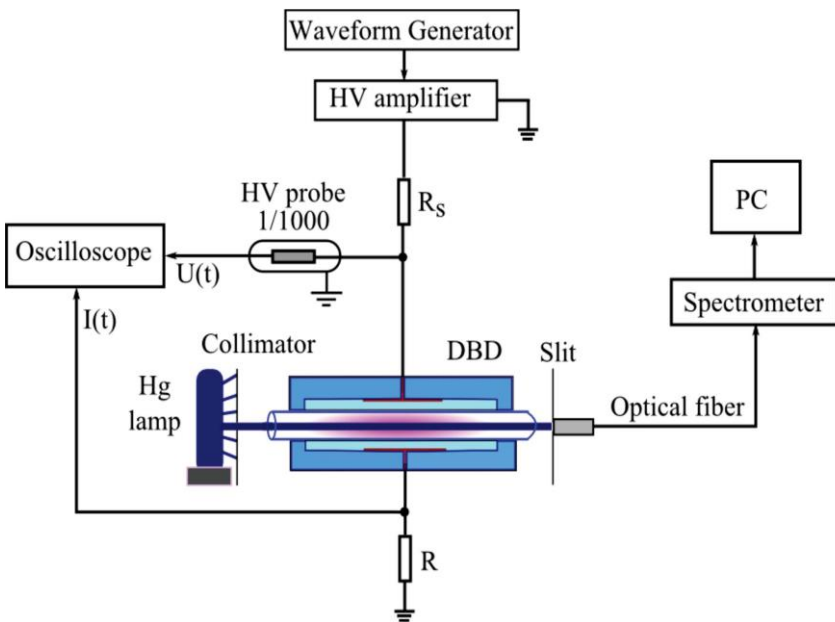


High Power Impulse Magnetron Sputtering (HIPIMS): simplified schematic of the experimental device (FPI—Fabry-Pérot interferometer, PD—photodiode, BS—beamsplitter, ESP—electrostatic probe, EMP—emissive probe, S—substrate, L—optic distance of the laser beam probing the plasma volume); TD-LIF signal area, Fe neutral mean density and deposition rate dependence on the argon pressure (30W average discharge power, 4 μ s pulse duration).





EXAMPLE:

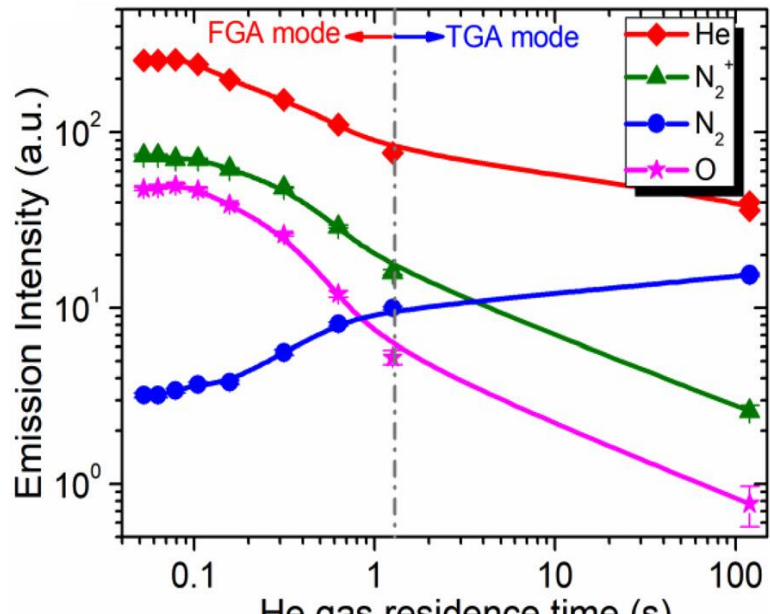


Dielectric Barrier Discharge: schematic of the experimental setup and Variation of the average absolute density of O_3 in the He + 0.5% O_2 -DBD plasma with the total gas flow rate. Voltage pulse width and its amplitude were kept constant at 35 μ s and 5.2 kV, respectively, while its frequency was 6 kHz.

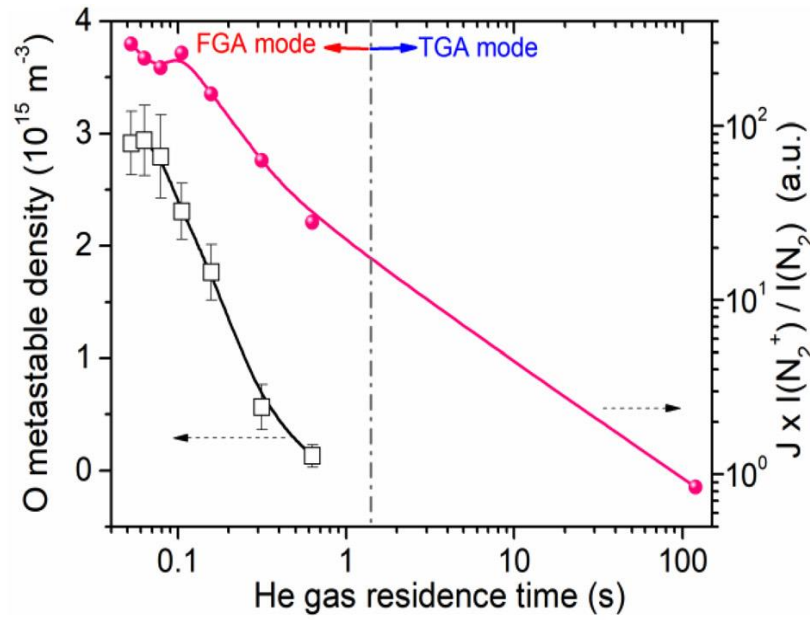




EXAMPLE:



(a)



(b)

Relative emission intensities of various excited species (a); O ($3\ ^5S_2$) metastable density and relative density of He metastable (b) vs helium gas residence time. In the FGA mode, the helium flow rate varies from 6 L/min to 0.25 L/min.



Optical diagnosis: photography



UNIVERSITATEA "ALEXANDRU IOAN CUZA" din IAŞI

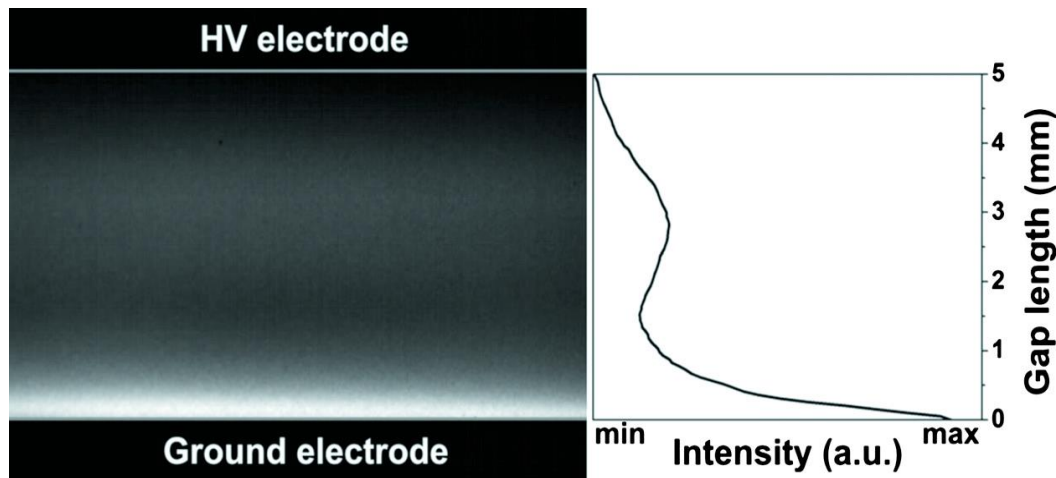
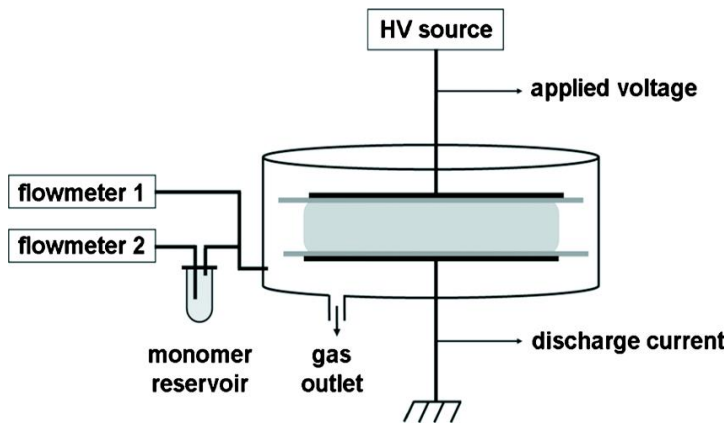
www.uaic.ro

Equipment and materials:

- Camera
- Spectral filters
- Computer



EXAMPLE:



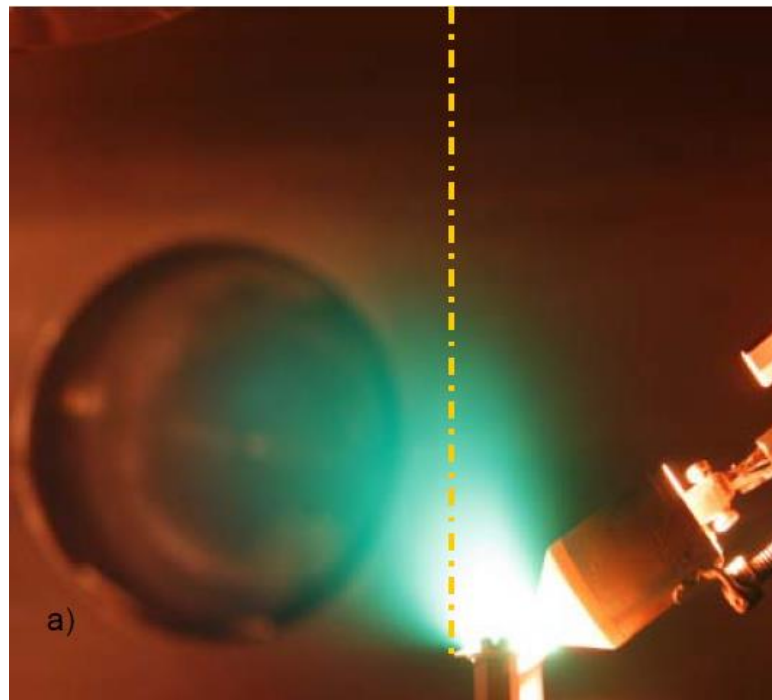
The axial intensity of a plane-parallel Dielectric Barrier Discharge, 7.5 W dissipated power (HV pulse parameters: 3 kV, 2 kHz, 250 μ s, positive polarity). The negative glow is uniformly distributed in the cathode vicinity, while the positive column can be also identified in the space between electrodes which is in accordance with the classic behavior of a Townsend glow discharge.



<https://doi.org/10.1063/1.3506528>



EXAMPLE:



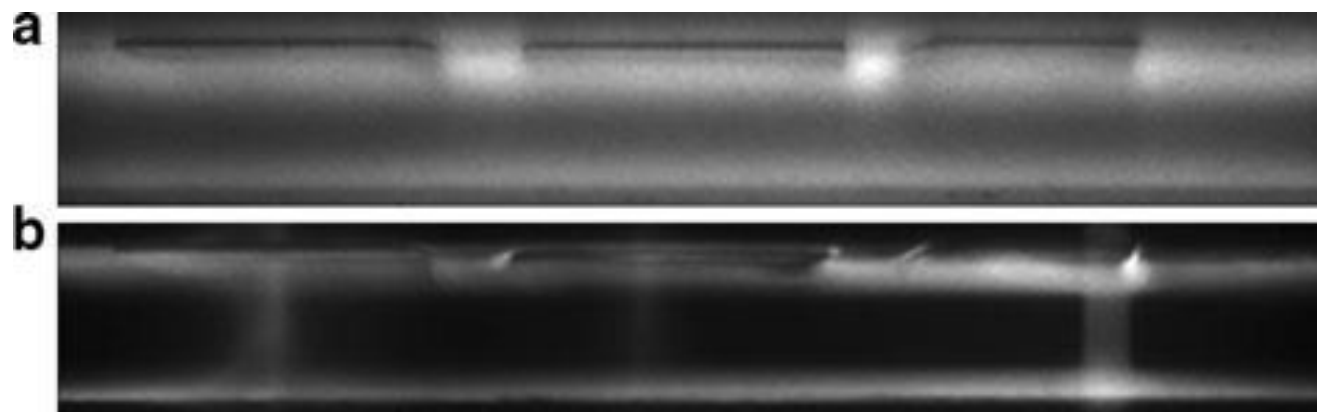
Thermionic vacuum arc plasma (TVA): plasma image and dashed line - emissive probe path.



https://rjp.nipne.ro/2011_56_Suppl/RomJPhys.56s.p41.pdf



EXAMPLE:



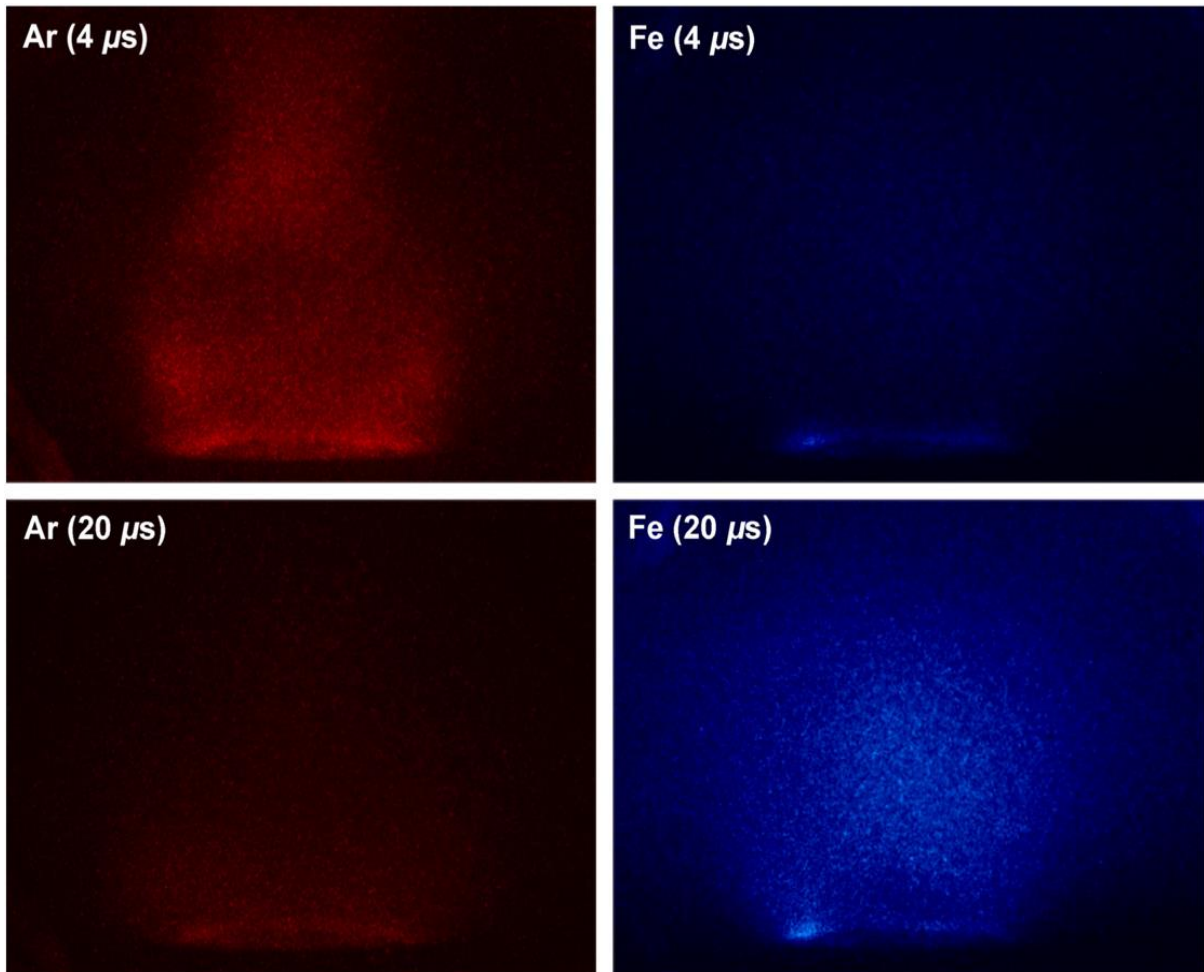
Dielectric Barrier Discharge: Plasma image (integral light emission) in the He-DBD (a) and Ar-DBD (b), during polymers treatment.



<https://doi.org/10.1007/s11090-013-9442-z>



EXAMPLE:



High Power Impulse Magnetron Sputtering (HIPIMS): On-pulse fast ICCD images registered at $4\text{ }\mu\text{s}$ and $20\text{ }\mu\text{s}$ respectively, with red (Ar) and blue (Fe) optical filters (1.33 Pa argon pressure and 30W average power).



<http://dx.doi.org/10.1016/j.surfcoat.2014.03.015>

Mass spectrometry



UNIVERSITATEA "ALEXANDRU IOAN CUZA" din IAŞI

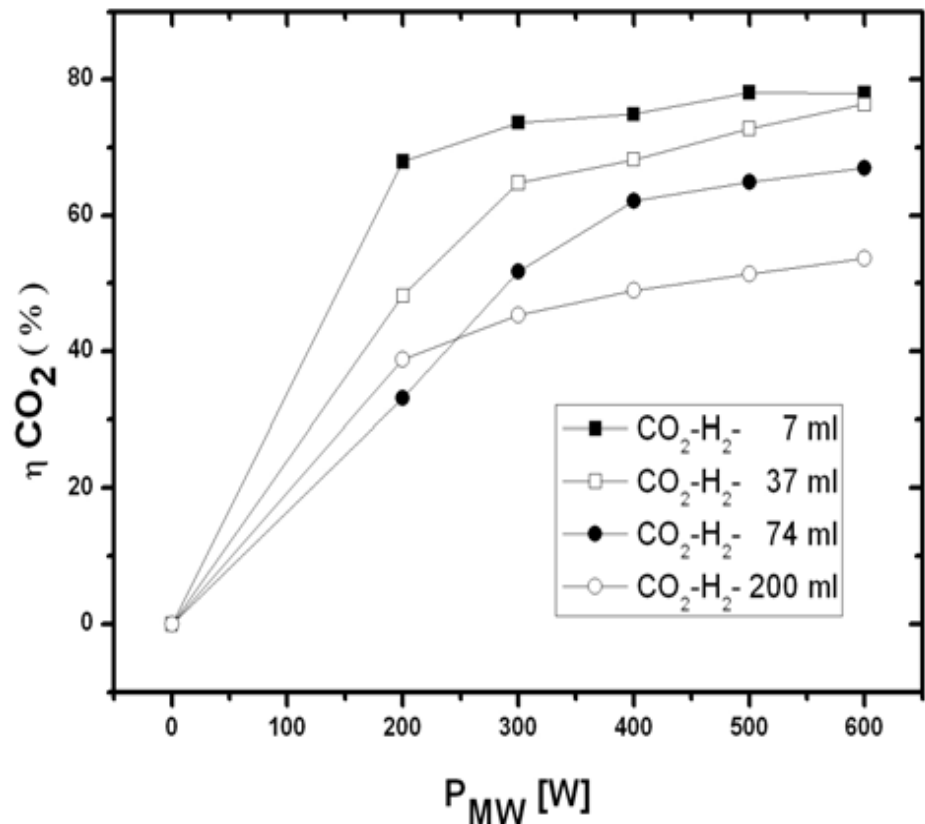
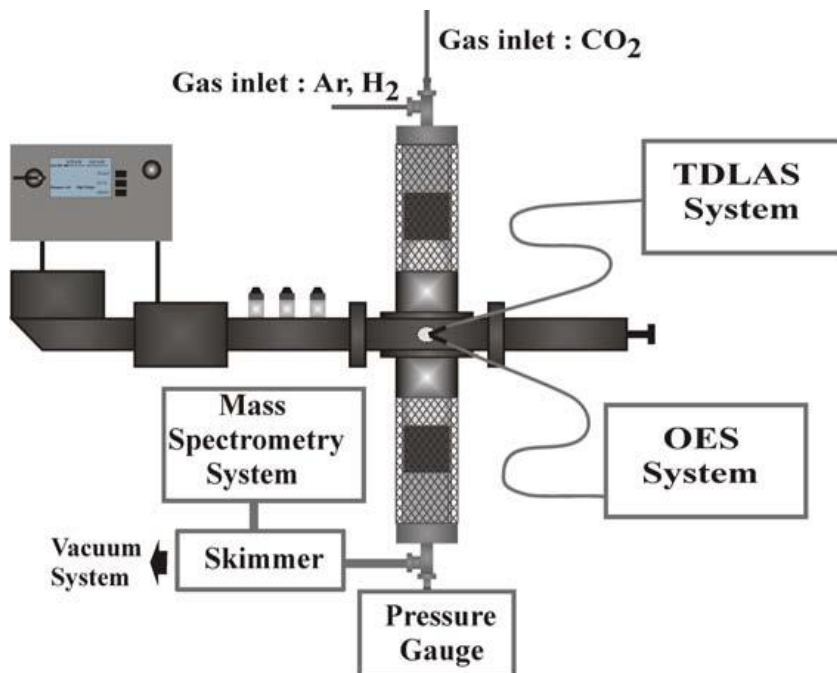
www.uaic.ro

Equipment and materials:

- Mass spectrometer
- Computer



EXAMPLE:



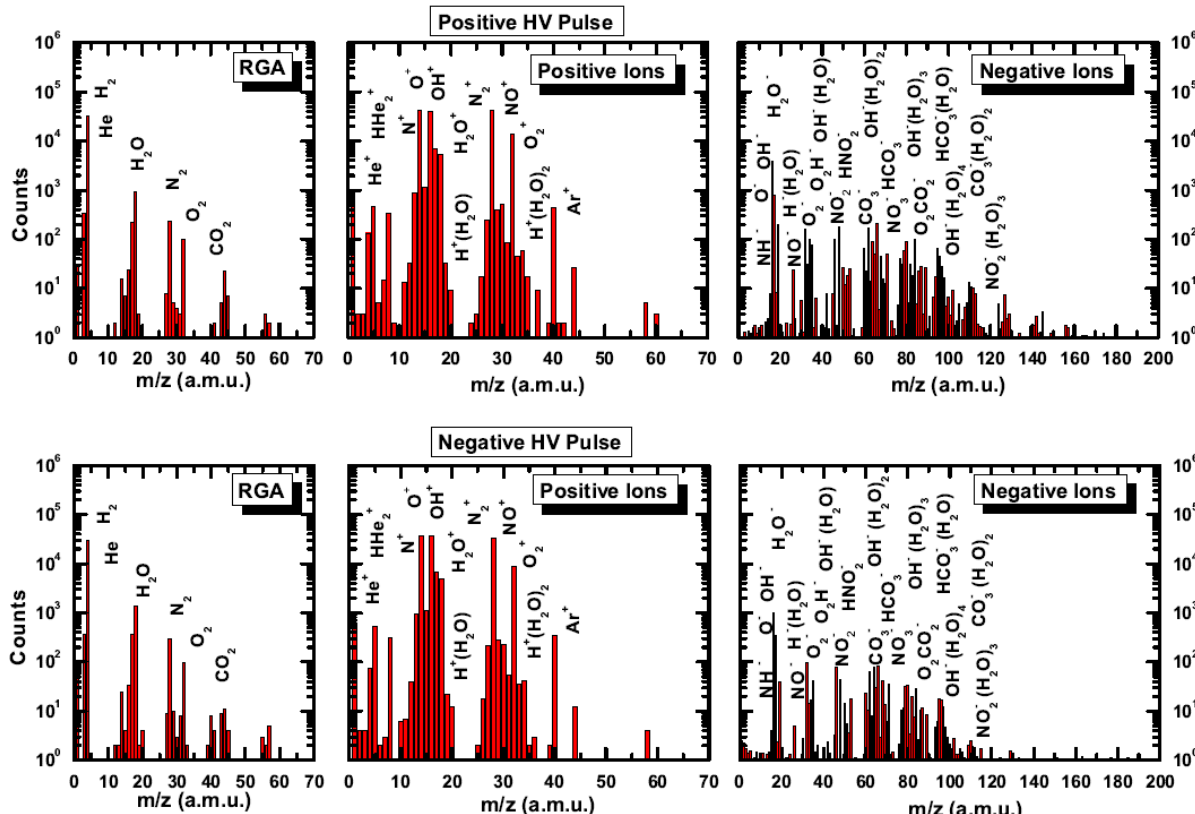
Microwave discharge: the percentage of CO₂ dissociation in microwave discharge plasma produced in CO₂ and H₂.



https://rrp.nipne.ro/2014_66_4/A22.pdf



EXAMPLE:



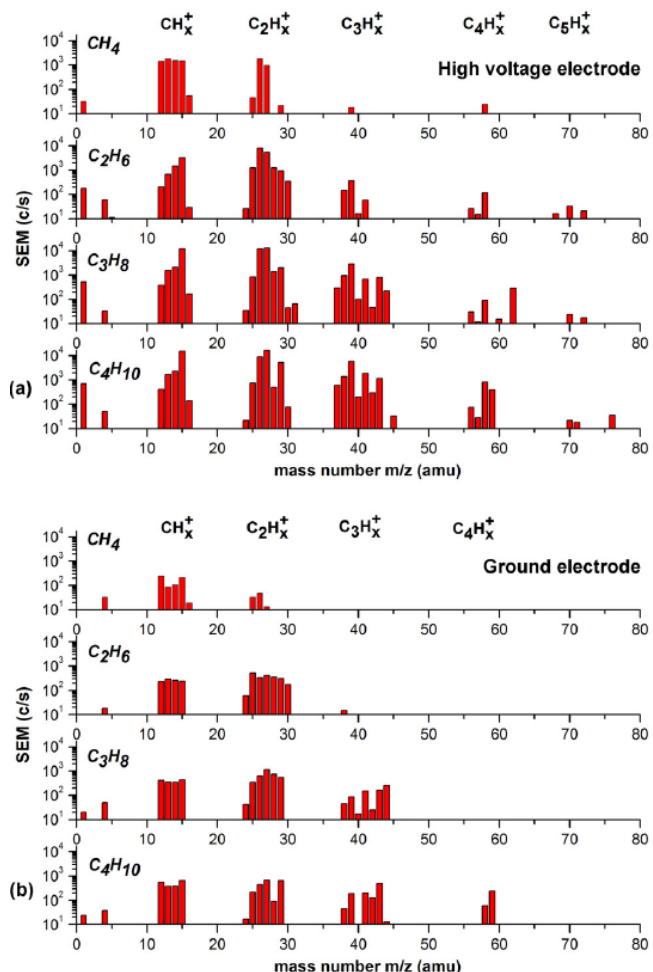
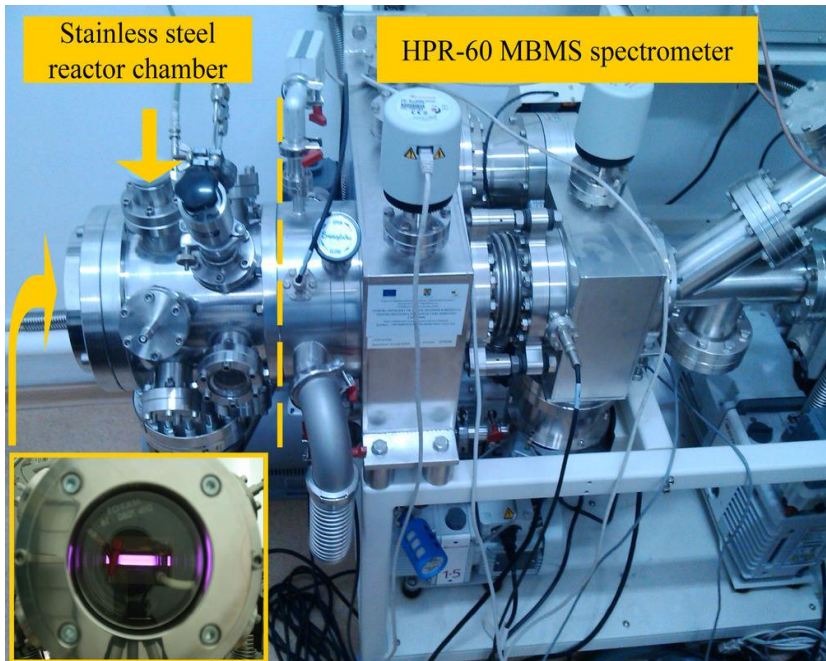
Typical residual gas analysis (RGA), positive and negative ions spectra of the helium Atmospheric Pressure Plasma Jet (APPJ) (HV pulse parameters: 6.5 kV, 4 kHz, 50 µs, positive and negative polarity; 10 mm distance between discharge tube nozzle and sampling orifice of HPR 60 MBMS).



<https://doi.org/10.3390/app7080812>



EXAMPLE:



Parallel plate DBD: subtracted positive ion mass spectra of plasma fed with $\text{He}/\text{H}_2=\text{C}_n\text{H}_{2n+2}$ ($n = 1-4$) relative to He/H_2 plasma.

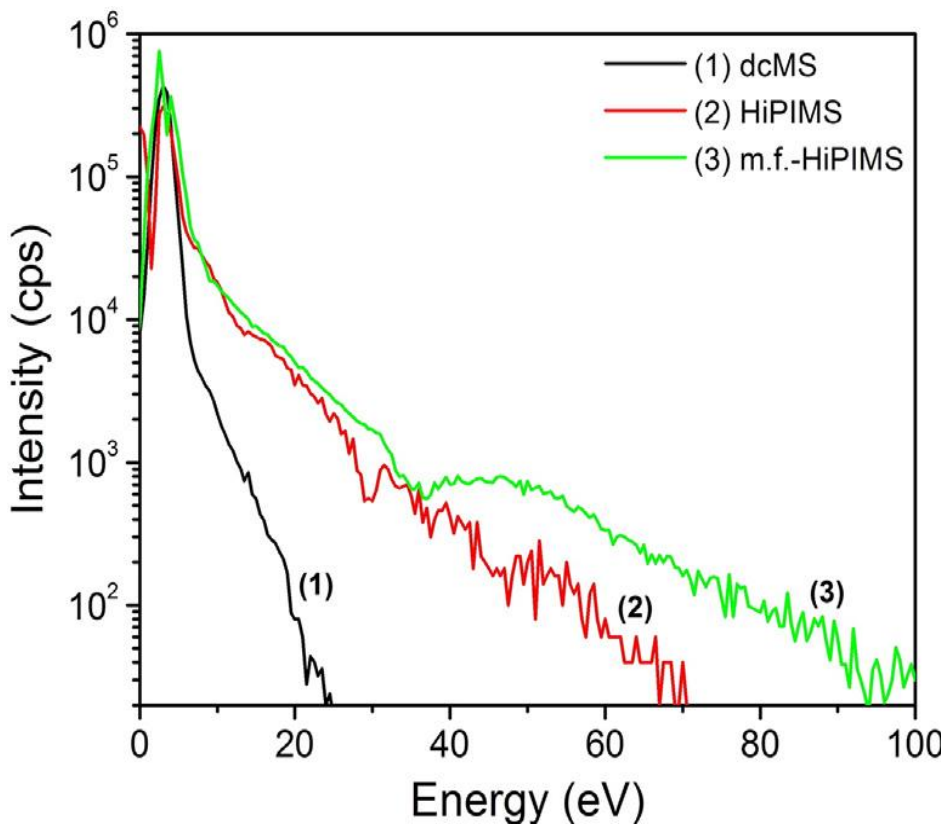
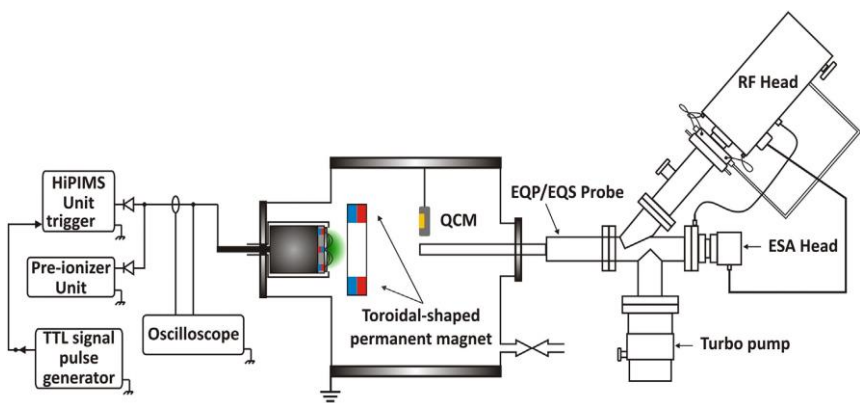
Sampling from high voltage electrode region (a) and from ground electrode region (b).



<http://dx.doi.org/10.1016/j.asr.2016.08.010>



EXAMPLE:



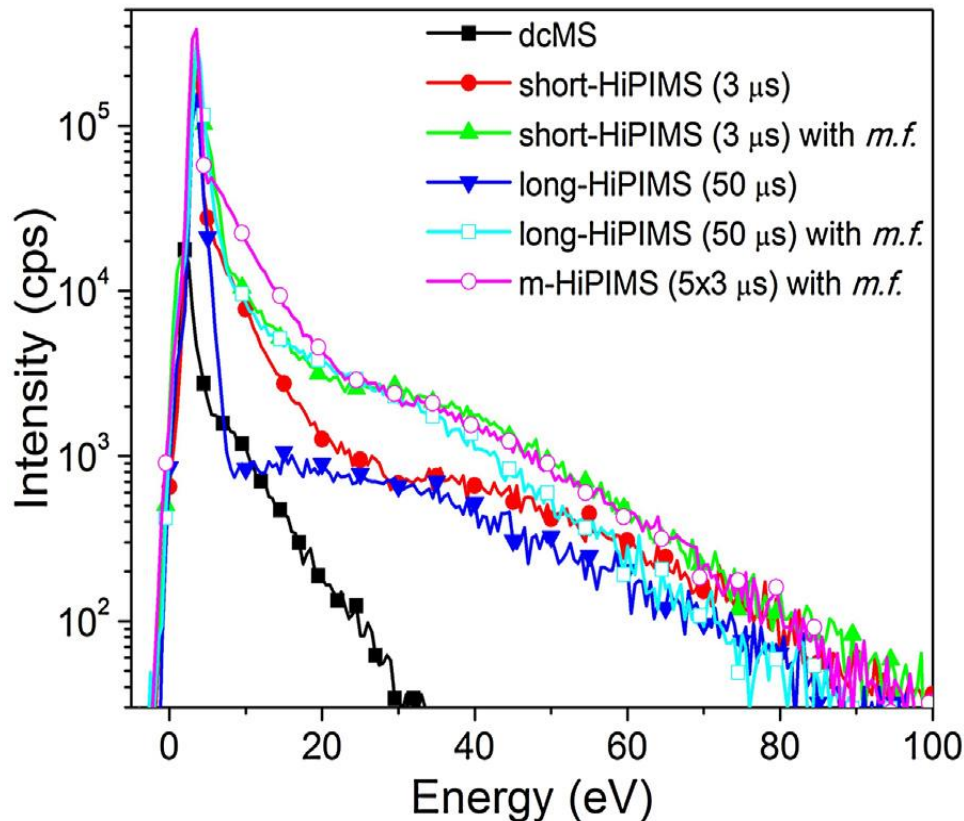
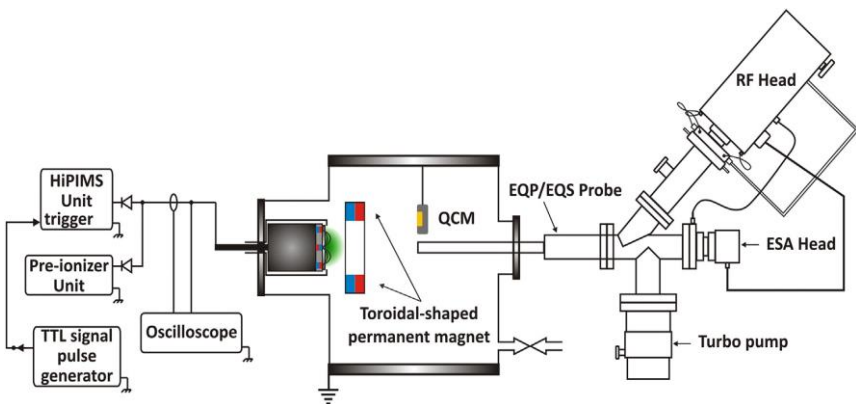
Time-averaged energy distributions of Cu^+ sputtered in dc magnetron sputtering and HiPIMS with and without external magnetic field, respectively.



<http://dx.doi.org/10.1016/j.surfcoat.2016.11.001>



EXAMPLE:



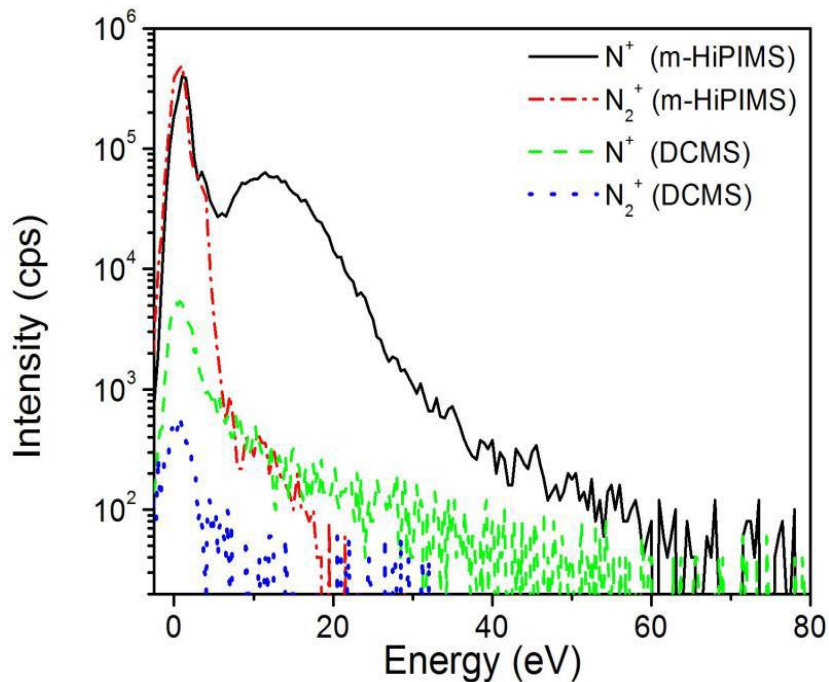
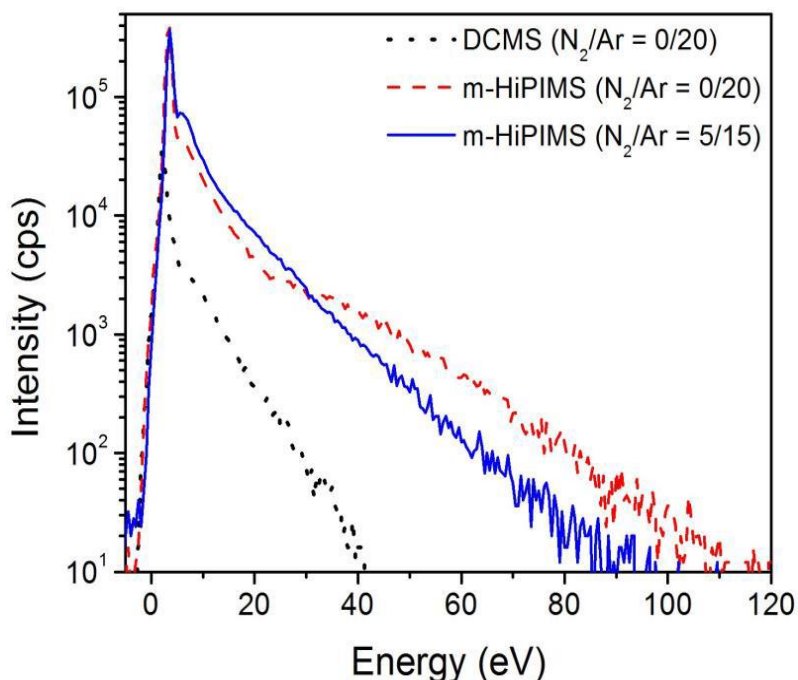
Time-averaged energy distribution functions of W^+ ions sputtered in: dcMS, short-HiPIMS, short-HiPIMS with m.f., long-HiPIMS, long-HiPIMS with m.f., and m-HiPIMS with m.f.



<http://dx.doi.org/10.1016/j.apsusc.2017.01.067>



EXAMPLE:



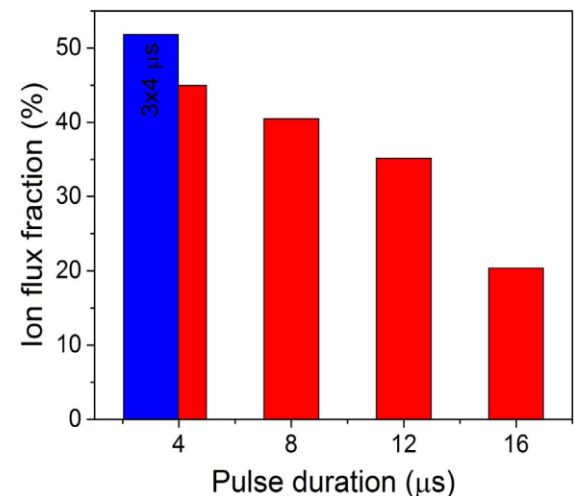
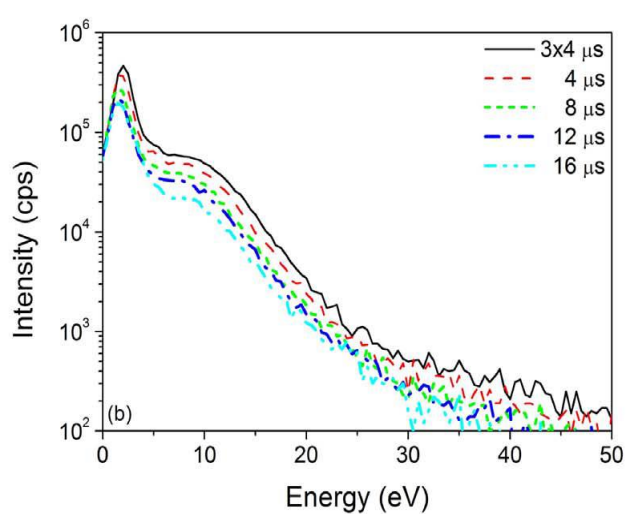
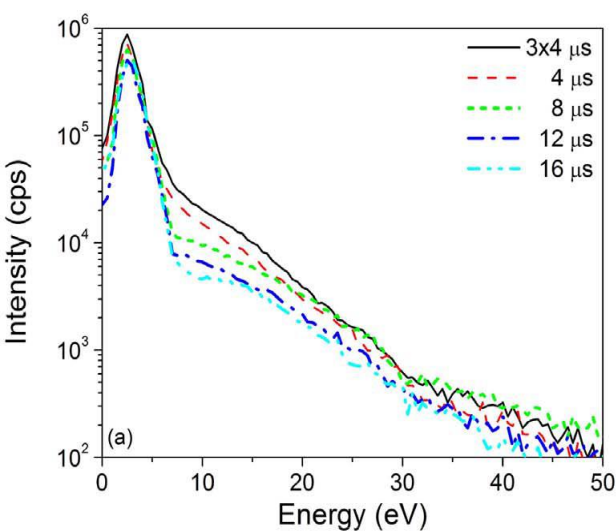
Time-averaged energy distributions of W^+ sputtered, N^+ and N_2^+ in DC magnetron sputtering and m-HiPIMS, respectively.



<http://dx.doi.org/10.1016/j.apsusc.2017.04.183>



EXAMPLE:



Titanium (a) and nitrogen (b) ion energy distribution functions versus pulse duration.
Ionized flux fraction in m-HiPIMS and HiPIMS versus pulse duration.



<https://doi.org/10.1016/j.surfcoat.2017.11.048>

Gas-phase FTIR spectroscopy



UNIVERSITATEA "ALEXANDRU IOAN CUZA" din IAŞI

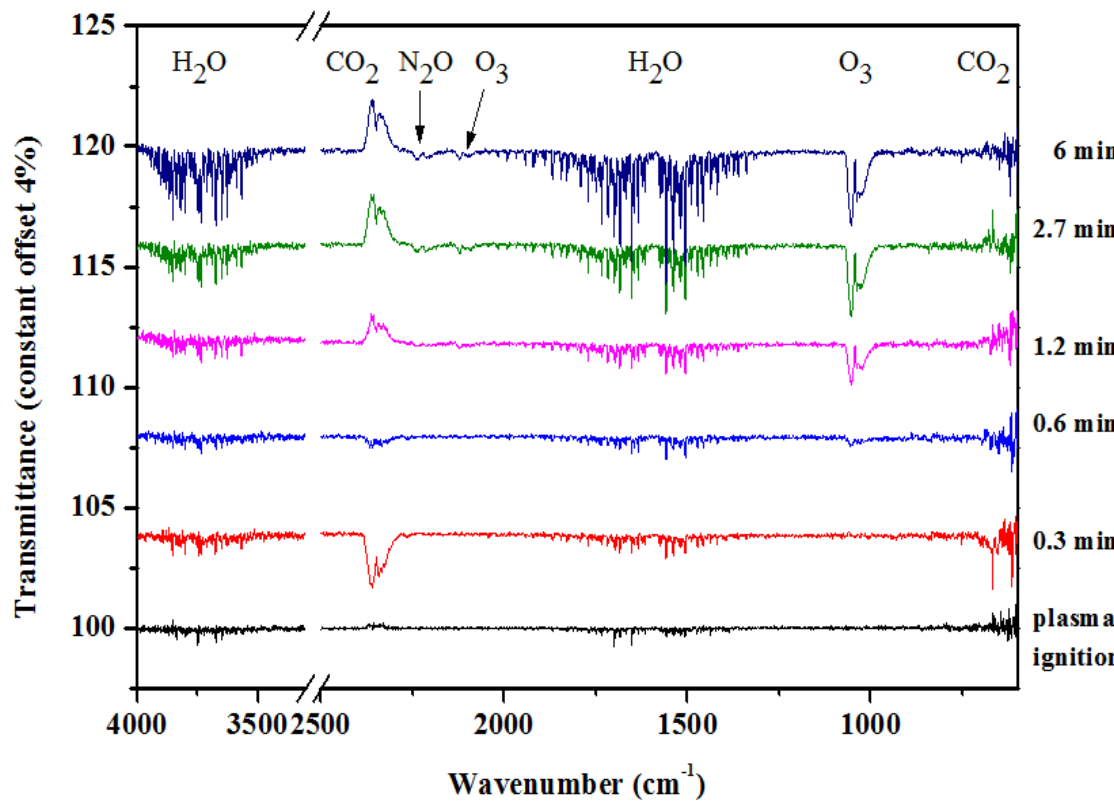
www.uaic.ro

Equipment and materials:

- FTIR spectrometer
- Gas cells and IR optics
- Computer



EXAMPLE:



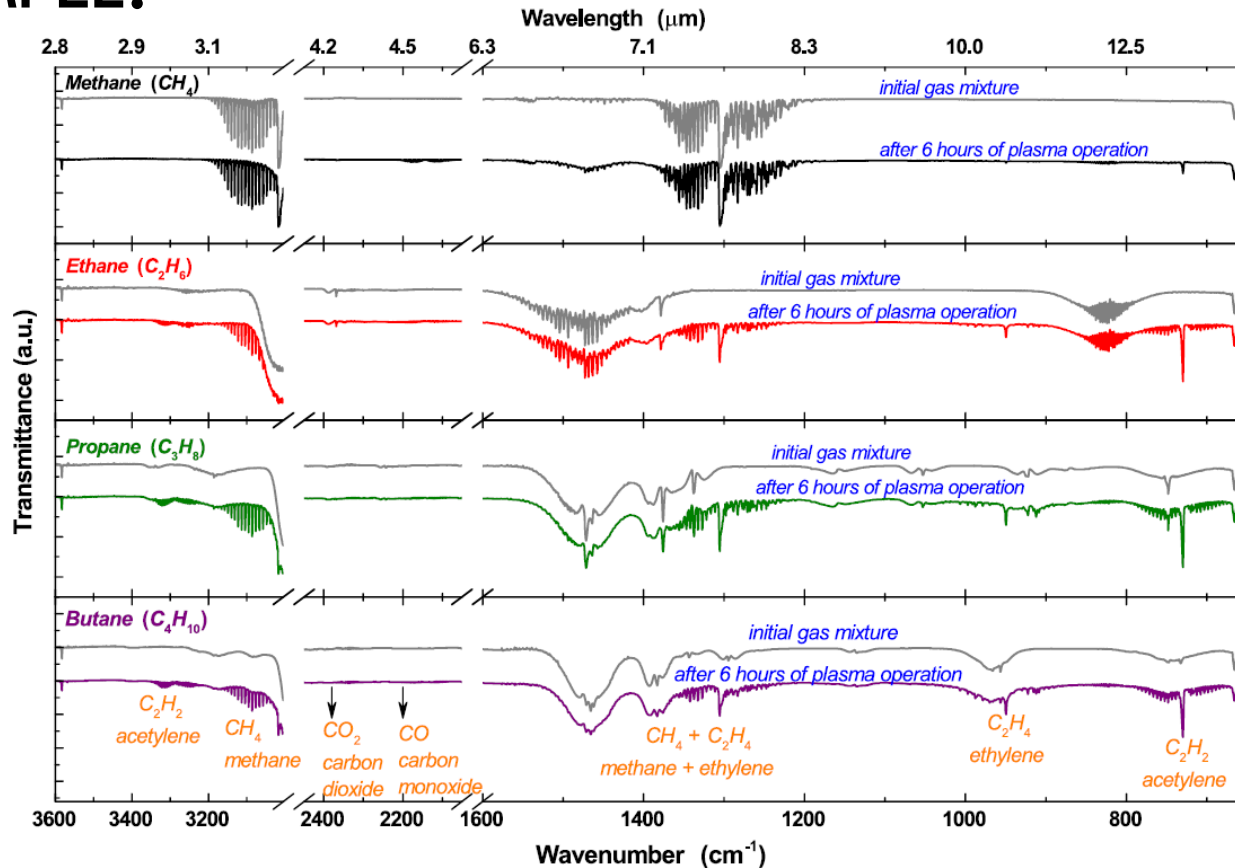
Kinetic gas phase analysis by infrared measurements (transmittance values of all spectra, except the initial spectrum, are intentionally shifted for clarity reasons) for a DBD plasma reactor used to expose wheat seeds.



https://rjp.nipne.ro/2018_63_7-8/RomJPhys.63.905.pdf



EXAMPLE:



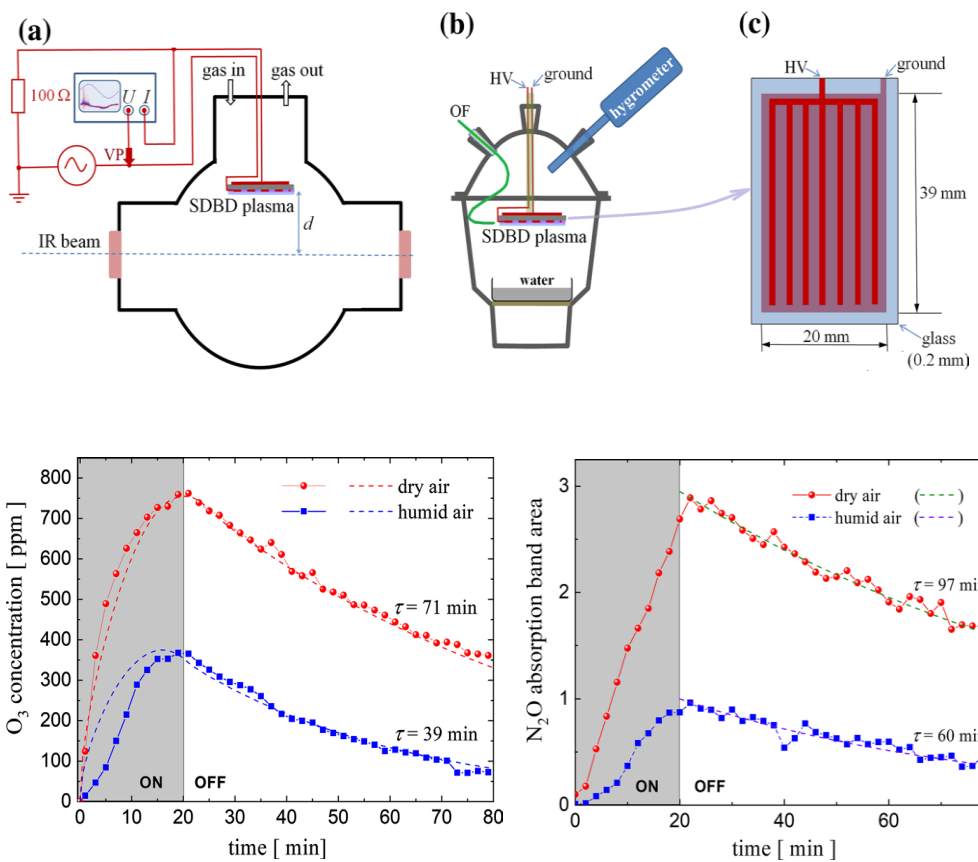
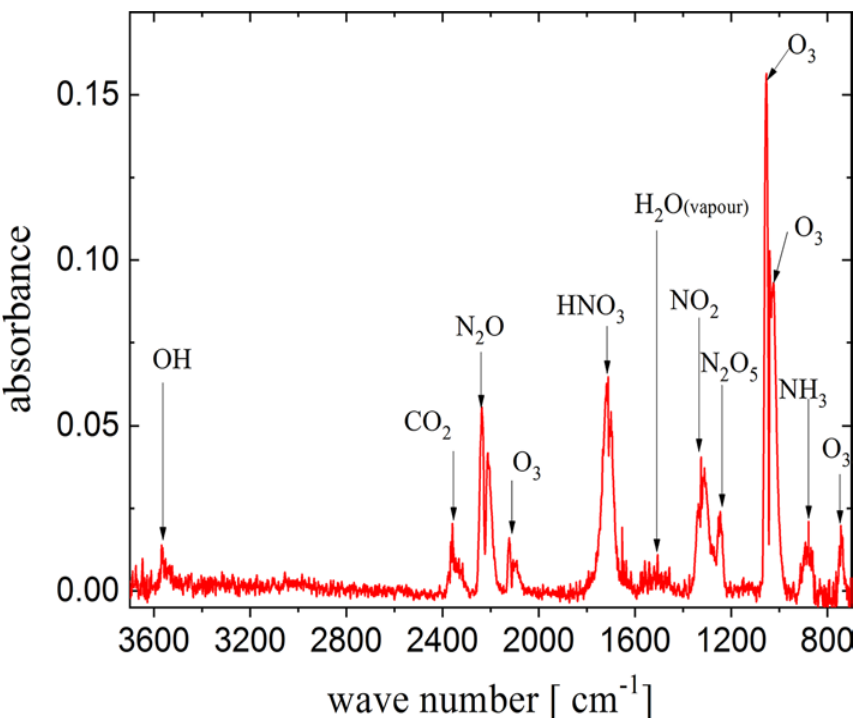
FTIR spectra of the He/ C_nH_{2n+2} gas mixtures, sampled before and after 6 h of DBD plasma processing.



<https://doi.org/10.1093/mnras/sty2497>



EXAMPLE:



Assignment of IR absorption bands to molecular species generated by SDBD plasma in air. This particular FTIR spectrum has been acquired with IR beam path at distance $d \approx 0$ cm after 4 min of SDBD working in dry air. Time variations of the average ozone and N₂O concentration.

